International Journal of Machine Tools & Manufacture 164 (2021) 103718

Contents lists available at ScienceDirect

International Journal of Machine Tools and Manufacture

journal homepage: http://www.elsevier.com/locate/ijmactool

Surface integrity in metal machining - Part II: Functional performance

Andrea la Monaca [a], James W. Murray [b], Zhirong Liao [a,**], Alistair Speidel [b], Jose A. Robles-Linares [a], Dragos A. Axinte [a,c], Mark C. Hardy [d], Adam T. Clare [b,c,*]

[a] Machining and Condition Monitoring Group, Faculty of Engineering, University of Nottingham, NG7 2RD, United Kingdom
[b] Advanced Component Engineering Laboratory, Faculty of Engineering, University of Nottingham, NG8 1BB, United Kingdom
[c] Faculty of Engineering, University of Nottingham, Ningbo, China
[d] Rolls-Royce plc, PO Box 31, Derby, DE24 8JB, United Kingdom

ARTICLE INFO

Keywords:
Surface integrity
Machining
Service life
Fatigue endurance
Corrosion resistance
Wear resistance

ABSTRACT

Material removal operations play a pivotal role in the manufacture of key components, required for engineering systems to operate safely and efficiently under ever more advanced functional requirements and over extended life cycles. To further step up the loading capability of machined parts, fundamental understanding of how of machining-induced features can influence the performance of advanced materials under complex service conditions is necessary over finer temporal and spatial scales. As discussed in Part I of this review, when engineering surfaces are generated by material removal processes, a wide range of physical mechanisms (e.g. mechanical, thermal, chemical and their combinations) drive the characteristics of workpiece surface integrity. In Part II of this review, the interplay between the metallurgical and micro-mechanical condition induced by material removal processes and their in-service response will be thoroughly explored, by a critical analysis of the state-of-the-art in the field. Specifically, attention is focused on recent advances made towards the understanding of the mechanisms determining the resistance of machined surface to fatigue crack nucleation (Section 2), corrosion and stress-corrosion cracking (Section 3), and wear (Section 4). Furthermore, the impact of relevant post-machining treatments on the in-service behaviour of machined surfaces is analysed, and the possible strategies for the enhancement of the functional performance of machined surfaces are presented (Section 5). Finally, the current research gaps and the prospective challenges in understanding the in-service behaviour of machined surfaces are critically discussed, providing an interpretation of the possible directions of future scientific development of this field.

1. Introduction

Machining processes allow realisation of desired component geometry through removal of material volumes from a target workpiece – the component. In fact, subtractive manufacturing operations employ varying strategies to locally interrupt the workpiece continuity by breakage of atomic/molecular bonds giving rise to material removal. However, due to the nature of the physical effects used to separate contiguous material volumes, presence of metallurgical alterations can be induced to the machined workpiece surface. The scale of these ranges from the atomic, through 'grain' to the macroscopic. In this context, the concept of 'Surface Integrity' is employed to describe the ensemble of process-induced characteristics (topographical, metallurgical, micro-mechanical, etc.) produced by machining operations in the workpiece surface and subsurface volume.

As discussed in Part I of this review [1], different types of anomalies can be induced by machining processes depending on the physical effect (s) they employ for material removal, e.g. mechanical, thermal, chemical and their combinations. Because of the modifications that can be induced in machined surface layers, their micro-mechanical properties can have a significant influence on the in-service behaviour and load-bearing performance of advanced materials. In this context, it has been long recognised that machining-induced surface quality plays a critical role on component performance. Classically, surface finish is carefully controlled, and finishing techniques are often prescribed for most mission imperative machined parts. However, as shown in this review, the material sensitivity to even minor variation in surface integrity can be sufficient to significantly undermine the performance of

* Corresponding author. Advanced Component Engineering Laboratory, Faculty of Engineering, University of Nottingham, NG8 1BB, United Kingdom.
** Corresponding author.
E-mail addresses: Zhirong.Liao@nottingham.ac.uk (Z. Liao), Adam.Clare@nottingham.ac.uk (A.T. Clare).

https://doi.org/10.1016/j.ijmachtools.2021.103718
Received 28 December 2020; Received in revised form 9 March 2021; Accepted 10 March 2021
Available online 16 March 2021

machined surfaces, with implications not only on component functionality but possibly concerning the safe operation of whole engineering systems. The implications are therefore potentially disastrous. In fact, controlling the response of advanced materials to small-scale machining-induced modifications represents a primary enabler for the manufacture of advanced systems capable of meeting the ambitious efficiency targets set for future applications in aerospace, nuclear, and automotive industries. Thus, this implies a critical need for a much more in-depth understanding of the mechanisms governing the behaviour of machined parts under complex service conditions (e.g. cyclic thermo-mechanical loads, exposure to corrosive agents, etc.).

In this context, addressing the origins and implications of the machining-induced surface integrity has been moving from macroscopic descriptions of machined surface states, to more fundamental material investigations on ever smaller scales. For this to be possible, a clear change in the culture and way of thinking of manufacturing specialists is necessary, obliging them to apply investigative approaches involving methods more typical of material science disciplines, as explored in this review study. Further, dealing with surface integrity as a "black box" where the functional performance is a result of statistically-optimised machining parameters is not believed to represent a viable option for the future, especially in presence of the fast-evolving machining challenges in terms new material systems, increased process efficiency and functional requirements characterising high-value engineering fields. Thus, to reach a solid and long-lasting understanding of the relationship between machining condition and in-service part functionality, current and future research needs to substantially advance the existing knowledge of the physical mechanisms induced by machining operations, particularly focusing on their intimate link with the resulting metallurgical state produced in machined surfaces, which ultimately determines the in-service part performance. For this reason, systematic analysis of the effect of machining parameters is beyond of the scope of this review, which in contrast aims to direct the attention of the reader to the role played by physical mechanisms of material removal (mechanical, thermal and chemical effects, as defined in Part I of this study [1]) on the machining-induced surface integrity and the resulting functional performance.

Against this background, this review discusses advances in our understanding of the behaviour of machining-induced layers when exposed to relevant working conditions. As shown in Fig. 1, after the analysis of the fundamentals of machined surface characteristics in Part I of this review study [1], Part II will explore the impact of the machining-induced surface integrity on the resulting component performance in context of key environmental conditions, which include: fatigue loading (Section 2), corrosion and stress-corrosion resistance (Section 3), and wear performance (Section 4); furthermore suitable post-machining treatments for the enhancement of the functional performance of machined surfaces are additionally discussed (Section 5).

2. Fatigue performance of machined parts in presence of process-induced anomalies

2.1. Considering fatigue – a manufacturing perspective

From fundamental solid mechanics, when external loads are applied to a body, continuum stress and strain fields (where they can be accommodated) arise in its volume. Under low magnitude loading conditions, metal volumes deform elastically, i.e. they are able to return to their original shape once external forces are removed. However, if the stress experienced by a metal overtakes a threshold defined as yield strength (YS), irreversible deformation occurs under a regime that is referred to as plastic. In the context of uniaxial tensile testing, the maximum engineering stress displayed by a metal before fracture is called ultimate tensile strength (UTS). Analysis of stress-strain fields and availability of constitutive material models hence enables engineers to design components that safely withstand service loads under static conditions. However, this approach is not sufficient when dealing with time-dependent or transient loading conditions.

Fatigue as a phenomenon was first identified during the industrial revolution of the 19th century, as cyclically-loaded components encountered sudden rupture loads which did not invoke failure when applied statically [8]. Frequent rail axels failures that occurred in that period were found to be linked to metal fatigue [9], with historic consequences such as the tragic Versailles accident in May 1842. Systematic studies from Wöhler later demonstrated how alternate stresses significantly below the material ultimate tensile strength (UTS) could cause metal fracture after several load reversals or cycles. Subsequent research throughout the 20th century followed to address fatigue phenomena from both an engineering and material science perspective [10]. Progress in fracture mechanics [11,12] revealed the mechanisms by which infinitesimal cracks nucleate and grow during loading cycles, which later explained dramatic fatigue accidents such as the in-flight failure of the de Havilland Comet I [13]. Thus, damage-tolerant approaches have been developed along with non-destructive inspection procedures to control the structural integrity of safety-critical parts as-manufactured and throughout their service. In this context, modern approaches investigating the behaviour of metals under cyclic loading are supported by the advances made in material science, which allow understanding of fatigue-induced failure mechanisms on ever smaller scales.

Micro and even nano-scale anomalies resulting from manufacturing process or damage accrued in service play the foremost role in determining the number of cycles a component can safely perform. Because of the physical effects introduced within the manufacturing route, the processed material can locally develop micro-scale features exhibiting a mechanical behaviour distinct to that of the bulk material. In the most critical cases, manufacturing-induced anomalies can undermine a material's performance by facilitating premature fatigue crack nucleation under in-service loading conditions. The understanding of these phenomena prompts new definitions of manufacturing quality where fatigue is a concern. In this context, researching the mechanisms by which manufacturing-induced alterations influence fatigue behaviour of metals is essential to meet the increasing technological demand for advanced materials processing and improved component performance of current and future times.

2.2. Material subtraction and fatigue performance

Material removal processes are key manufacturing operations, making machining processes culpable for much of the final part quality for key industrial fields such as aerospace [14], nuclear [15], power generation [16], or rail [17]. One of the factors traditionally related to fatigue performance of machined parts is represented by surface topography. In fact, although surface roughness has been known for many years to be a key aspect influencing fatigue strength, the role played by material removal processes still represents a traditional and still active topic of research in this area. As discussed by Novovic et al. [18], even in absence of other defects, influence of surface topography on fatigue is in general non-negligible from $Ra > 0.1$ μm. In fact, surface asperities that may result after machining can induce stress intensifications under loading and hence promote early crack nucleation in machined surfaces [19,20]. An additional aspect traditionally considered when investigating the fatigue performance of surfaces generated through material removal involves the analysis of the residual stresses (RS) apparent in the workpiece after operation [21]. Machining-induced RS induce a local stress condition that persists in the component sub-surface when external loads are no longer applied [22]. Several studies reported how the nature of the RS field can influence nucleation of fatigue cracks. Presence of compressive residual stresses are generally found to retard fatigue crack occurrence while tensile states have an opposite effect [23–25]. Specifically, the more energetic a machining process (e.g. higher feed rates, and depths of cut) is, the larger the RS field magnitude is to be expected. Hence, roughing

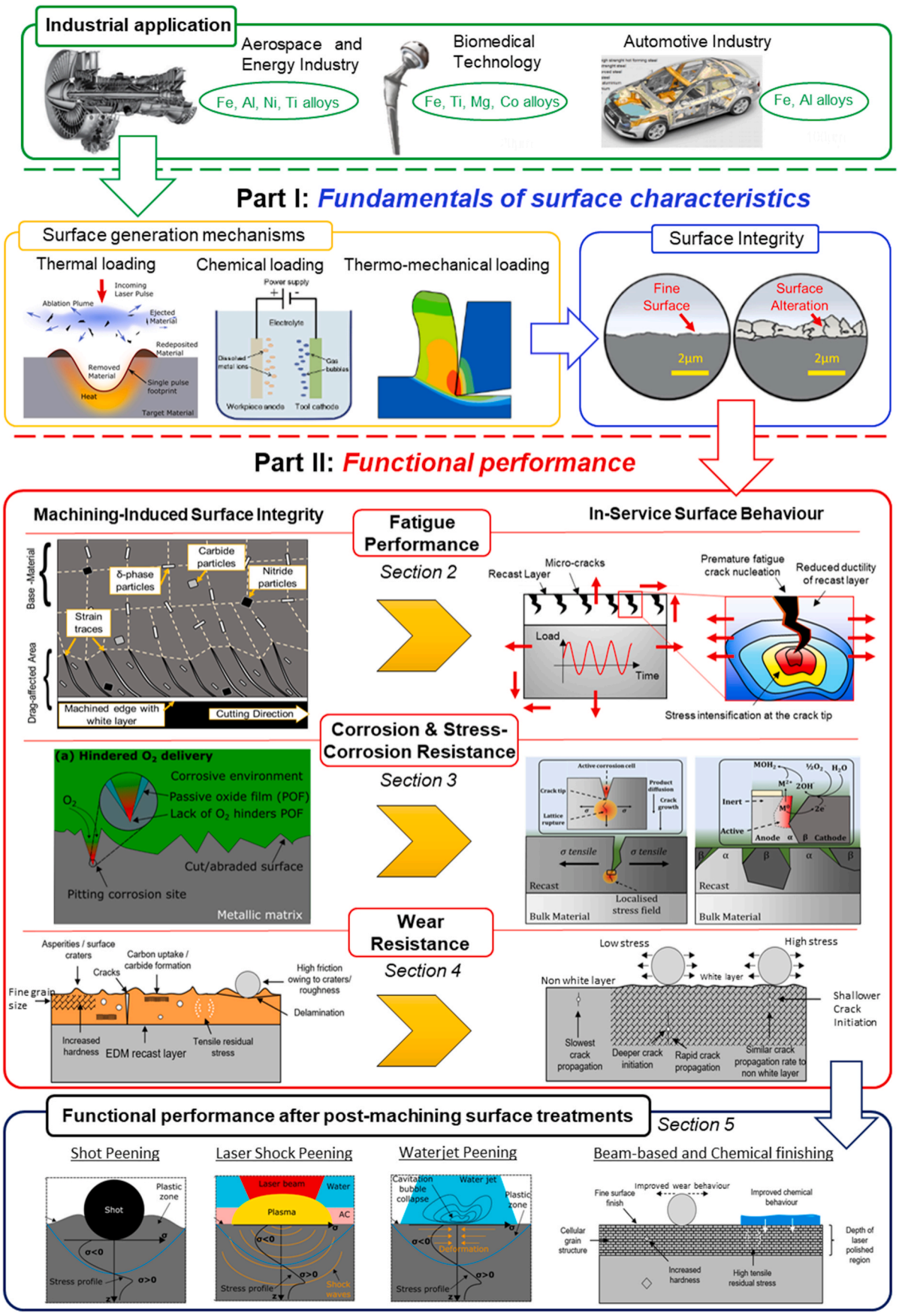

Fig. 1. In order to aid the reader in navigating this review, an overview is presented above. Part I [1] focused on fundamentals of surface characteristics and here, Part II describes the influence of surface integrity upon the functional performance of machined parts [2–7].

processes are expected to have a bigger impact in terms of RS than finishing operations, which can represent a trade-off between the material removal rate and resulting surface integrity. Put simply there is a balance to be struck between economy in process and resultant surface quality.

Nevertheless, the impact of machining-induced RS and surface roughness on fatigue life is a topic widely investigated, as documented in prior reviews on this subject [22,26]. To guarantee component performance in ever more challenging environmental conditions, interest in a deeper understanding of the implications of manufacturing route on in-service performance has sharply increased in recent years.

New concepts are being developed by the research community to understand the influence of micro-mechanical states locally generated by machining (as outlined in Part I of this review [1]) and address their influence on the fatigue performance of machined parts. A close relationship exists between the machining-induced surface integrity, the behaviour of the machined surface under dynamic loading, and its sensitivity to fatigue crack nucleation. In fact, microstructural surface modifications can be induced when high energy densities are delivered to the processed workpiece. This is illustrated in Fig. 2 for an exemplar operation, in this case laser machining, which can be responsible for the formation of recast layers and several micro-cracks adjacent to the machined surface. These types of anomalies can locally alter the material ductility on small scales and might additionally induce stress intensifications in the machined surface layer. As a result, the rate at which fatigue cracks nucleate are no more controlled only by the unprocessed material properties, but additional deformation mechanisms can be activated in the machined subsurface and interface with the bulk potentially influencing on overall component performance.

Against this background, wider concepts for the description and understanding of the integrity of machined surfaces have been developed, including analytical methods within the machining research community, as outlined in detail in Part I of this review [1]. This has led to the development of intertwined approaches arising from a mix of disciplines involving metallurgy, advanced manufacturing technology and solid mechanics. Thus, disclosing the mechanisms by which process-induced anomalies affect the fatigue performance of advanced materials after machining operations is attracting increasing research effort both industry and academia.

2.3. Fatigue performance of advanced alloys after mechanical machining

As a result of the thermo-mechanical fields induced by metal cutting at the tool-workpiece interface, small-scale metallurgical alterations of different types and degrees can be induced. In fact, microscopic observation of machined subsurfaces can reveal the existence of layers of material with a deformed microstructure, which can present traces of strain propagating from the machined surface into the workpiece volume, as shown in Fig. 3a. Such machining-induced strain is frequently encountered when analysing the microstructure of cut subsurfaces, and it is usually referred to as material drag (MD). Moreover, a severely strained material layer with nanocrystalline grain structure can be induced in machined sub-surfaces under aggressive cutting conditions. This is commonly referred to as white etching layer (WEL) or simply white layer (WL) because of its white and featureless appearance when observed via light microscopy following chemical etching. Examples of WLs are reported in Figs. 3 and 4b and c. Formation and extent of MD and WLs is dependent on the severity of the thermo-mechanical fields in cutting, with advanced strategies being developed to investigate their microstructural [6] and micro-mechanical [27] characteristics. In the following, the analysis of cutting-induced material deformation on fatigue performance will be considered for the most relevant alloys employed in high performance industrial systems, while parallels can be drawn to other alloys. Specifically, the focus will be first placed on Ni-base superalloys and Ti alloys, whose surface integrity and performance after machining has notoriously high relevance especially when it comes to the aerospace propulsion field. In addition their performance is often the limiting factor of the engineering systems in which they reside. Moreover, the machining-induced fatigue performance of steels and aluminium alloys will be also discussed in terms of their different machining challenges and in-service requirements.

2.3.1. Influence of mechanical machining on the fatigue performance of Ni-base superalloys and Ti-base aerospace alloys

Polycrystalline Ni-base superalloys enable the manufacture of components required to exhibit long-term structural performance in a high-temperature environment, which poses significant challenges in terms of both mechanical properties and corrosion resistance, especially in presence of combustion products. Thus, wrought Ni-based superalloys find key applications within the aerospace gas-turbine industry or in advanced-ultra supercritical (AUSC) power plants [30]. Even though

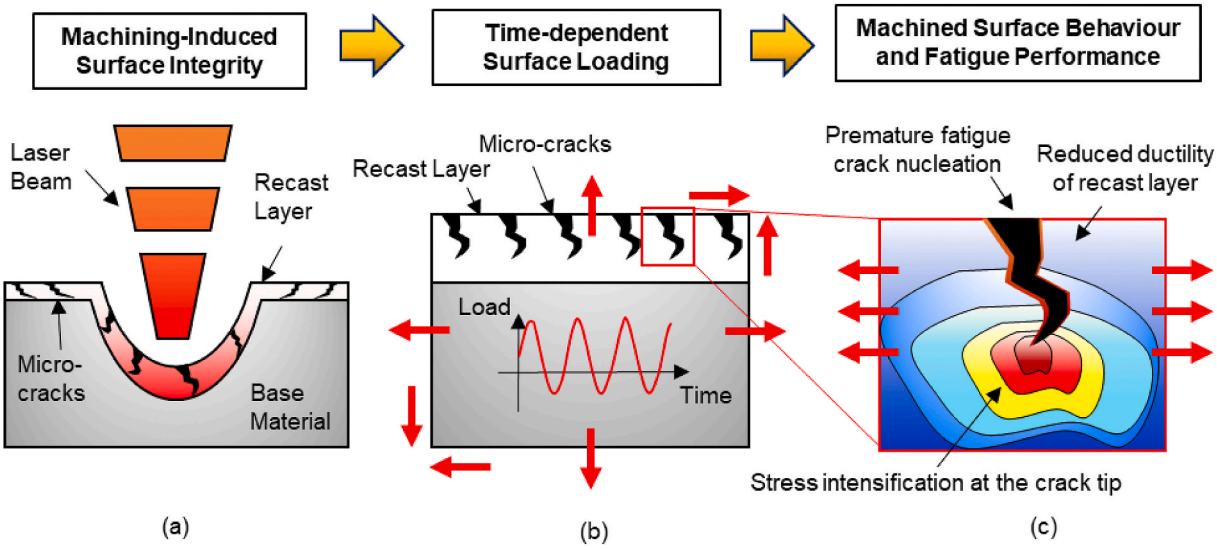

Fig. 2. –Schematic representation of the interplay between surface integrity and functional performance of machined parts. (a) Microstructural surface integrity induced by metal machining considering laser machining as an example, (b) its interaction with in-service cyclic loading conditions, and (c) its influence on the fatigue failure mechanisms of machined surfaces.

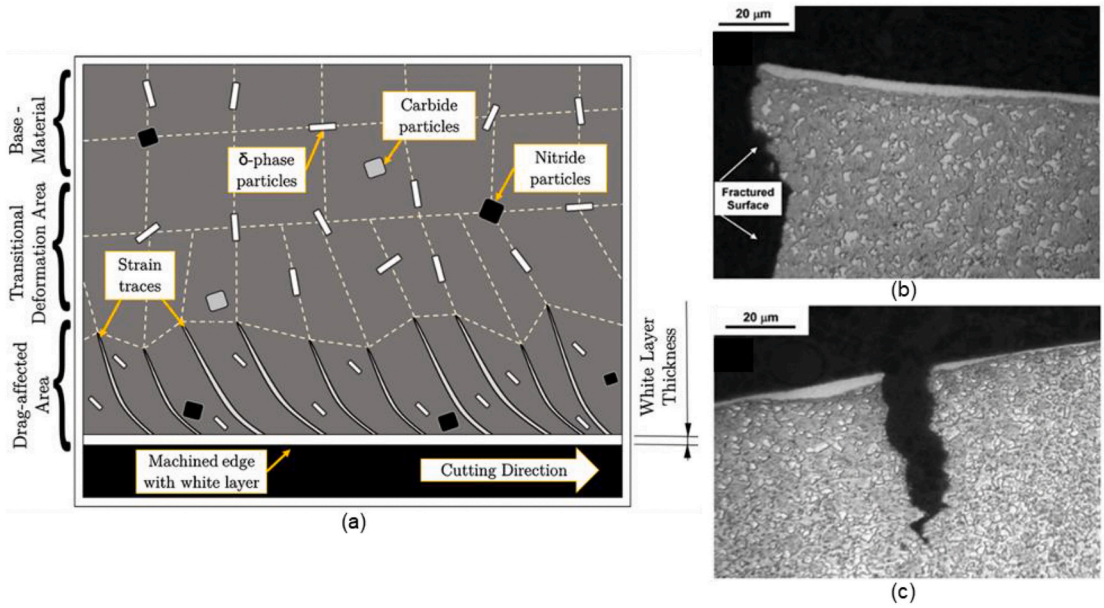

Fig. 3. Microstructural deformation and crack initiation in Ni-base superalloys after mechanical machining operations. (a) A schematic representation of the main microstructural surface features that can be induced by mechanical machining, such as Material Drag (MD) and White Layer (WL) features in a Ni-base superalloy [6] (b) Wusatowska-Sarnek et al. [28] showed the formation of the WL (clearly shown as a white band at the surface) and the origin of cracking which results. The onset of cracking at 530K and 640 MPa can be clearly related to the presence of the WL. (c) Additionally, a secondary crack developing at the sample surface was observed in the same specimen [28].

machining this class of materials involves significant challenges for their elevated mechanical properties, cutting processes are fundamental to the manufacture many nickel-based superalloy components [31]. As an example, the mechanical coupling between compressor or turbine blades and rotor discs is possible through 'fir-tree' roots geometries, which can be obtained through broaching, fir-tree milling, grinding or wire electrical discharge machining. Although mechanical machining operations such as broaching represent an effective way of realising the desired profiles in heat resistant superalloys, it has been shown that if excessively deformed material drag layers are induced in the workpiece subsurface after machining, the material's high-temperature fatigue performance can be compromised [32].

The presence of nanocrystalline layers induced by material removal may not be acceptable for most safety-critical components where low-cycle fatigue (LCF) is a concerned [14,29]. In fact, WLs have been shown to reduce the fatigue endurance of mechanically machined Ni-base superalloys under LCF regimes, e.g. for the case of fine-grain IN100 after milling [28] where it was revealed how metallurgical anomalies promoted early crack-initiation under cyclic stresses. Among polycrystalline nickel-base superalloys, RR1000 is a proprietary state-of-the-art material currently employed for the manufacture of safety-critical components, including modern high-pressure aero-engine disc rotors [33]. When new alloys are introduced, understanding and hence controlling of the effect of machining-induced microstructural anomalies on in-service performance is essential. This acts as a research driver for the development of a systematic definition of acceptability levels of machined parts presenting cutting-induced microstructural deformation.

SEM analysis has revealed that mechanical operations such as hole-making via drilling or plunge milling can introduce significant levels of material drag and invoke white layer formation in this superalloy, as shown in Fig. 4a–(d) [29]. High-temperature LCF performance of RR1000 specimens can be significantly influenced by the microstructural state induced by machining in the vicinity of the new surface, which can be particularly complex for the elevated properties of this alloy [34–36]. An analysis of the cycles to failure of RR1000 specimens under high-temperature LCF conditions is reported in Fig. 4 (d), for different levels of subsurface deformation induced by hole-making operations both in terms of WLs and MD. In fact, the study by Herbert et al. [29] reports that the effect of MD layers with thickness below 10 μm have negligible influence on fatigue performance. Differently, MD layers become unacceptable when presenting greater extent (in the range of ~20 μm), as this condition reduced fatigue performance and coexisted with highly tensile stresses in the hoop direction. Additionally, this study showed how white layers were not tolerable in any of the extents considered (5 and 10 μm), further indicating how thicker WLs are associated to higher tensile stresses due to greater thermal effects during aggressive cutting. Post-failure fractography presented in this study revealed that the presence of a WL compromised the fatigue endurance of RR1000, as it promoted early crack nucleation because of the reduced ductility induced in this workpiece surface by aggressive cutting conditions. In this context, to understand the small-scale behaviour of WLs under loading, new possibilities are offered by in-situ micro-mechanical testing of these machining-induced layers. Cyclic micro-pillar compression of WL regions recently showed that machining-induced nanocrystalline layers present a dominating micro-plastic behaviour with low elasticity, thus revealing the micro and nanoscale loss of ductility occurring in such material regions, which accounted for the macroscopic reduction in fatigue performance [27].

A difference in constitutive behaviour would explain why metallurgical anomalies such as WLs are so critical in the context of LCF, where the number of cycles to failure under high cyclic stresses is dictated by the material response in the plastic domain. Recent advances in cutting-induced fatigue behaviour of nickel-base superalloys include studies of the response after hybrid cutting processes such as laser-assisted machining (LAM) [37,38], where complex RS induced by thermal and mechanical effects can coexist with drastic microstructural alteration. However, the way metallurgical anomalies interact under alternate loading is in most cases not fully understood. This should represent a key question for future research as machining-induced alterations frequently occur simultaneously and their coupled effect on crack initiation is unknown.

With excellent strength-to-weight ratio, titanium alloys find an increasing number of applications in the aerospace and medical sectors.

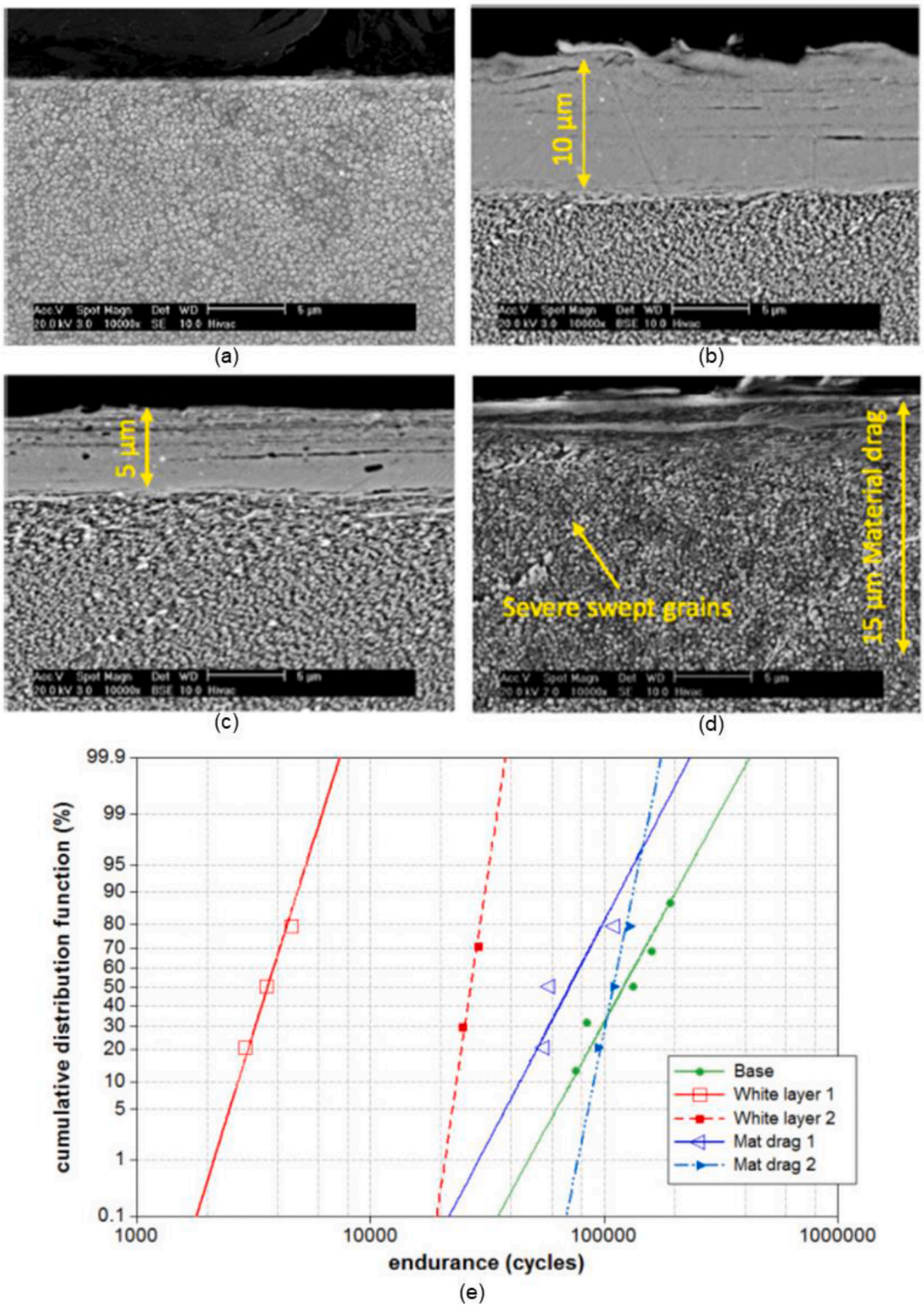

Fig. 4. Herbert et al. [29] analysed by SEM the nature of machining-induced layers as a result of hole-making operations, which are later related to the resulting fatigue endurance of a Ni-base superalloy (RR1000). (a) damage-free surface; (b) white layer I; (c) white layer II; (d) material drag I; (e) Endurance data from 600 °C fatigue tests on single hole test pieces of a Ni-base superalloy (coarse grain RR1000). These test pieces showed "damage–free" (base) and 2 heavily deformed surfaces, a white etch layer (1 = depth of 10 µm, 2 = depth of 5 µm) and severely distorted γ′ structures to a depth of 15 µm (mat drag 1) and 10 µm (mat drag 2) [14].

However, these alloys are notably characterised by low machinability consistent with their high mechanical properties and low thermal conductivity [39]. Hence, when they are cut, aggressive processing conditions can locally develop and induce a highly-deformed surface [40–42] with potential influence on fatigue performance. For the case of beta titanium alloy Ti-5553 processed through end-milling, it has been shown that a 50% increase in material removal rate (MRR) reduced by 50% the number of LCF cycles to rupture, despite the higher

compressive RS state generated [43]. This is illustrated in Fig. 5, where higher MRR also generated severely deformed subsurface layers, which acted as preferential fatigue crack nucleation sites in spite of the increased compressive RS state [43]. Hence, investigating the machining-induced fatigue behaviour from a metallurgical perspective is necessary to understand the material response to cyclic stress conditions, where more conventional metrics (e.g. RS measurement) cannot fully account for the observed phenomena. For their superior mechanical properties and corrosion resistance combined with a low density (~4.0 g/cm^3), TiAl-based alloys also find an increasing number of applications in the aerospace field [44]. Fatigue behaviour of these materials after mechanical machining however, appears to be complex. For example, when turning a gamma XD™ titanium aluminide, increased micro-hardness can be generated in the subsurface layer up to a depth of 100 μm, and the formation of defects such as material pull-out and cracking are observed [45]. Nevertheless, although the turning process produced cracks at depths up to 20 μm from the new surface, no evidence of crack initiation at these defects was discovered, leading to a similar fatigue response of specimens that were single-point machined or polished. Although this result is not fully explained, it is suggested that in this case the reason might reside in the generation of compressive residual stresses during turning. If this is the case, the trend would be opposite to what was found in Ref. [43] where crack nucleation occurred from machining-induced anomalies *despite* the presence of compressive RS. However, to better understand these phenomena, further research work should be focused to identify how the presence of local anomalies interacts with residual stresses field under cyclic loading conditions, especially for Ti-based materials presenting different metallurgical properties. Moreover, it should be remarked that not all cracks are equal. In fact, crack growth is also influenced by the amount of plastic deformation to which the nearby material had been subject, together with its RS state. Hence, further research should be focused on understanding the interaction of multiple anomalies induced in machined surface layers to fully address macroscopic component performance.

2.3.2. *Influence of mechanical machining on the fatigue performance of high performance steels and Al-base alloys*

The aerospace industry is notoriously focused on guaranteeing that finish cutting operations generate excellent surface integrity, to limit the effect of machining-induced anomalies on fatigue crack nucleation. The use of steels for some key aerospace components, e.g. aero-engine shafts or landing gear components, still persists since their fatigue properties have been very well understood throughout the years. For instance, controlling of machining-induced integrity is crucial when it comes to ultra-high-strength (UHS) steels for landing gear systems. Early studies on UHS steels investigated their HCF strength after grinding, turning and milling, with best performance exhibited by ground surfaces [46]. However, at that time it was not possible to fully address the nature of the observed performance, as understanding of the cutting-induced micro-structural conditions was still limited. State-of-the-art research has now identified how a presence of cutting-induced WL's and RS has a damaging effect on the performance of AISI 52100 material [47,48]. Inadequate levels of machining-anomalies including microstructural distortion, residual stresses and surface roughness represent potential crack nucleation sites under cyclic loading [20,48]. Statistical modelling and fractography material analysis (as in Fig. 6) has shown how previous approaches for fatigue life of machined parts, such as Murakami's equation, can underestimate the severity of surface condition when machining-induced defects are present [49]. However, although phenomenological and statistical approaches have produced significant steps forward, the introduction of this new knowledge based on fundamental material mechanisms in fatigue life calculation models still leaves something to be desired. Because of the increasing attention focused on the levels of microstructural alteration induced in machined surfaces, emerging approaches introduce surface integrity-oriented decisions from the design stage of machining processes.

Comparing drilling with and without pre-drill and helical milling for hole-making in AISI 4340, better fatigue performance has been associated with higher cutting speeds and lower feed, as shown in Fig. 7. In addition, a pre-drilling approach has been found to generate thinner white layers and consequently an improved fatigue performance [50], which may be expected when considering the reduced loading induced by the follow-up drilling operation. In contrast with these results, when considering carbon steels such as STS410, fatigue cracking seemed to be mainly influenced by morphological imperfections such as sharp corners and scratches, while local variations in component metallurgy and material properties induced by machining did not appear to have a primary influence on LCF endurance of this alloy [51]. As previously remarked, the presence of RS in machined surfaces can have either a beneficial or detrimental effect on component fatigue performance, depending on the direction of the RS field itself. When it comes to rolling contact fatigue life for instance, the expected component endurance can be significantly improved by controlling the machining condition. Recent research has in fact demonstrated that higher tool rake angles are able to induce a compressive residual stress of greater magnitude in the

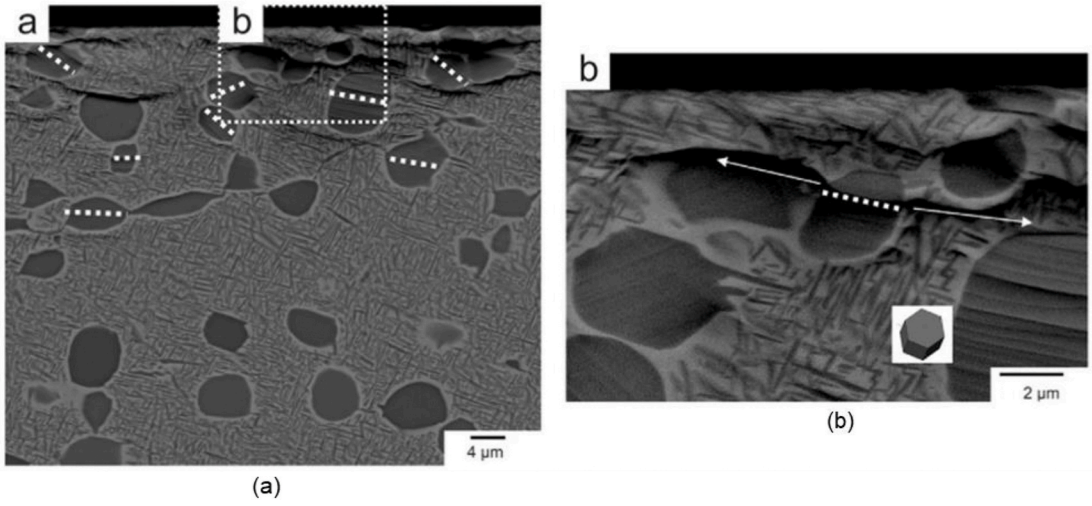

Fig. 5. Cox et al. [43] showed the initiation of fatigue cracking from a mechanically machined surface affected by a significant level of machining-induced plastic deformation. In particular: (a) shows the nucleation site presenting macroscopic and microscopic striations, where the dashed area is additionally magnified in (b) further highlighting presence of microscopic striations propagating from the machined surface.

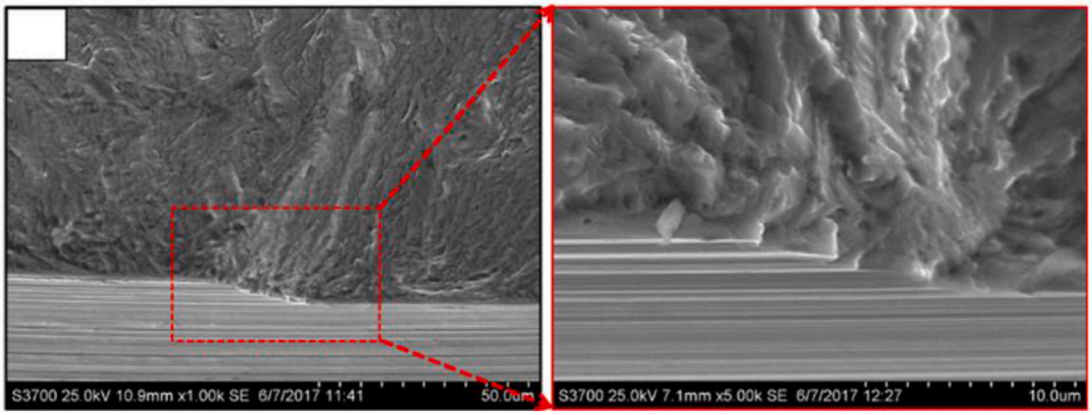

Fig. 6. -The fractographic analysis of a hard turned 300 M steel (55 HRC) shows that fatigue crack initiation is associated to the presence of a feed mark, which promoted machined surface failure at $\sigma_a = 965$ MPa, $N_f = 1.75 \cdot 10^6$ cycles [49].

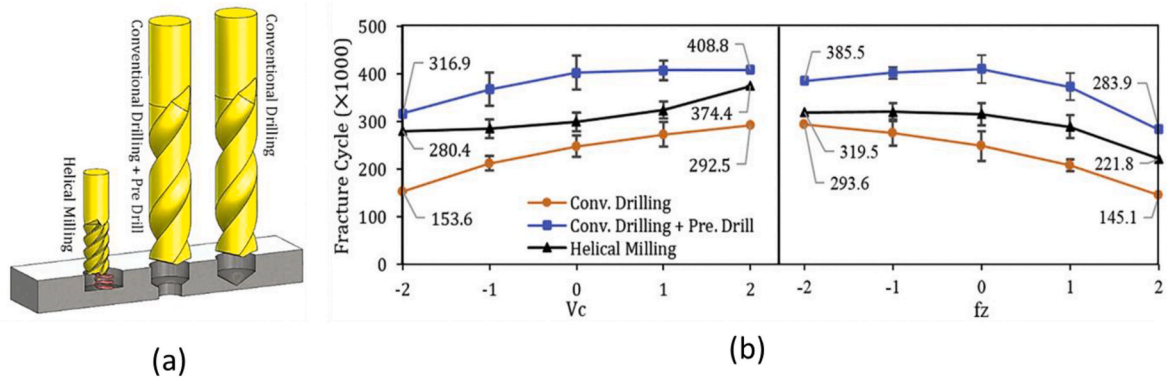

Fig. 7. The impact of different hole-making strategies on fatigue performance was studied by Rasti et al. [50]. The figure shows the kinematics of hole-making strategies in (a) and the variations of average fatigue life versus cutting speed and feed rate for the different drilling strategies in (b) reported by this study.

machined surface in face-turning AISI 1053 steel with CBN tools, consequently improving the material's resistance to crack initiation under rolling contact fatigue [52].

Aluminium alloys are widely used for aerospace applications such as airframe structures. These alloys are cost-effective, lightweight and relatively easy to manufacture [53]. High speed machining (HSM) is widely employed for this class of applications. Surface roughness, residual stresses and work hardening, that can be induced by HSM can have a direct effect on High-Cycle Fatigue (HCF) component performance [54]. Surface roughness degradation has been proven to have a direct impact on fatigue performance of Al-alloy components. Analysis of experimental data based on a large number of surface defects on different geometries allowed topography-oriented approaches to be developed, investigating the influence of scale effects on HCF performance of a AA7050 based on statistical description of real surfaces [55]. The thermal effects induced by metal cutting can also be strongly influential on resulting workpiece microstructure and surface integrity [1]. Therefore, for key mechanical machining processes, several strategies have been developed to efficiently remove heat from cutting zones with consequent effect on component surface quality and resulting fatigue behaviour. Namely, if different machining strategies in terms of lubri-cooling condition are compared, the resulting surfaces can exhibit very different fatigue performance. For 7075-T6 Al alloy, it has been proven how cutting under dry, minimum-quantity lubricant (MQL), cryogenic or high-pressure air jet (HPAJ) generates significantly different grain-size distributions and a different surface finish, especially at higher cutting speeds [56] compared to more conventional processes. With respect to the other strategies, cryogenic machining was demonstrated to be able to generate surfaces with retarded crack initiation behaviour, enabling the combination of high surface integrity and resulting fatigue performance together with high productivity. Hence, understanding the thermo-mechanical phenomena involved in metal cutting operations represents a key aspect to bridge processing conditions, productivity, component integrity and performance.

Summarising the considerations discussed in Sections 2.3.1-2.3.2, different challenges are introduced by mechanical material removal operations depending on the class of material being machined. In fact, the machining complexity will be influenced by both the workpiece material response to plastic deformation, but as well by the fatigue performance requirements dictated by the specific application, as schematically reported in Table 1.

2.4. *Influence of non-conventional machining on fatigue performance*

Aside from mechanical machining operations other physical mechanisms for material removal, processes such as electrical-discharge erosion, or chemical milling are able to achieve distinct surface characteristics. Nevertheless, the introduction of 'special' processes on a production stage not only requires expertise for effective process performance, but it also calls for in-depth understanding of the in-service behaviour of such machined parts, to enable the definition of quality standards.

2.4.1. *Influence of electrical discharge machining on the fatigue performance of the components*

Through electrical discharge machining (EDM), material removal is performed trough a potential difference generating sparks that erode workpiece material in the proximity of the electrode tool. When

Table 1
Summary of key challenges posed by mechanical machining with respect to the fatigue performance of advanced engineering alloys.

Materials	Typical Applications	Machinability	Impact of mechanical machining on fatigue – main research focus
Ni-base superalloys	High-temperature structural components for: aero-engines, land-based turbines, AUSC plants	Low	Impact of machining-induced layers (e.g. white layers, material drag layers) [14,29,28,37] – especially on high-temperature LCF performance
Ti alloys	Aero-engine parts, gas turbine industry, biomedical industry	Low	Impact of micro-cracks combined with complex residual stress states and machined surface layers [43,45]; - especially on LCF performance
High-performance Steels	Nuclear components, aero-engine shafts, landing gear components, bearings, die and tool industry	Medium	Impact of residual stress [47,48,52], surface roughness [20,48] and machined surface layers [47,48];
Aerospace-grade Al alloys	Airframe structures	High	Impact of surface topography and residual stress on HCF performance – especially after high-speed machining [54–56]

performing wire EDM, high process temperatures are reached, in the range of 8000–20,000 °C [57]. Although this allows efficient workpiece erosion, thermally-induced microstructural alterations are observed in components processed by EDM [58], such as the recast layer shown in Fig. 8a. The main factors affecting the extent of EDM-induced recast layers include peak discharge current, pulse duration and energy per spark, while electrode type and duty cycle have been reported to have reduced influence on this phenomenon [59]. Recast layers exhibit increased hardness compared to the bulk material along with a tensile RS state and often incorporate micro-cracks [59,60]. Therefore, understanding their influence on material in-service performance is mandatory for high-valued systems operating under time-dependent loads. Specifically, recast layers of 20–70 μm thickness induced by spark-EDM have been found detrimental to the fatigue performance of Inconel 718 [61], as a tensile RS state generated in such surface layer was accounted for early fatigue crack nucleation. The fatigue behaviour of Udimet 720 Ni-base superalloy after wire EDM has been studied by Antar et al. [62] under HCF loading conditions at room temperature. This research reported how sensitivity to fatigue crack nucleation of EDM'd surfaces was influenced by the EDM strategy (i.e. roughing and finishing). In fact, greater extent of surface tensile stresses and recast layers were associated to more aggressive machining conditions and promoted premature fatigue failure (Fig. 9). The presence of process-induced micro-cracks combined with tensile RS has been found responsible for a 10% reduction in HCF fatigue strength ($\sim 10^6$ cycles) of Inconel 718 wire-EDM specimens with respect to ground equivalents, while the same trend is however not found when moving towards scenarios with a number of cycles below 10^5 [63]. However, as recast layers possess a different metallurgy from the bulk material, it seems yet to be understood how the fatigue behaviour in the presence of micro-cracks and tensile RS differs when they are embedded in such altered layers.

For Ti-based alloys, fatigue life is directly related to the microstructural state induced by EDM. For Ti–6Al–4V, premature HCF failure has been attributed to the high volume of cracks generated in EDM-induced recast layers, however EDM influence on fatigue did not occur under more severe cyclic stresses [64]. This agrees with the results discussed for nickel superalloys, where fatigue response of EDM-ed specimens was influenced mainly in the HCF regime. On the other end, this diverges from the analysis previously carried out for WLs induced by mechanical machining, which transpired to be critical for LCF performance. The generation of EDM-induced layers takes place under high thermal conditions while in cutting processes a severe thermo-mechanical action is applied. Hence, even if these anomalies can present similarities when observed by SEM, they can result in very different in-service behaviour. Nevertheless, the mechanisms by which their fatigue response differs is not yet fully defined, and should be investigated by further understanding of their physical metallurgy. Reductions in fatigue strength of Ti–6Al–4V specimens processed through state-of-the-art EDM are reported to be in the range of 15–30% with respect to mechanical milling, which is a promising result considering that outdated processes could reduce fatigue strength of titanium alloys up to 2–5 times (Fig. 10) [65]. Achievement of these results has been possible thanks to an increased awareness of the processing conditions generating detrimental microstructural alterations. Since this material region is characterised by the presence of multiple micro-cracks, local stress intensifications combine with a less ductile metallurgical response of white layers. However, their mechanisms of interaction under cyclic loading is still unclear. Following an approach based on EDM parameters selection, research conducted on SKD11 tool steel shows the possibility of producing different types of recast layers with thicknesses increasing at higher pulse currents (4–32A) and pulse-on durations (4–6μs), but with the presence of cracks diminishing when this last parameter is reduced [66]. This study thus analyses how different parameter sets enabled suppression of cracks in recast layers with improved part performance under cyclical loading. However, it would be interesting to study this tendency also in terms of the physical effects induced by the process on the resulting surface integrity and fatigue performance, as it was for example demonstrated for AISI D6 tool steel, the fatigue performance was related to the EDM process discharge energy, recognising how moving towards lower energy settings (at low currents and pulse on time) improved the fatigue behaviour of EDM-affected layers [67].

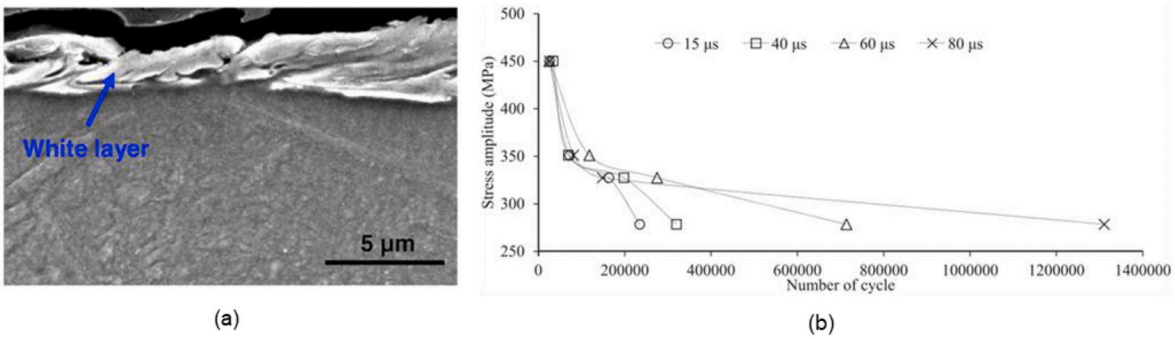

Fig. 8. Machined surface condition and functional performance in the context of Electrical Discharge Machining. (a) Example of EDM-induced white layer, with reference to a NiTi alloy [60]; (b) Relationship between stress and number of cycles before failure for specimens produced by wire EDM under different pulse-off times [64].

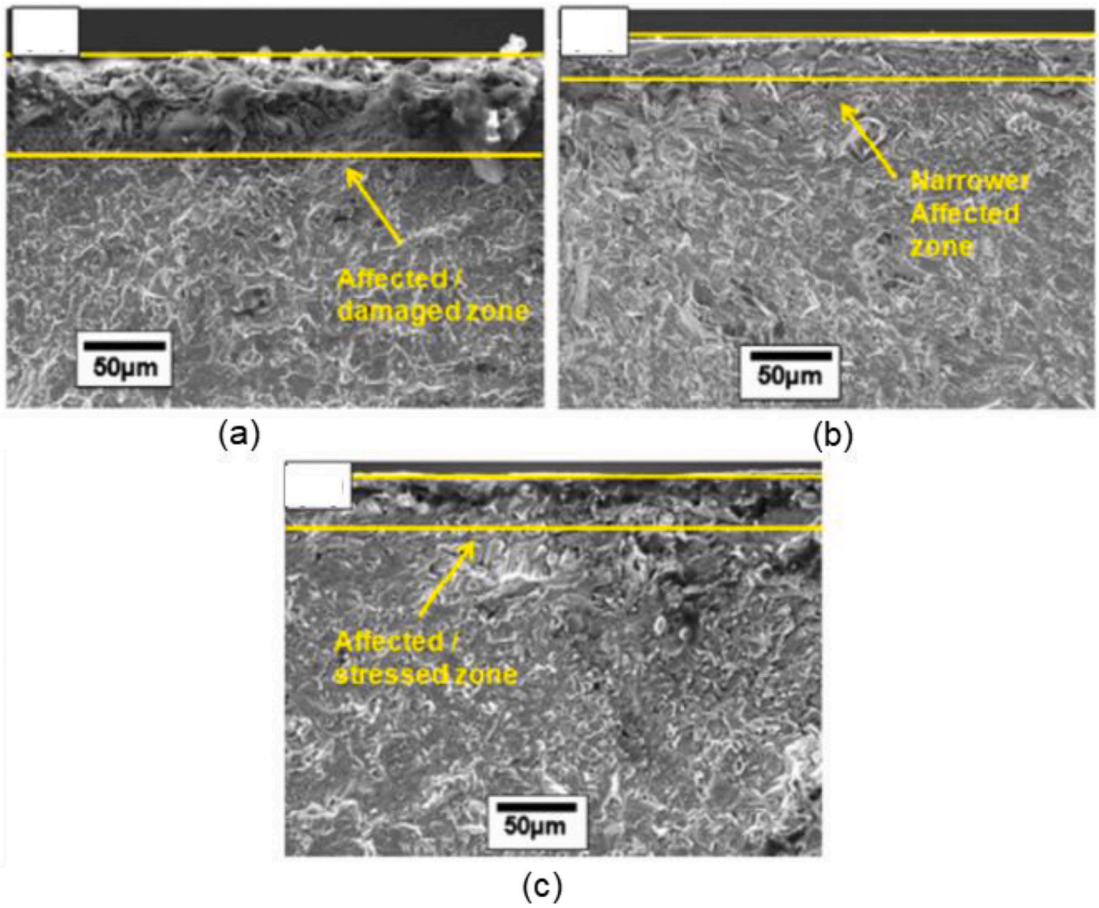

Fig. 9. Antar et al. [62] studied the influence of machined surface layers on the fatigue performance of Udimet 720 Ni-base superalloy. Machining-induced zones are clearly visible from fracture surfaces for (a) wire EDM roughing, (b) wire EDM finishing, (c) flank milling.

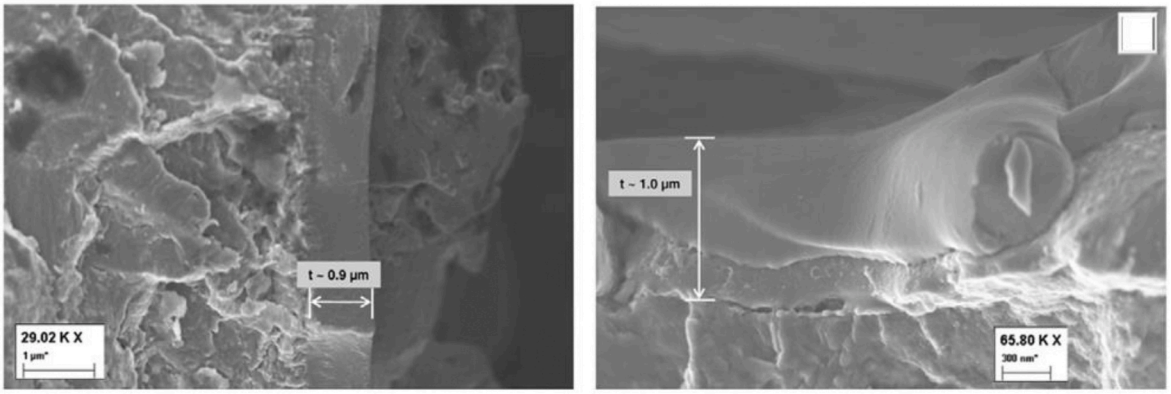

Fig. 10. Mower [65] showed that thick recast layers induced by EDM could facilitate fatigue crack initiation, as represented in this figure where recast layer measurements are carried out on fracture-surface edges.

2.4.2. Influence of laser machining on the fatigue performance of the components

High thermal energy density is delivered in laser machining, making the influence of process-induced surface integrity on fatigue of high relevance when processing critical parts. As discussed in Part I of this review work [1], crucial thermal anomalies that need to be controlled in laser processing of advanced aerospace alloys are micro-cracks and recast layers, along with thermal softening and occurrence of heat-affected zones (HAZ). For high-strength steels it has been reported that optimal fatigue conditions rely on the control of HAZ's and near-edge microstructure induced by laser cutting [68]. Premature crack initiation from laser-induced anomalies such as pores, burr and recast layers has been observed. In this context, Pessoa et al. [69] disclosed how the fatigue limit of laser cut AISI 304 could encounter up to a 40% reduction in fatigue life of polished samples, with crack initiation regions originating from laser-induced defects, as shown in Fig. 11c. On the other hand, HAZ's have been found to play a secondary role in the fatigue response of laser-cut Ti–6Al–4V, suggesting that the influence of workpiece surface roughness was predominant in defining microstructural surface integrity [70].

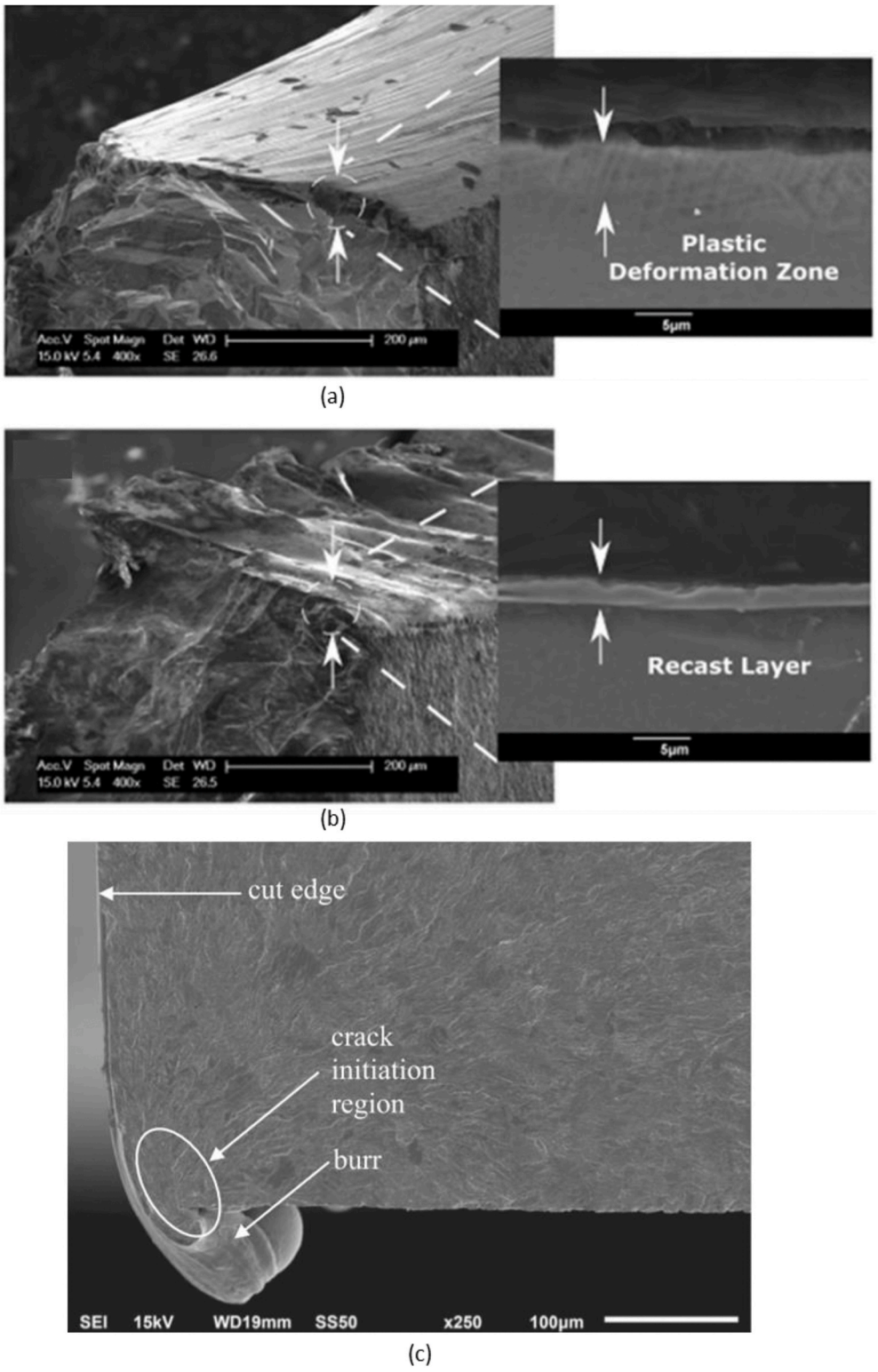

Fig. 11. Fractographic analysis (by SEM imaging) of a blade repaired through thermal and mechanical machining strategies. (a) Mechanical and (b) PLA repaired blades, showing a tilted fractured surface with top view section [71]. (c) SEM micrograph of a laser-cut fractured surface in presence of edge burr. Adapted from Ref. [69].

Due to its ability to machine advanced alloys (Ti and Ni-base superalloys) with μm-scale accuracy and no forces, pulsed laser ablation (PLA) finds extensive use in high-value industries [7]. Fig. 11a and b show fractographic analyses of two nickel-base superalloy high-pressure turbine blades, the first one in Fig. 11a presenting a plastically affected region induced by mechanical machining, and the second in Fig. 11b being affected by a recast layer induced by material removal through PLA. Testing component endurance under alternate loading, these two processes have been proven to deliver comparable HCF part performance ($>10^7$ cycles), demonstrating the applicability of PLA for in-situ repair operations of turbine blades [71]. Thus, the surface integrity induced by processes involving high thermal energy densities (i.e.

laser-cutting, PLA and EDM) significantly depends on the way the thermal energy is delivered to the workpiece. The resulting fatigue performance is hence dependent on the physical conditions generated by machining in the workpiece material.

2.4.3. *Influence of chemical machining on the fatigue performance of the components*

Through electro-chemical machining (ECM) operations, features are realised through anodic dissolution of workpiece material [72,73]. Due to the electrochemical effect employed, ECM processes are able to deliver machined surfaces displaying excellent mechanical integrity with absence of microstructural deformation or formation of recast layers [74]. This characteristic is also shared with chemical etching or/pickling processes. As these material removal mechanisms do not involve any thermo-mechanical gradient or machining forces, surface anomalies are minimal and surface quality through ECM and etching is considered best in class. However, when chemically machining multi-phase alloys, dissolution of different metallurgical phases occurs at different rates depending on their chemical properties [75]. This means that material inhomogeneity such as grain boundaries or sub-phases can directly influence the resulting microscale topography of the ECM-ed surface, as shown in Fig. 12a.

Hence, electrochemical processing of high value components requires a deep understanding of the behaviour of ECM micro-features in presence of cyclic stress conditions. In this context, research has shown that LCF life of cast Ti-6242 presented a significant reduction as a result of chemical milling, with formation of corrosion pits influencing crack initiation sites [77], as shown in Fig. 12b. Influence of chemical milling on LCF crack initiation has been studied also for Al–Mg–Si alloys, showing that fatigue life of chemically milled specimens was reduced by ca. 50% with respect to electropolished ones, with most of the crack initiation sites associated to process-induced micro pits [76]. Focusing on a γ-TiAl, research by Sharman et al. [78] observed that turned surfaces were able to display a better fatigue revealed how relatively rough surfaces (1.43 μm Ra) induced by selective etching in ECM caused significant stress intensification under alternate loading despite the absence of cracks. Differently, the same study shows how turned specimens with shallow cracks (<5 μm in depth) were able to perform better under fatigue conditions. This was attributed to presence of a compressive RS layer that favoured overall performance. Hence, this further highlights how the understanding of the physical link between machining effect, surface condition and specimen performance is fundamental to control the quality of machined products.

2.5. *Discussion: fatigue-life oriented approaches for machining process design and directions of future research and development*

A wide spectrum of studies reporting on machining-induced fatigue performance have been reviewed in the context of conventional and non-conventional material removal operations. In-service behaviour of machined induced surface anomalies has been explored and linked to the physical effects that led to their generation, which must be considered when optimising material removal processes aiming to deliver premium metallurgical and micro-mechanical integrity. In Fig. 13, the link between machining-induced microstructural surface integrity and fatigue performance is represented by linking key machining-induced anomalies and the context under which they develop (on the left hand side of the table), to their influence on fatigue crack nucleation with analysis of fracture surfaces (on the right hand side). WLs have been observed both under severe thermo-mechanical conditions characteristic of aggressive mechanical machining (e.g. milling, drilling, LAM) and under machining processes delivering high densities of thermal energy (e.g. EDM, PLA).

Depending on the physical conditions under which they are generated, WLs can have very different impacts upon fatigue performance. In mechanical machining, a combination of mechanical and thermal conditions in terms of ultra-high strain rates compounded by extreme cooling rates induces a nanocrystalline WL microstructure that is highly strained, with high lattice misorientation and high dislocation densities, which results in a reduced micro-ductility [27]. Thus, thermo-mechanical WLs are unfavourable for cyclically-loaded components, especially when it comes to higher stress states typical of LCF scenarios, where the number of cycles to rupture is highly dependent on the material behaviour in the plastic domain [27,29]. WLs resulting

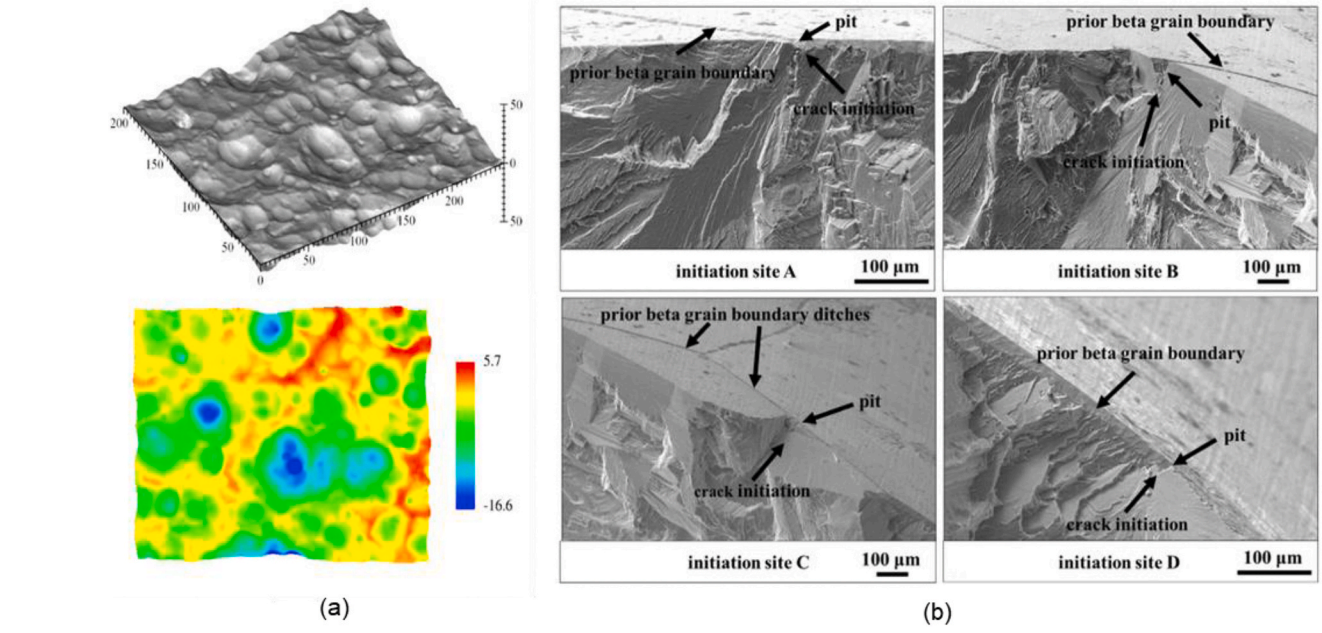

Fig. 12. Surface integrity and functional performance of surfaces produced by chemical machining. (a) Topography of a chemically milled surface of an Al–Mg–Si alloy. This figure shows the presence of several micro-pits which may act as a preferential fatigue crack nucleation site under LCF conditions (dimensions in μm). Adapted from Ref. [76]. (b) Fractographic SEM micrographs of six crack initiation sites in machining-induced surface layers in a Ti alloy (Ti–6Al–2Sn–4Zr–2Mo), with reference to a chemically milled LCF specimen. Adapted from Ref. [77].

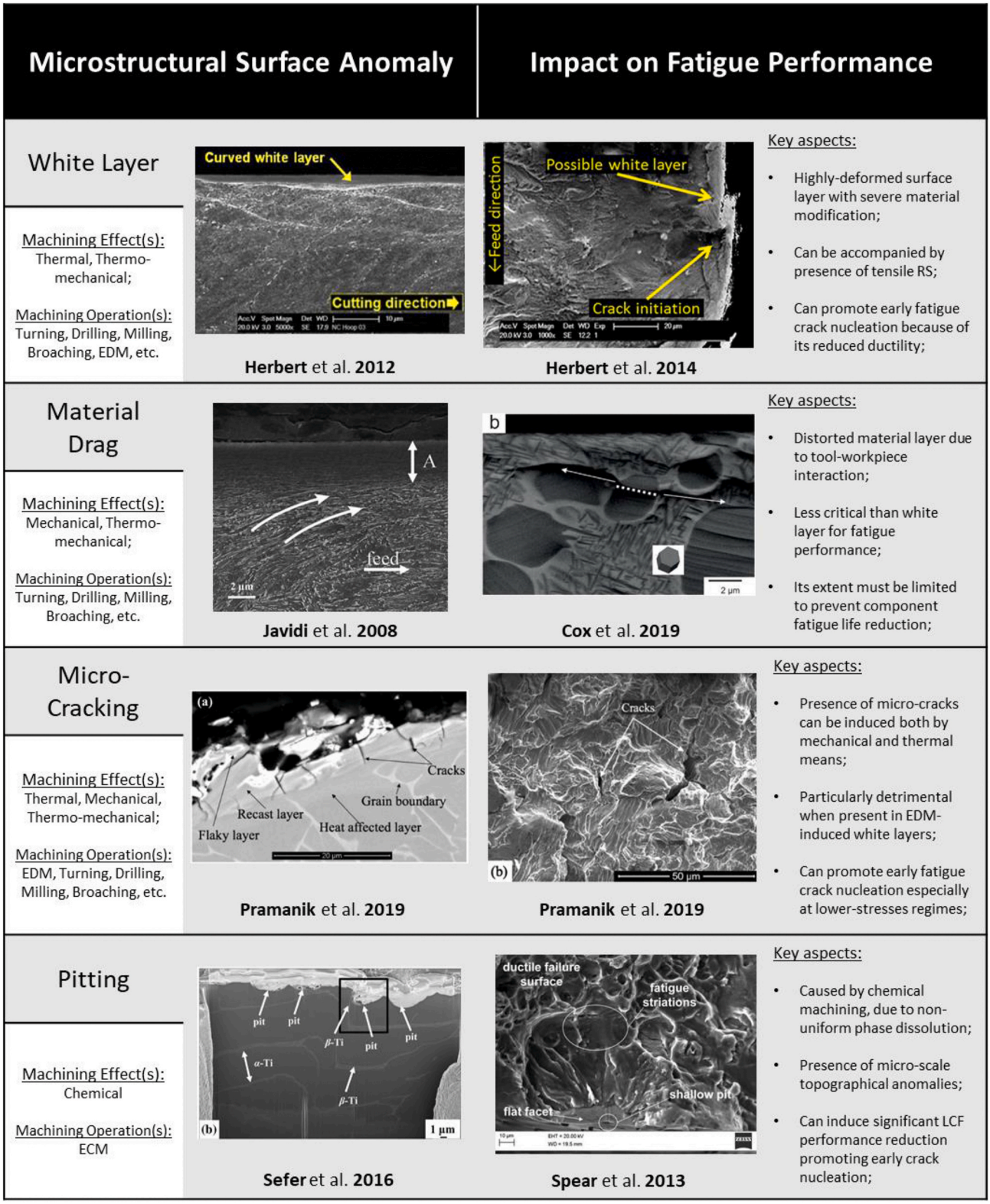

Fig. 13. Examples of key machining-induced microstructural anomalies and their influence on fatigue life. Typical machining-induced layers associated with different physical effects are reported on the left-hand side of the table, while the right-hand side correlates them with their in-service behaviour and fatigue performance.

from thermal material removal are generated by ultra-high-temperature conditions but with absence of external mechanical action. Moreover, because of the extreme thermal gradients induced in the workpiece material, thermally-induced WLs are often accompanied by presence of micro-cracks, introducing stress intensification that can lead to premature fatigue failure [64]. The presence of tensile RS instead has been found to characterise WLs obtained both by thermo-mechanical and thermal machining effects [1], which in both cases gives a detrimental

contribution to fatigue performance.

Nevertheless, strategies to mitigate the surface RS state (e.g. shot peening) proved to be unable to fully address the fatigue performance of WL-affected machined surfaces, therefore requiring WLs to be removed by a subsequent non-aggressive machining operation [29]. Along with thermal effects, surface micro-cracking can also result from mechanical machining, with similar undesirable consequences on part integrity under alternate loading. However, the influence of micro-cracking on fatigue endurance can be mitigated when a compressive RS state is induced by the machining process, acting as a retardant effect for crack nucleation [45,78]. Differently from WLs and micro-cracking, material drag (MD) and pitting defects are material features typical of a predominant physical mechanism, i.e. mechanical and chemical machining effects, respectively. Fatigue testing demonstrated that the occurrence of MD is less critical than WLs, as its impact on fatigue was limited when MD layers thickness was small (up to ~10 μm) [14,29]. Even though its impact on fatigue performance has been reported in the literature, the mechanisms governing MD-induced crack initiation are still not fully understood from a metallurgical perspective. Hence, further research effort should be focused in this sense. Within chemical removal processes, no significant forces or thermal gradient are generated, resulting in a high-integrity micro-mechanical and metallurgical surface condition. In fact, absence of deformation or process-induced RS is observed after ECM. However, ECM surfaces tend to present geometrical defects in the form of corrosion pits and can result in relatively high roughness due to uneven electro-chemical phase dissolution, condition that can be responsible for early crack nucleation by inducing local stress intensifications.

Thus, the relationship between surface integrity, near-surface material behaviour, and the resulting fatigue performance is considered in Fig. 14 for two different classes of machining-induced anomalies, i.e. metallurgical (e.g. material drag or white layers), and micro-geometrical (e.g. corrosion pits or micro-cracks). High lattice distortion occurring in metallurgical alterations such as machining-induced nanocrystalline layers can reduce dislocation mobility, which can in turn affect local yield stress and a induce micro-softening under cyclic loading conditions in plastic regimes [27,79]. However, sharp features such as micro-cracks tips can undergo stress-intensifications that locally lead to early plasticity, even if the constitutive material response can be considered unchanged and under loading conditions that would be otherwise considered below the yield point of a defect-free material. Thus, in the presence of metallurgical alterations (e.g. WLs), the failure mechanism is provoked and potentially accelerated by an altered constitutive response of machined layers, in the absence of significant stress

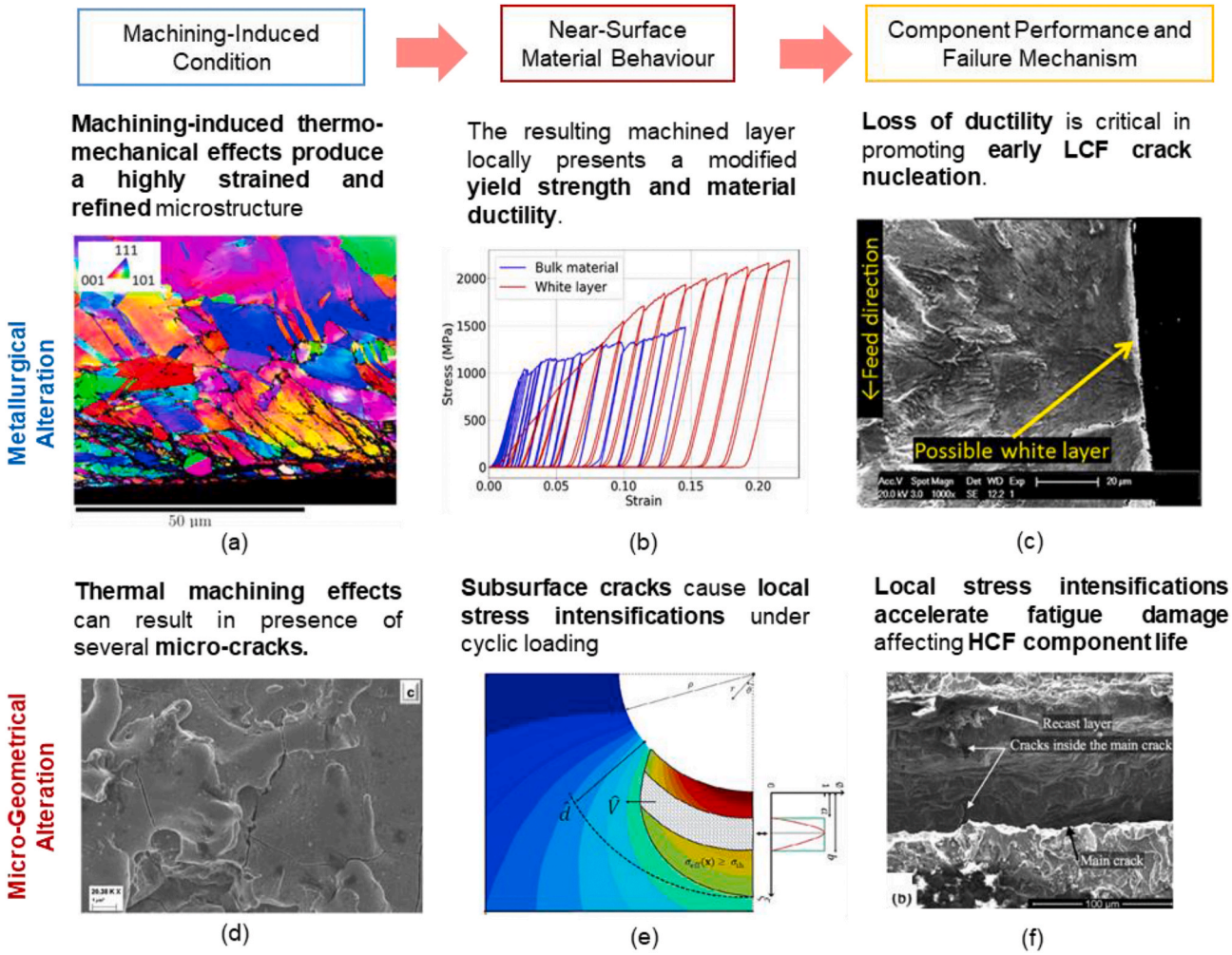

Fig. 14. This figure explores of the link between fundamental surface characteristics induced by machining, machined layers behaviour under loading, and resulting fatigue failure mechanism. (a) Material drag layers generated in a Ni-base superalloy (Inconel 718) [6] significantly alter the near surface metallurgy. (b) Metallurgical alterations can induce a locally different constitutive response, as for the nanocrystalline layers considered in [27]. (c) Different constitutive response of machined surface layers (e.g. white layers) can influence the LCF crack initiation, as shown by fractographic analysis [29]. (d) On the other hand, geometrical anomalies such as EDM-induced micro-cracks [65] will introduce different mechanisms under cyclic loading. (e) In fact, stress intensifications can be induced as a result of machining-induced micro-cracks [80]. (f) Thus, local stress intensifications can promote fatigue failure from micro-cracks populated recast layers [64].

intensification factors. On the other hand, even if machining-induced micro-geometrical features (e.g. micro-cracks) do not significantly affect the material's constitutive response, fatigue crack nucleation can be promoted by a local intensification of the material stress state. Thus, to fully understand the machining-induced fatigue performance of advanced alloys, the failure mechanisms of machined layers need to be investigated in relation to both the physical effects under which they were generated and the environmental loading conditions to which they are subject when in-service.

3. The influence of surface integrity on corrosion resistance of machined parts

Machining processes induce local alterations to the material surface, which could have a detrimental effect on their functional performance both at the micro- and macroscopic levels. These represent a significant opportunity for machining induced defects to impact resistance to corrosive environments. For instance, several industrial sectors require the use of metallic components within corrosive media (Table 2), such as stainless steel (SS) or copper alloys, which are highly employed in nuclear reactors and heat exchangers, respectively. A poor surface integrity in combination with an aggressive environment will result in premature component failure because of machining-induced surface defects promoting corrosion. In some cases, corrosion in critical components (i.e. aircraft structural elements) has resulted in catastrophic failure [81]; therefore, the relationship between surface integrity and corrosion resistance is hugely important.

Corrosion can manifest in a material in various forms (e.g. pitting, crevices, stress corrosion cracking) and the type and extent of surface defect could promote one more than another. Naturally, different machining techniques (e.g. mechanical, thermal, chemical) imply different surface characteristics and hence, result in different mechanisms that alter the corrosion resistance of machined parts, even when referring to the same material. Since corrosion takes place often in combination with mechanical and/or thermal loading complex interactions between these are often observed in application.

As a first instance, many industries rely on the employment of protective coatings (e.g. paint, anodizing) or corrosion inhibitors on metallic surfaces to protect them against corrosion [86] and while this is a practical solution, it cannot be applied in specialist applications nor in situations where the cost or extra-processing steps are unaffordable. In these cases, the metallic surface of the alloy is exposed to corrosive media in a direct contact manner. Thus, the corrosion resistance of the metal plays a more relevant role, and so, the machining effect on corrosion resistance must be revised.

3.1. Influence of mechanical machining on corrosion resistance of metallic alloys

Mechanically machined surfaces associated with cutting or abrasive material removal methods can possess different sub-surface characteristics (e.g. grain size and orientation, residual stresses, hardness) than the bulk material, which translates into different behaviour under a corrosive environment. Hence, the machined near surface can display different corrosion resistance than the bulk material, plus the local machining-induced anomalies (e.g. grooves, pits) significantly affect the local corrosion propagation.

Corrosion damage in a machined surface can be enhanced through various mechanisms, such as hindered oxygen delivery in the pits created by machining which becomes an obstacle for the passivation process in the surface (i.e. difficult to create the associated protective oxide film) (Fig. 15a), formation of intermetallic compounds that act as pitting corrosion sites (Fig. 15b) and stress corrosion cracking (Fig. 15c).

Table 2
Industrially relevant (machined) metals that are usually exposed to corrosive environments.

Metal	Usual corrosive agents
Stainless steels	Chlorides, acid chlorides, high-temperature water [82]
Carbon steels	Alkalis, nitrates, acid gasses (e.g. CO_2, H_2S), water [83]
Copper alloys	Ammonia, biocides [84]
Titanium alloys	Chlorides, bromides, iodides, physiological fluids [85]
Aluminium alloys	Acids, alkalis, salts [81]

3.1.1. Mechanical machining effects on corrosion resistance of aluminium, magnesium and copper alloys

Aluminium, especially the 2XXX and 7XXX series alloys, possess desirable properties for aerospace components [81], plus their auto-passivation protective oxide film generally provides acceptable corrosion resistance to various aggressive environments. In the case of milling AA7150-T651 alloy, the machining process induces dynamic recrystallisation and high plastic deformation in the subsurface, which in this case results in an increased number of grains, which are ultrafine (50–100 nm) and have Mg and Zn alloying elements segregated at the grain boundaries. Elemental segregation in these fine grains favours the anodic behaviour of the machined subsurface, even more than the bulk material [87]. Therefore, in the presence of a corrosive environment, the bulk material remains protected from corrosion via the cathodic protection that the highly anodic machining-induced layer provides. This effect is similar to that of the EWL in Mg-alloys.

Residual stresses in Al-alloys also play a role in corrosion resistance. For instance, a larger tensile strain on the surface facilitates the exposure of the true surface area (i.e. greater width-to-depth ratios of the machining grooves in the surface) with corrosive agents, incrementing the pitting corrosion depth. Thus, large machining-induced tensile stresses compromise the corrosion resistance, while compressive ones enhance it [88]. In the case of Al7050-T7451, for example, a compressive stress of −47.5 MPa on the surface, produced pitting depths of up to 7.5 μm, while a tensile stress of 33.1 MPa resulted in a 59.4 μm depth [88], i.e. about 8 times deeper; however this does not translate to an overall corrosion contribution to failure that is 8 times larger.

Abrasive processes in Al-alloys are commonly employed to achieve a desired surface roughness on machined parts. However, these processes usually leave grooves in the material, whose dimensions depend on the grinding conditions and the grit size. Depending on the topology of the grooves and the true surface area of the surface, the surface will react differently under pitting corrosion. For instance, surface roughness of 2297-T87 Al–Li alloy showed that grooves with small values of width-to-depth ratios ($R_a = 0.918$ μm) promote pitting corrosion (Fig. 16a) due to the hindered access of the reactant element (i.e. oxygen) to the deeper regions of the pits (Fig. 15a). The lack of oxygen is an obstacle for the auto-passivation process, which translates to a failed formation of a robust oxide film in the deeper areas of the grooves. On the other hand, grooves with large values of width-to-depth ratios ($R_a = 0.082$ μm) represent a more uniform surface area (i.e. more true area easily exposed to oxygen), which favours corrosion resistance by hindering pitting corrosion (Fig. 16c) on the surface [89].

Abrasion processes can also stress induce phase transformations. With respect to Al–Li alloys abrasion can induce the presence of AlCuMnFe intermetallic compound on the surface, and while this can be reduced by using finer grit sizes [89], the presence of these compounds on the abraded surface tends to behave in cathodic manner, hence facilitating the initiation of pitting corrosion locally [90] (Figs. 15b and 16d–f). In this type of alloy, the effect of intermetallic compounds on the surface's corrosion resistance is more significant than that of surface roughness alone.

The effect of machining-induced fine grain sizes (or increased grain boundary density) on metallic components has been studied, showing a general good agreement that finer grains increase the corrosion resistance for at least Mg, Al, Ti, Ni, Cu and Zn alloys, with Fe alloys showing either an increase or a decrease that is highly influenced by residual

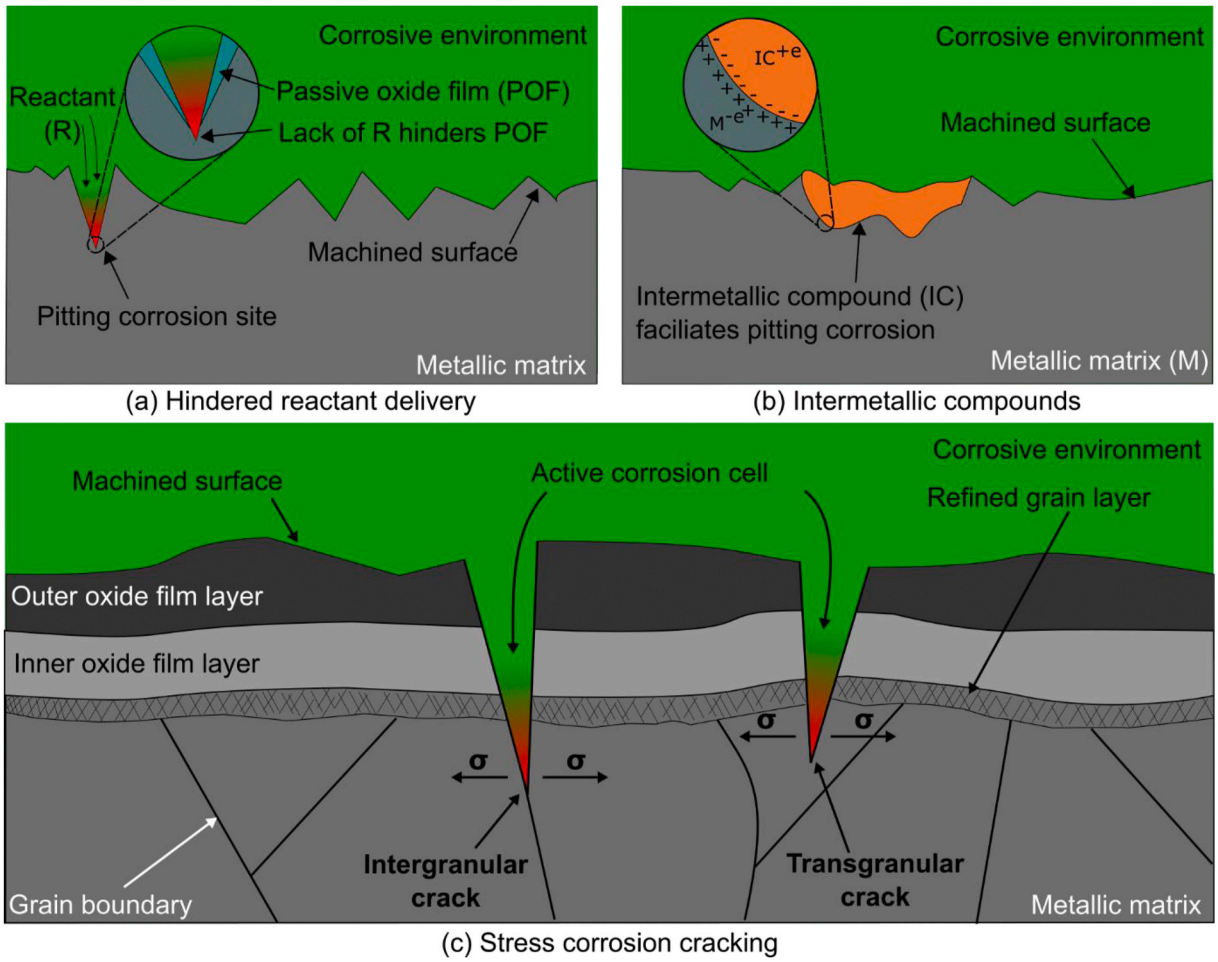

Fig. 15. Corrosion-enhancing mechanisms in mechanically machined surfaces. (a) Large width-to-depth ratios of the surface grooves hinder delivery of the passivation reactant element (e.g. oxygen, nitrogen) to the metallic matrix, which results in a weak passive oxide film that facilitates pitting corrosion. (b) Formation of intermetallic compounds can occur during cutting or abrasive processes. These tend to behave in cathodic manner relative to the metallic matrix, which behaves anodically, thereby facilitating pitting corrosion in these sites. (c) The combination of tensile residual stresses and corrosive media facilitates the propagation of both intergranular and transgranular cracks.

stresses [91]. In copper, for example, a smaller grain size (i.e. 80 nm) hinders the corrosion rate by about 3 times when compared to coarse-grain (i.e. 500 μm) copper in the bulk material [92]. The reason for this is not trivial. The high dislocation density in the crystal structure within the fine-grained region of the material (e.g. machined subsurface) results in an enhanced passive oxide film that is easily produced by the highly-reactive effect that the fine-grain boundaries possess in contrast to coarse-grains and the crystal lattice inside the grains [91,93]. That is, the larger the grain boundary density on the surface, the more reactive the surface will be, and the more susceptible it will be to create an auto-passivation oxide film that protects the bulk material from corroding. This means that the machining and finishing conditions of metallic components can be tailored to produce a desired finer-grain layer that enhances the quality or condition of the passivation layer, thereby producing a targeted corrosion resistance. Nevertheless, this is not extended to all metals, since corrosion resistance is not only dependent on grain size and other aspects such as the cathodic/anodic role of alloying elements must be taken into account.

Magnesium alloys are extensively used in the aerospace, defence, automobile and electronics industries due to their favourable strength-to-density ratio. However, due to their appropriate biodegradation properties, they are also important materials in the medical industry (e.g. temporary implants). Hence, their corrosion resistance in physiological environments is of upmost relevance for a proper understanding of implant in-service lifetime. Similar to other metallic alloys, the machining-induced EWL also manifests in Mg-alloys if the cutting conditions allow [94], producing fine nanocrystallized grains as small as ca. 45 nm [95]. In this case, the EWL can act as a coating that slows down the corrosion rate and displays uniform pitting along the cut surface, but an absence of EWL not only accelerates the corrosion rate, but the pitting occurs in inhomogeneous manner, which could also translate into more noticeable stress concentrators [95], which highlights the importance of assessing and improving the surface integrity using engineering methods. The usage of cryogenic or dry machining in Mg-alloys can significantly alter the EWL in terms of its depth, sub-surface grain size, crystallographic orientation and residual stresses, which finally results in a specific corrosion rate [96]. Hence, the appropriate control of the white layer in Mg-alloys not only yields better corrosion resistance to pitting under physiological environments, but the machining parameters can be tailored to provide a specific corrosion rate that translates into the specific desired implant lifetime before the biodegradation occurs. Nevertheless, since the EWL could have a detrimental effect on other aspects (e.g. fatigue, osseointegration), it is imperative to consider them along with the enhancement of corrosion resistance to make a compromise.

3.1.2. Mechanical machining effects on corrosion resistance of stainless steels (SS)

SS are widely employed in all types of industries due to their excellent mechanical and corrosion resistance properties. Additionally, the

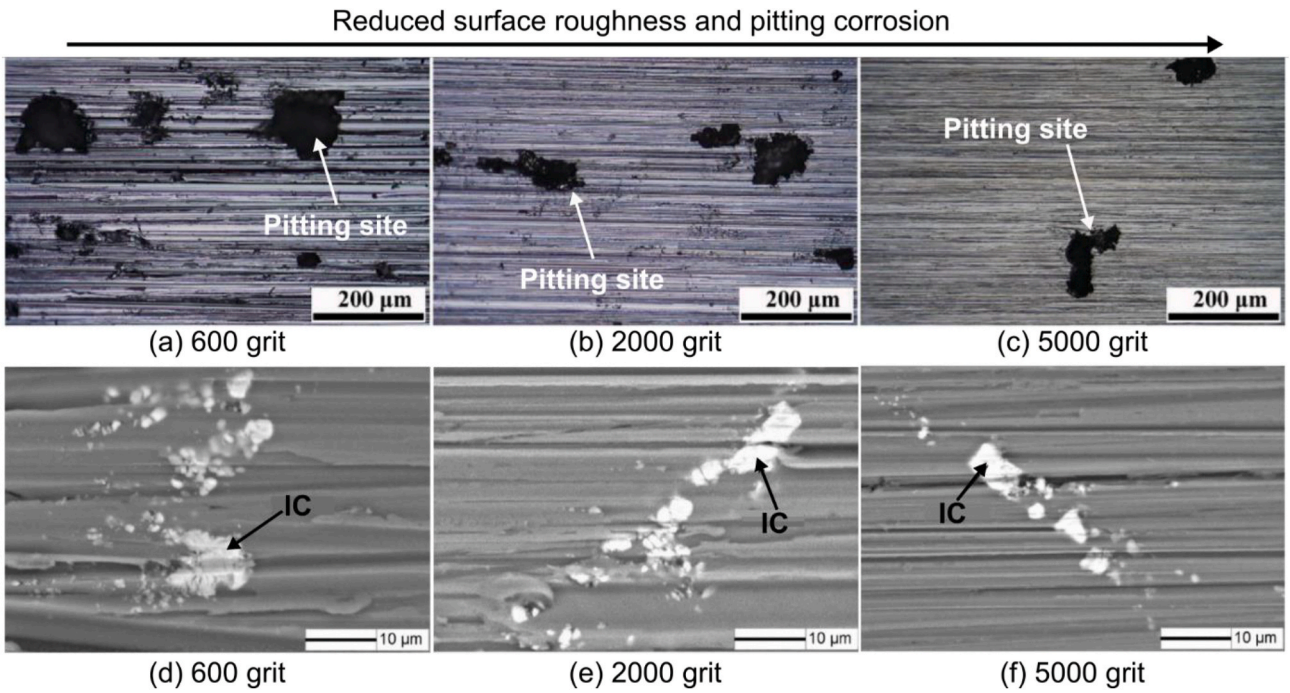

Fig. 16. In their work, Liu et al. [89] **discussed the effect of grooves and intermetallic compounds on corrosion resistance.** Pitting corrosion can be inhibited by: (a–c) reducing the surface roughness in 2297-T87 Al–Li alloy due to the increased exposure to oxygen delivery (i.e. ease of passivation process) in most of the surface, and (d–f) by minimising the formation of intermetallic compounds (i.e. AlCuMnFe) in the surface since these sites act represent a cathode with respect to the metallic matrix (anode).

properties of steels are, generally, well understood under different working environments (e.g. high temperatures, LCF, HCF, etc.) and therefore, they have continued to be rigorously employed in many applications (e.g. nuclear, automotive, aerospace, food, medical). As such, the corrosion resistance of these materials under various environments has been thoroughly studied and related to the machining characteristics that produced them.

It is well known that aggressive machining conditions may result in an EWL that exhibits superior hardness than the bulk material [34] and under some cutting or grinding scenarios, intermetallic compounds may appear on the surface [90]. Pitting corrosion has been reported to be more susceptible in hard surfaces [97]and in local intermetallic compound clusters along the cut surface [98] (see Figs. 15b and 16d–f), in low carbon martensitic SS and super duplex SS, respectively.

Machining and grinding operations significantly alter the passive oxide film of austenitic SS. For instance, the as-machined passive oxide films in these alloys are composed of an outer and an inner layer, with the first being composed of single oxide particles rich in iron, i.e. orthorhombic magnetite (Fe_3O_4), and the second one being chromium-rich [99] with the most stable oxide being chromite ($FeCr_2O_4$) [100]. The thickness of each passive layer is affected by the machining process, showing that, in general, a rougher surface (e.g. as milled) possesses a thicker non-uniform inner layer with low chromium and high molybdenum concentrations, whereas a smoother surface (e.g. electro-polished) exhibits a thinner, uniform inner layer with high chromium and low molybdenum content (Fig. 17) [99]. This occurs since the diffusion rate of ions at the grain boundaries is much larger than in the crystal lattice, therefore the larger grain boundary density in the machined surface (i.e. compared to a polished one) results in an increased outward diffusion of metal cations and inward diffusion of oxygen [99], thereby promoting passivation.

Furthermore, electrochemical tests performed in a 52100-steel showed that the EWL possesses more anodic potential than the bulk material, which facilitates metal ion diffusion in the as-cut surface, hence increasing the corrosion rate of the material. Additionally, discontinuities and defects within the top surface of the EWL work as local anodic and cathodic areas that facilitate corrosion [101] due to their increased capability for ion diffusion.

Stress corrosion cracking (SCC) is a major concern in SS, since the combination of an aggressive media (e.g. chlorides [82]), high temperatures and tensile stresses provide a favourable scenario for surface defects (e.g. grooves, pits, microcracks) to act as precursors of cracks that are prone to propagate into the material [102]. In the case of austenitic SS, machining induces high levels of plasticity and work hardening in the subsurface, which is a characteristic feature of the EWL [34]; this produces a shift from austenite in the coarser-grain matrix to martensite in the fine nanocrystal grains in the highly deformed sub-surface [15]. Martensite possess less corrosion resistance than austenite; hence, SCC is more susceptible to occur faster in as-machined surfaces with stress-induced martensite within the subsurface [15]. Any surface defects will work as starting points of SCC [103], with the principal propagation direction being mostly driven by the stresses in the subsurface. For instance, SCC cracks tend to follow surface defects (e.g. grinding groove direction, feed marks) [102,104], regions with high dislocation density [15], through the grain boundaries (i.e. intergranular propagation) [105,106] and through the grains (i.e. transgranular propagation) [107]; refer to Fig. 18 and Fig. 15c. It has been reported that under a chloride environment, if tensile residual stresses exceed 190 MPa in 316 SS, SCC will occur, with cracks propagating more rapidly at increased values of stress [103]. However, the role of tensile stresses in SCC in 316L SS is less significant in non-chloride corrosive environments (i.e. slow strain rate testing in high purity water) [108], which proves that the SCC phenomena in SS is a complex issue that depends not only on the material and machining characteristics, but also on the environment and working conditions.

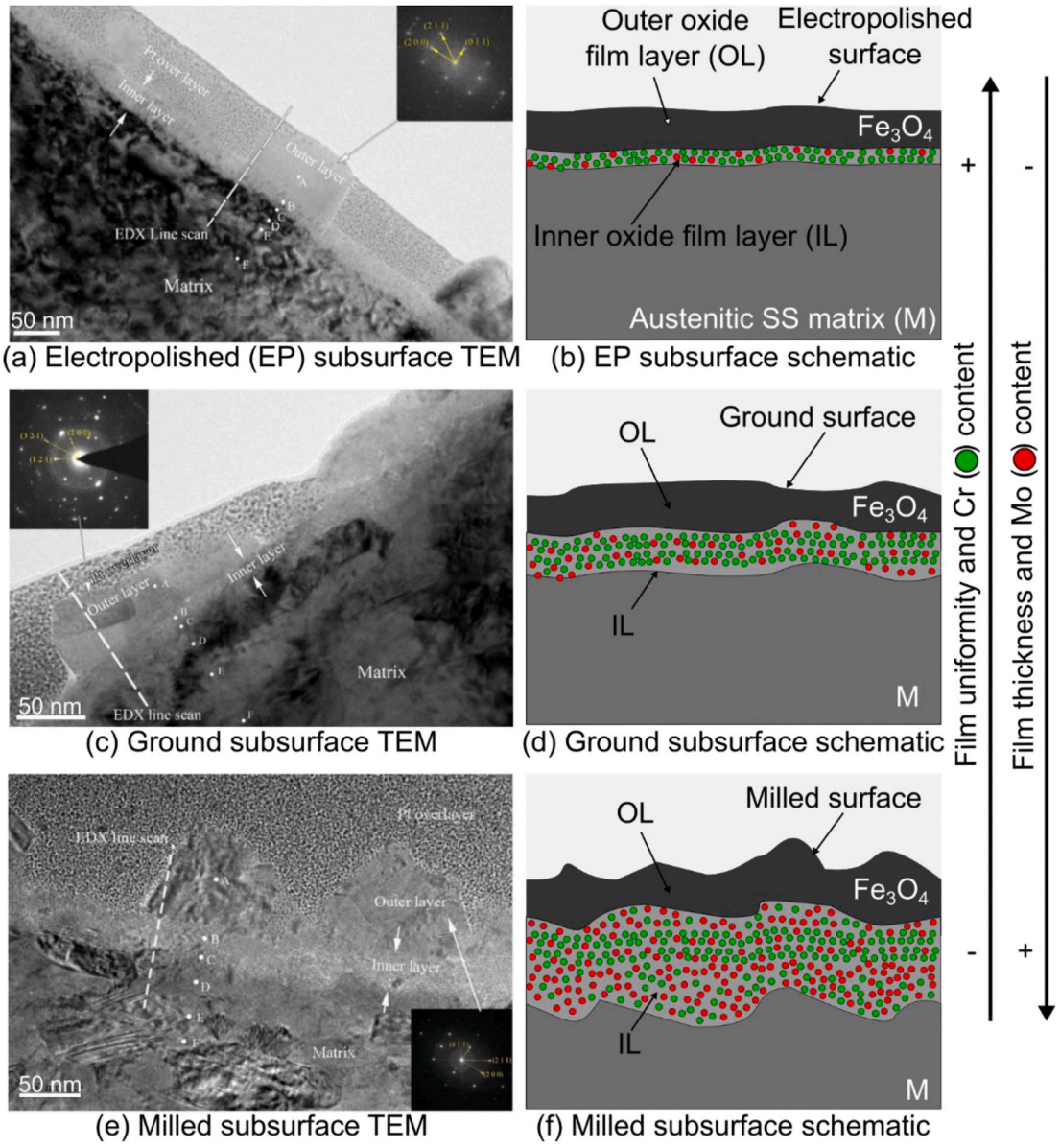

Fig. 17. Different surface preparation methods produce variations in the passive oxide film layers in austenitic steels. According to their work, Wang et al. [99], showed via TEM end EDX the characterization of the passive films after different surface preparation methods (a,b) Electro-polishing resulted in a thin (ca. 10 nm). Cr-rich (green colour) inner film, with a smooth surface. (c,d) Grinding produced a thicker film with increased roughness and heterogeneity (e,f) Milling yielded the thickest (ca. 30 nm). and Mo-rich (red colour) film with the roughest surface. (For interpretation of the references to colour in this figure legend, the reader is referred to the Web version of this article.)

3.2. Influence of thermal and chemical machining on the corrosion performance of the components

3.2.1. Influence of thermal machining processes on the corrosion mechanisms of machined parts

Non-contact thermal machining methods, such as those employing energy beams or discharges, do not remove material by mechanical shear, and therefore do not affect surface integrity in the same manner as conventional machining processes. However, the heat-affected regions associated with thermal processing methods, such as recast layers, change the chemical and mechanical condition of the near-surface material, and can significantly impact corrosion resistance and the mechanisms through which corrosion progresses. As such, there is an overall desire to limit recast layer depths. Thermal methods, such as electrical discharge machining (EDM) and laser beam machining (LBM), are widely used for subtractive machining and shape-generation in high-value manufacturing of parts designed for use in corrosive environments, in marine, biomedical, and aerospace applications [109]. This section will explore the types of defects associated with thermal processing and understand the role in which the transformed surfaces influence mechanisms of corrosion. Fundamentally, the processes resulting from the input of thermal energy into the material, for example melting and solidification, lead to distinct metallurgies, local compositions, and stress distributions from the bulk material [110]. This depends on cooling rates that are influenced by the input energy, the material, and the machining environment. The resulting differences in chemical and mechanical properties can enable different corrosion mechanisms. These compositional changes can affect corrosion resistance, among other properties.

Corrosion is broadly understood to be initiated at active pitting sites, such as regions of relatively high surface free energy, like pre-existing cracks, oxide layer defects/discontinuities, and some types of grain

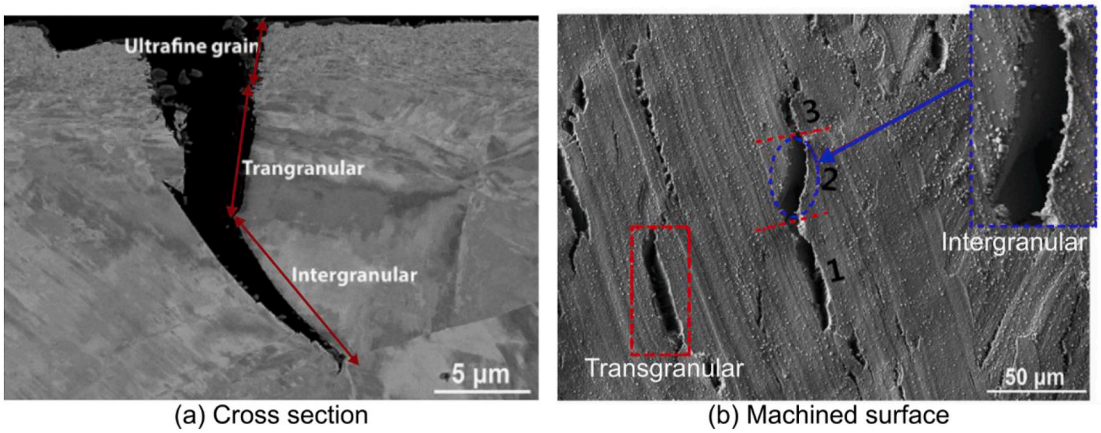

Fig. 18. Stress corrosion cracking (SCC) mechanisms in a machined metallic component. In their work on 304L SS, Chang et al. [107] show that after being machined and immersed in high temperature hydrogenated water at slow tensile strain rates (i.e. 10^{-5} s^{-1} followed by 2×10^{-8} s^{-1}), SCC occurs with cracks that propagate either in the trans- or intergranular directions, as shown in (a) the cross section, and in (b) the machined surface.

boundaries. This is relevant as both EDM and LBM can lead to micro-crack formation in recast layers, depending on cooling rates that can be up to 106 K/s in EDM [111]. Surface micro-cracks generally form in regions of tensile residual stress, which are caused by material volume contraction upon cooling; this facilitates the activation of corrosion sites over the material surface. The high aspect ratios of micro-cracks compared with non-cracked surface topographies lead to discrete internal chemistry [112]. This activates the metal surface to further attack. In such cases, metal atoms are oxidised to their respective cations, which draws corrosive anions to the local crack zone as the system works towards electro-neutrality. Complexed metal-anion species react with water to form generally insoluble metal hydroxides and increase the concentrations of protonated species like H3O+, acidifying the local environment. Local acidification also provides a reducing chemical environment that inhibits the formation of metal oxide species that may offer passive protection and de-activate the corrosion site. This accelerates the local corrosion rate (Fig. 18a).

In some cases, the existence of tensile stresses within recast layers can lead to stress corrosion cracking (SCC), depending on temperature, the chemical environment, and the material. In SCC, the propagation of cracks occurs below the yield strength of the material and within a chemical environment that would normally be considered benign towards the unstressed material. While the initiation phase is considered to be purely electrochemical as previously discussed, the propagation stage is also caused by strain localisation at the crack tip. This can lead to deformation of the surrounding material, propagating the crack perpendicular to the tensile stress field (Fig. 19b). Corrosion reactions that also evolve hydrogen gas can further embrittle the local area. These enable reactions within the material, ahead of the crack tip, dependent on the solid-state diffusion of hydrogen through the material. Amelioration of tensile residual stresses by annealing will reduce SCC mechanisms, however this may not be practical in all cases. Poorly controlled recast layer solidification can result in local compositional differences as certain elements are rejected from dendritic core areas into the inter-dendritic regions. In the context of high-performance alloys and steels, certain elements are incorporated in concentrations designed to improve the corrosion resistance, for example Cr in steels and Ni-alloys, however local compositional differences can enable corrosion, where locally depleted elements are responsible for corrosion-resistant properties. In this case, the formation of Cr-carbide compounds locally deplete solid-solution Cr, sensitising the grain boundaries, enabling inter-granular corrosion (Fig. 18c). Furthermore, compositional differences within the recast layer and between the bulk material and the heat-affected layers can result in the formation of micro-galvanic corrosion cells within the material. Local compositional differences can arise from i) the vaporization of more volatile elements upon thermal activation, ii) solid-state diffusion of elements through heated regions, iii) precipitation and rejection from the melt upon solidification. The created galvanic couples can exaggerate corrosion effects, removing the anodic material and exposing additional routes to failure (Fig. 18d) [113].

Techniques to reduce corrosion in thermally processed surfaces such as recast layers include annealing to reduce SCC mechanisms, post-processing steps to remove micro-cracks and areas of compositional difference, and appropriate parameter selection to control changes in metallurgy and stress condition during processing. While chemical coatings may be applied to enhance the corrosion resistance of machined surfaces, these cannot be applied to all surfaces and parts in all applications, for example those used under high thermal and mechanical loading conditions.

3.2.1.1. Influence of electrical discharge machining on the corrosion mechanisms of machined parts. In addition to compositional changes caused by thermal energy input, contamination of resulting surface layers can arise from the process and from material originating from both the dielectric fluid and the tool electrode in EDM [59]. These can alter the corrosion resistance. Both positive and negative influences on corrosion-resistance have been reported after EDM when compared with un-machined materials; the positive effects largely being attributed to grain refinements associated with the recast layer and integration of corrosion-resistant materials into the recast layers. Conversely, poor surface integrity like micro-cracks arising from EDM can accelerate corrosion mechanisms to occur over common manufacturing timescales, if the machined part is left submerged in dielectrics like deionised water. This can enable the formation of a galvanic cell between the workpiece and the vice, depending on the material type [114].

While Ni-superalloys possess desirable elevated temperature properties facilitating their application in turbomachinery, under extreme operating conditions the aforementioned material modifications in EDM recast layers can affect the corrosion resistance in comparison to bulk materials. For example, Wang et al. [115] found that the structural defects like cracks within EDM recast layers in Inconel 718 enabled the corrosion of EDM recast layers, while not affecting the bulk material, in a phosphoric acid and hydrochloric acid mixture. Corrosive liquid penetration through the crack networks enabled the separation of the recast layer from the bulk material (Fig. 20a), leading to a significant reduction in recast layer hardness after corrosion (<10 HV), compared to beforehand (450 HV). Hertweck et al. [116] also reported lower corrosion resistance of EDM recast layers in Inconel 718, compared to the un-machined material, after exposure to an acidic ammonium chloride environment. The authors reported Cr-depletion, as well as Cu

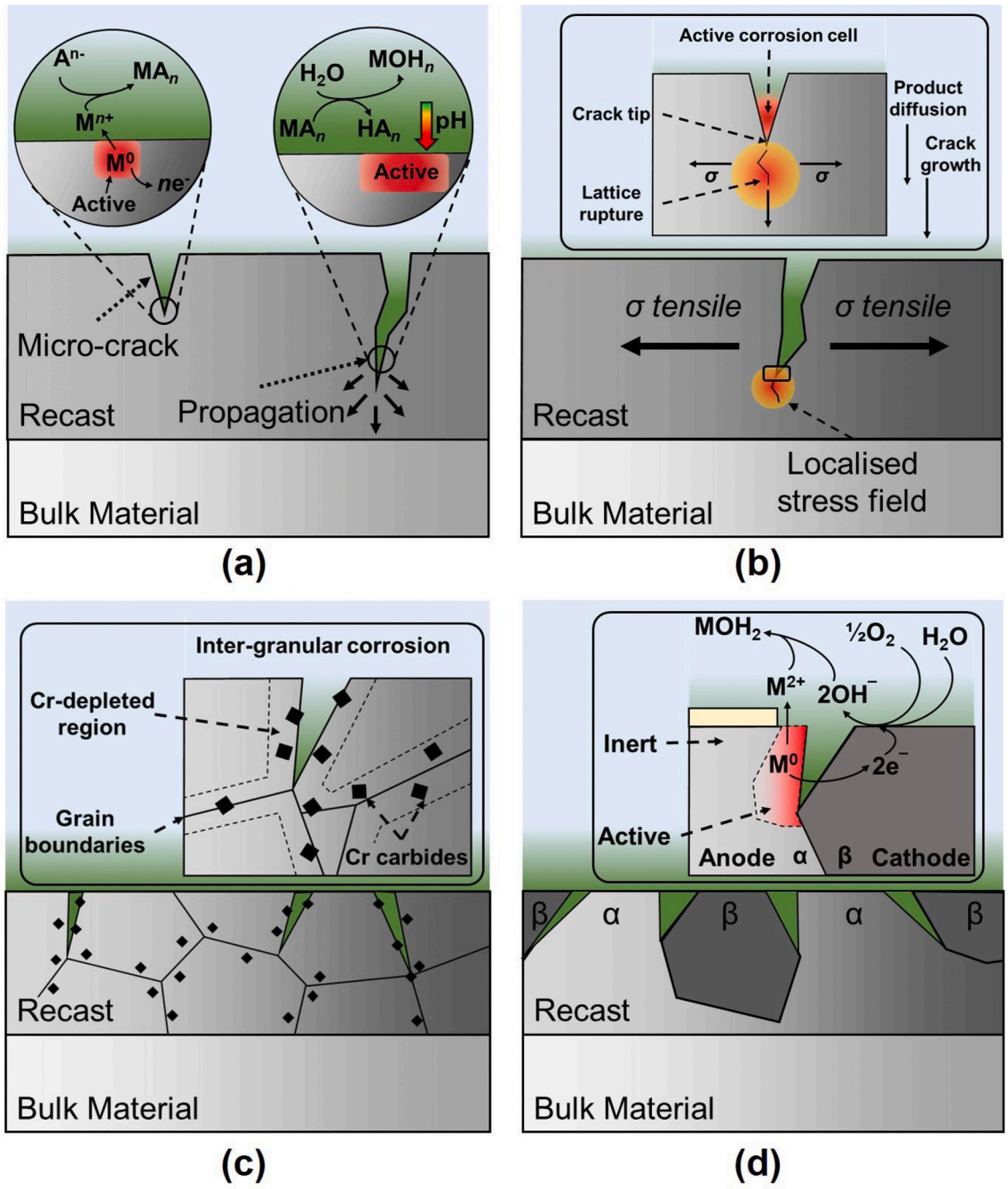

Fig. 19. Corrosion-enhancing mechanisms in thermal machining (EDM, LBM, etc.). (a) Thermally-induced micro-cracks present surface defects: i) active dissolution leads to metal loss resulting in cation formation, electrostatically attracting aggressive anions, ii) water reacts with metal anion complexes forming hydroxides and acidifies the local chemistry, activating the surface. (b) The existence of tensile residual stresses in thermally-affected layers can lead to SCC. (c) Grain boundaries can be sensitised by carbide formation, leading to inter-granular attack. (d) Compositional differences can lead to galvanic couples in the material.

and Sn, and surface cracking from the recast layers after corrosion, the latter possibly influenced by residual stresses within the layer. In loading environments, EDM-processed slits have been used to validate mechanistic understanding of SCC, for example in Ni-based Alloy 600 [117].

It follows that surface and sub-surface cracks are largely responsible for the generally inferior corrosion resistance of EDM surfaces compared with the un-machined material, especially under tensile loading conditions [119]. However, the EDM dielectric can influence both grain morphologies [120] and metallurgical transformations in Ni-superalloys associated with local compositional differences. The dielectric presents an additional route through which the chemistry of the recast layers can be modified or contaminated during machining. For example, Cr-depleted regions in EDM recast layers of Hastelloy X have been observed after subsequent heat treatments after machining with both deionised water and with kerosene [121]. In this study, Cr-depletion was associated with the formation of Cr2O3 phases upon machining with deionised water and high-order Cr-rich carbides (e.g. M23C6) when machining with kerosene. Local Cr-depletion is known to enable corrosion mechanisms such as sensitisation (Fig. 18c), and requires further investigation. The EDM tooling can also influence the recast layer composition, where additional elements can be alloyed with the surface layer to affect the corrosion and oxidation resistance. For example, Bai [118] used an Al–Mo composite electrode to modify the surface of Haynes 230 Ni-superalloy. The authors showed that using an

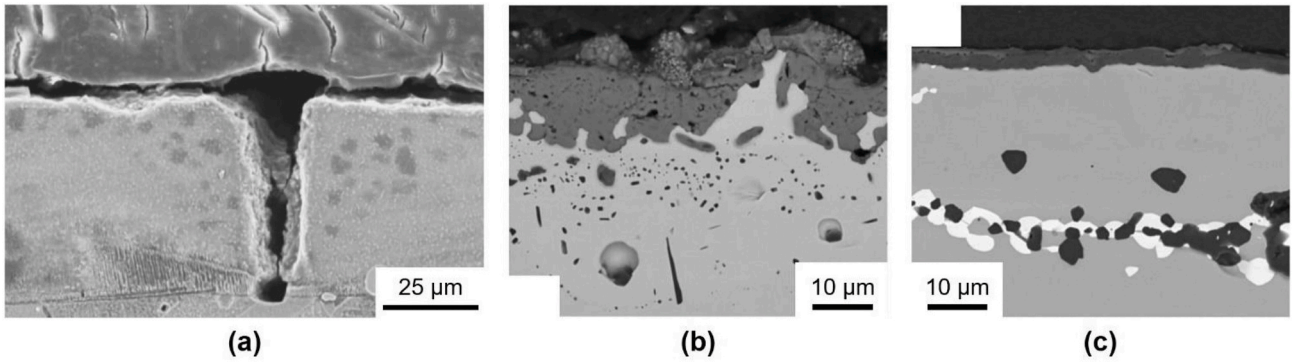

Fig. 20. Corrosion and oxidation in sectioned EDM recast layers of Ni-alloys. (a) Sectioned micro-crack in Inconel 718 showing corrosion through to the bulk material. (b) BSE micrograph of recast of unalloyed Haynes 230 exposed to air at 1100 °C (600 h) showing discontinuous oxide scale. (c) BSE micrograph of the same material processed with Al–Mo anode tool electrode, showing continuous Al_2O_3 protective surface oxide layer. (a) From Wang et al. [115], (b)–(c) from Bai [118].

anode tool electrode could improve oxidation resistance, while a cathodic tool decreased the oxidation resistance, in comparison to the unprocessed material. This was a result of the beneficial dense and continuous Al2O3 scale in the former, while the latter resulted in Ni- and Cr-oxides and discontinuous topographies leading to worse internal oxidation when compared with the unprocessed superalloy (Fig. 20b-c).

The limited number of studies appraising the effect of the EDM process on the resulting corrosion resistance in Ni-superalloys appears to result from the fact that common EDM surface defects, like micro-cracks and secondary phase formation, which accelerate corrosion also influence other failure modes, such as fatigue. Therefore, despite EDM being widely employed in turbomachinery manufacture, for example cooling holes, the associated recast layers are generally removed before application [122]. Accordingly, the susceptibility of Ni-alloy EDM surfaces to application-specific mechanisms, such as hot corrosion (650–950 °C) [123], is yet to be investigated.

Both the high specific strength and innate corrosion resistance drive selection of Ti-alloys for aerospace and biomedical applications. Corrosion resistance occurs by the formation of tenacious passive TiO2 oxide layers under ambient conditions, which prevent further oxidation and corrosion. However, EDM has been shown to decrease the corrosion resistance in comparison to conventionally finished surfaces, for example in commercially pure Ti (cp-Ti) in simulated biological environments [124], relevant for load-bearing parts applied *in-vivo*. In addition to surface cracks, crevices and pores, this could also be influenced by the incorporation of material from the EDM tool electrode into the recast layer. For example, Cu has been shown to influence the composition of the layer and the surface oxide films in cp-Ti [125]. Conversely, in the case of β-Ti alloys, the EDM surface layer has been shown to decrease the rate of corrosion in comparison to the un-machined alloy [126], which was attributed to the incorporation of Ti-, Nb, and Zr-oxides into the recast layers resulting from interactions with the deionised water dielectric. Corrosion resistance could be further improved by the incorporation of hydroxyapaptite phases into the dielectric. Other powder additives within the dielectric have been shown to alter the corrosion resistance of EDM surfaces. For example, when machining γ-TiAl materials, powder additions of graphite and Cr have been shown to improve corrosion resistance, while Fe and Al powders reduce corrosion resistance when compared with the EDM surface [127].

Steels and stainless steels are widely applied in corrosive environments throughout industry and can be conveniently machined using EDM. However, the precise influence of the EDM process on the corrosion resistance of steel is challenged by the broad range of steel types, compositions and metallurgies, in addition to the array of EDM processing parameters. For example, Uno et al. [128] reported a smaller equilibrium potential, correlating with a greater corrosion resistance, during linear sweep voltammetry experiments for an EDM-processed surface in comparison to the ground material, in this case mould steel. In addition, the authors noted lower rust formation in the EDM-processed regions of a sample left for 1 year under atmospheric conditions (Fig. 21a). It should be noted that the initial EDM surface appeared to have low density of micro-cracks, which likely aided corrosion resistance (Fig. 21b).

Conversely, Sidhom et al. [129] reported that the surface effects caused by the EDM process, including surface cracks, facilitate pitting and crevice corrosion compared with the bulk material (stainless 316L). In addition, the authors noted sensitisation that led to the preferential dissolution of inter-dendritic areas (Fig. 21c) due to Cr-depletion, caused by Cr7C3 formation at high temperatures (Fig. 21c-d). Furthermore, the combination of tensile stresses resulting from rapid cooling and exposure to chloride enabled SCC of the EDM surface (Fig. 21e-f). Bhattacharya et al. [130] demonstrated that EDM surfaces of P91 steel were uniformly corroded in comparison to the diamond polished material, where corrosion was localised at the grain boundaries. The authors studied the recast layer, reporting grain refinement and a reduction in the formation of carbides, restricting inter-granular corrosion. However, the presence of micro-cracks accelerated corrosion in acidified chloride environments.

Al-alloys are applied where weight minimisation and corrosion resistance are desired. The corrosion resistance arises from the strong affinity towards oxygen, which leads to surface passivation, similar to Ti. Cracking and other defects associated with EDM can affect the integrity of these passivating layers and decrease the corrosion resistance. Compositional changes caused by EDM, and specifically the incorporation of tool electrode material into the recast layers, have been shown to decrease corrosion properties over a range of Al-alloys. For example, Arunachalam et al. [113] showed that the incorporation of Cu electrode material into the recast layer increased the corrosion potential compared with the milled surface, implying that these could act as a galvanic couple, accelerating corrosion. The authors reported corrosion potential and rates an order of magnitude greater than the comparative milled surfaces in the same alloy, for example corrosion rates of 0.330 mm/year were reported for 2024-T351 Al-alloy, when compared with the milled material (0.005 mm/year). The type of intermetallic formed within the recast layers of Al-alloys has also reported to affect corrosion resistance. In an investigation by Pujari et al. [131], the presence of AlCu3-phase promoted galvanic corrosion mechanisms in comparison to AlCu-phase; where the formation was influenced by the EDM parameters. In addition, compositional changes can also be designed using appropriate EDM tooling to improve this aspect of surface integrity. For example, Stambekova et al. [132] alloyed the EDM recast layers using a Si tool electrode to generate Al–Si alloyed regions, and showed that the resulting recast layers possessed similar corrosion resistance to the un-machined base material (5083 Al-alloy).

The literature has indicated that the corrosion resistance of materials

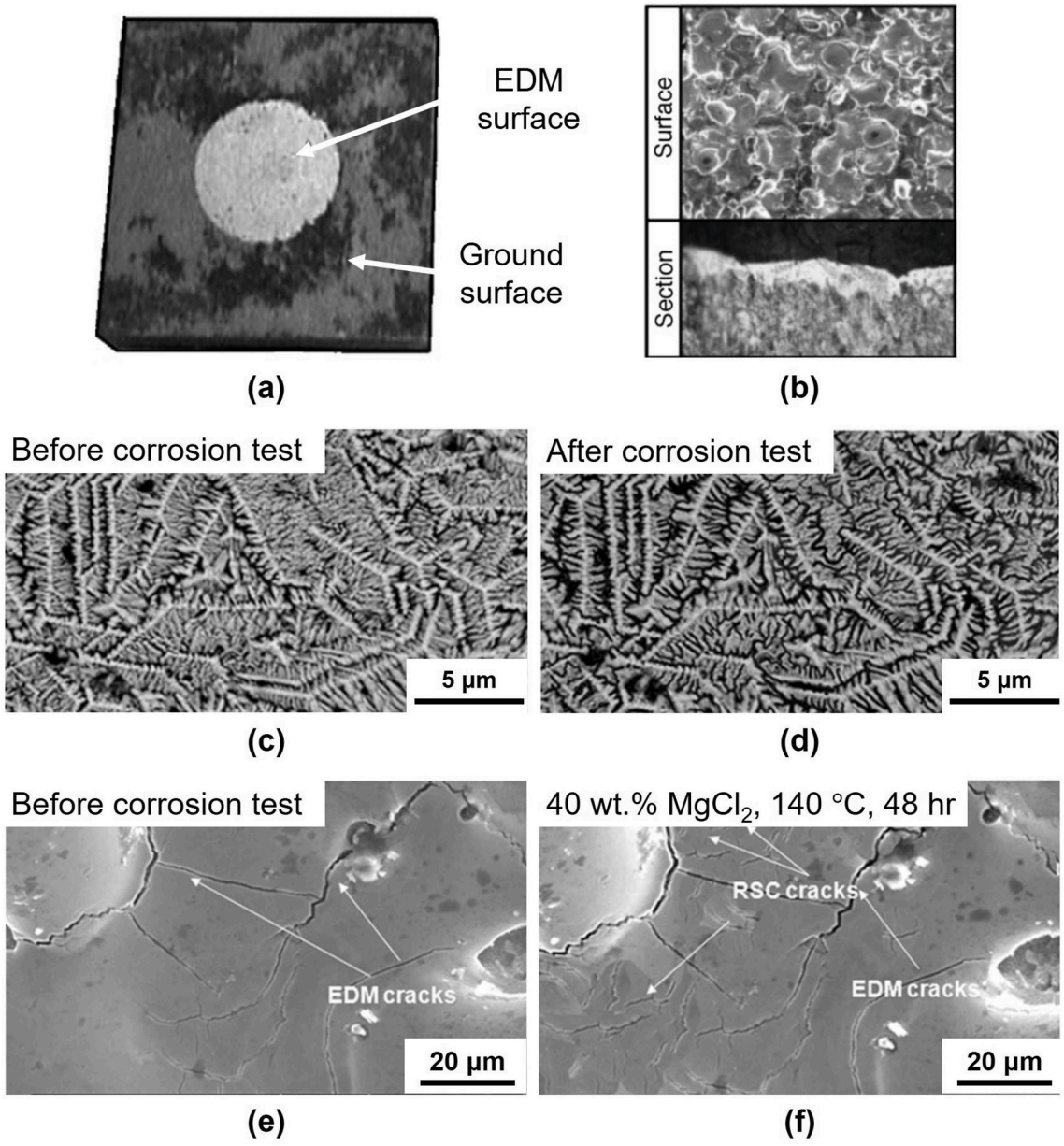

Fig. 21. Corrosion in EDM-processed steels. (a) EDM pocket manufactured in AISI steel showing less corrosion than the ground material under ambient conditions (1 year exposure), (b) recast layers appear relatively free from micro-cracks. (c) Dendritic recast in 316L stainless before, and (d) after corrosion testing, showing removal of the inter-dendritic regions. In the same material, (e) primary EDM micro-cracks, and developed SCC networks after exposure to high chloride environment (140 °C, 48 h). (a)–(b) Taken from Uno et al. [128] (c)–(f) taken from Sidhom et al. [129].

can change significantly after EDM. Differences have been associated with cracks, tensile stresses, and compositional changes. Compositional control is challenged by submersion of the workpiece in dielectric media and incorporation of tool electrode material into the recast layers, which has been reported to enable micro-galvanic corrosion. However, both positive and negative impacts on corrosion resistance have been reported, depending on the material and machining conditions. It should be noted that i) EDM-processed materials are almost never applied in high-loading applications without subsequent treatment, like recast layer removal, and ii) corrosion resistance is often measured in laboratory conditions, where the chemical environment is not necessarily representative of the chemical environment in which the machined part will be applied. As such, more investigations are required to understand the nature of EDM surface defects on corrosion resistance, and how the EDM process can be adapted to inhibit defect formation, in the context of the application as well.

3.2.1.2. Influence of laser beam machining on the corrosion mechanisms of machined parts. Generally, the effect of laser energy on corrosion resistance is influenced by heat input and laser pulse duration, where relatively long pulse durations lead to extensive heat conduction away from the machining zone and the development of heat-affected layers and associated stress distributions, and recast layers. Conversely, ultra-short pulses (e.g. femtosecond order of magnitude) may not allow significant heat conduction into the workpiece, and removal occurs by near immediate vaporization and plasma debris formation [133]. As a result, metallurgical and compositional changes to the near surface can largely be avoided when applying fs-pulses, and the changes to corrosion resistance can be avoided. Exceptions to this exist where pre-existing residual stresses in the near-surface of a workpiece are removed upon fs material removal, where the corrosion resistance will tend towards that of the underlying bulk material. However, for macroscale machining operations in LBM, >ns-pulse or even continuous mode

high-power laser operation are often applied [134], leading to the metallurgical and structural changes that can influence corrosion behaviour. Despite this, it is challenging to understand the influence of a given microstructural change on the corrosion resistance, for example changes to the grain size have been reported to both enhance and diminish corrosion resistance depending on the material and the range of grain sizes investigated [91]. In addition, the direct application of energy in gaseous or vacuum environments restricts surface layer contamination to that originating from the working atmosphere in LBM. Alternate gas environments, such as inert Ar or high-vacuum conditions can reduce oxide formation, where the material has a strong affinity to oxygen, such as in the case of Ti-alloys [135]. However, the presence of thermodynamically and/or kinetically stable oxide phases within LBM recast layers has in some cases been shown to improve corrosion resistance. Many investigations regarding the corrosion resistance of laser-processed materials concern both laser beam welding (joining methods) and selective laser melting (additive manufacturing methods) rather than LBM. The relatively small number of studies pertaining to LBM is related to the fact that as a machining method, finishing processes are generally applied to remove thermally-affected layers, especially in safety critical applications, thus making protracted corrosion experiments somewhat redundant.

This is generally the case for Ni-superalloys that are widely applied in high-temperature and high-loading conditions and in corrosive environments. In most safety-critical applications, like gas turbines, the existence of thermally-affected surface layers such as recast are unacceptable from a fatigue (Section 2) and corrosion fatigue [136] perspective, and therefore great care is taken to ensure removal of these near-surface layers resulting from LBM prior to application. Accordingly, there is a limited amount of literature regarding the corrosion performance of LB-machined Ni-superalloys. Furthermore, such materials are often applied in service with additional coating layers with stable oxide compositions (e.g. yttrium-stabilised zirconia), which offer protection from corrosion, particularly at elevated temperatures. However, in other load-bearing Ni-alloy material systems, for example NiTi-alloys that have potential application in biomedical implants, corrosion performance upon laser processing has been investigated given the physiological effects associated with *in-vivo* Ni-ion release. In NiTi alloys, the affinity of Ti to oxidize to TiO2 has been exploited in laser material removal and processing techniques creating passive phases in the near-surface that can improve the corrosion resistance [137]. For example, Man et al. [138] reported a higher concentration of TiO2 and a higher Ti/Ni ratio upon laser surface melting of NiTi, which the authors considered was responsible for the increased corrosion resistance in NaCl (3%) solution. Subsequently, Micheal et al. [139] showed that the crystallinity of resulting surface oxide phases upon laser processing of NiTi increased with increasing pulse numbers, caused by increased heat input. The authors indicated this increase in crystallinity and associated conductivity was partially reducing corrosion resistance. This could be negated with appropriate post-processing.

The widespread application of Ti-alloys as a biomedical implant material and the health implications of in-vivo corrosion mean that corrosion behaviour of thermally machined Ti-alloys is often appraised in biologically simulated solutions. This is relevant for LBM operations that offer a convenient route to remove, rapidly and selectively, material for *bespoke to patient* implant creation. The reactivity of Ti and its alloys means that LBM operations are often undertaken in inert environments to retain surface integrity, and specifically corrosion resistance. For example, by Shanjin and Yang [140] investigated different assist-gases (air, N2, Ar) in the cutting of Ti-alloy TC1. The authors showed that surface cracking caused by both tensile cooling forces and brittle Ti-oxide and nitride reaction products in the case of air- and N2-assisted cutting severely limited the corrosion resistance of the HAZ upon exposure to an acidic chemical environment (HF/HNO3) compared with TC1 cut with Ar assist gas (Fig. 22a-c). Application of laser energy can improve corrosion resistance of Ti-alloys under appropriate parameters. For example, Sun et al. [141] reported the absence of pitting corrosion on the laser remelted (Ar-flushing gas) surface layers of cp-Ti and a higher electrochemical impedance compared with the base material. The authors proposed that this improvement to corrosion resistance was obtained due to microstructural changes, specifically acicular α' martensite, brought about by rapid cooling and solidification. Conversely, Gil et al. [142] laser processed both α- (cp-Ti) and α-β (Ti–6Al–4V) Ti-alloys in an Ar environment and performed corrosion tests in a simulated biological solution. In both cases, the laser processed samples showed slightly reduced corrosion resistance, which the authors indicated was a consequence of the induced residual stresses (in comparison to the control that had slight compressive residual stress), grain refinement, and other microstructural changes. Similarly to Ti-alloys, the affinity of Al to form thermal oxides represents a route through favourable corrosion resistance of laser processed Al-alloys has been enhanced upon laser processing [143]. Similarly, AlN surface phases have been reported after processing with N2, which alongside microstructural refinement, was reported to lower corrosion current densities [144].

The corrosion resistance of stainless steels results from the formation of passive layers of Cr- and Ni-oxides that form under ambient conditions that protect the bulk material. As such, changes to the composition and electrochemical structures of these surface layers upon heating can influence the corrosion resistance. Deleterious effects can be negated at ultra-short processing regimes, for example Valette et al. [145], applied fs-range laser pulses (10–15 s) to engrave both martensitic (Z30C13) and austenitic (316L) stainless steels. The authors reported lower susceptibility to corrosion for both materials after fs-laser processing, which the authors correlated with solutionising of metal carbide (M23C6) phases and partial transformation of the near surface from martensite to austenite in the case of Z30C13. The mechanism is somewhat unclear given the pulse times were significantly lower than those required for meaningful effect on diffusion. However, the pre-existing stress condition was not measured before laser processing. At much longer pulse durations (10-2 s), Pieretti et al. [146] reported that highly defective laser-machined surfaces resulting from engraving operations in stainless steel F139 resulted in increased corrosion susceptibility when exposed to phosphate buffered saline solution, even at open circuit potential. XPS

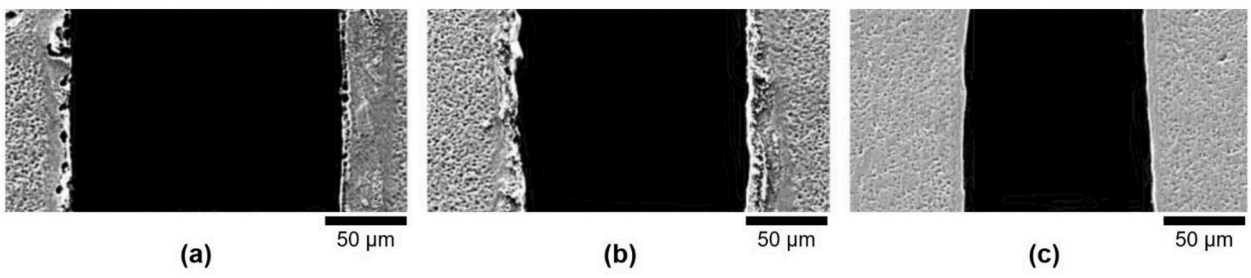

Fig. 22. Acid-etched (HF/HNO3) laser cut TC1 sheet with different assist gases: (a) air, (b) N2, and (c) Ar. Corrosion of recast layer is reduced on Ar flushing. Taken from Shanjin and Yang [140].

studies indicated Ni-depletion in the near-surface layers, while the electron donor defects where shown to increase on laser processing. The latter facilitates ion transport through the passive film and ultimately film breakdown. Furthermore, reattached melt material was shown to dissolve actively at open circuit potential and initiate crevice corrosion. Similar increases in corrosion susceptibility upon laser material removal have also been reported in 304 stainless steel, wherein corrosion resistance was improved where surface ferrite and oxide-phase concentrations were reduced. This was achieved at lower heat inputs [147].

Other microstructural and compositional changes have been shown to influence the corrosion resistance of steels after LBM, for example Wang et al. [148] reported differences in corrosion potential when machining 305 stainless steel with different assist gases (O2, Ar, N2). The authors observed increased nitrogen concentrations in the recast layers in the order O2<Ar < N2, and corresponding increases in corrosion resistance, although the microstructural morphologies were not shown to change. The authors proposed that sulfide inclusions that are known to initiate corrosion pitting in steels were redistributed and reduced from the near-surface upon LBM,

Ferrous alloys are susceptible to SCC, particularly in the chloride-containing chemical environments to which they are often applied, for example marine and nuclear applications. The tensile surface stresses within the near-surface layers that can arise from LBM can activate this failure mode. Accordingly, Eto et al. [149] investigated the role of laser processing (10-9 s pulse width) in the initiation and development of SCC failure modes in 304L stainless steel when exposed to synthetic seawater (80 °C, 35% relative humidity). The authors reported the development of two SCC crack types: i) those starting from the top surface, and ii) those starting at the base of large corrosion pits, the propagation of both arresting in regions of compressive stress, which was subsequently measured (Fig. 23a). As such, higher pulse energies and cycles that induced tensile stresses further away from the top surface led to deeper SCC (Fig. 23b). Gupta et al. [150] directly compared SCC-resistance between LBM and conventional milling in 304L stainless steel, indicating the LBM surface possessed a greater resistance to SCC when the machined parts were exposed to boiling MgCl2 solution (155 °C, 10 h). While both machining processes induced tensile residual stresses and led to significant SCC, the lack of cold working and the laser-induced microstructural variation (predominantly ferrite with γ-austenite) present in the LBM recast layer was reported to retard the rate of crack propagation compared with the conventionally milled sample. Krawczyk et al. [151] investigated laser-induced SCC in 316L stainless steel in addition to aqua-blasting post-processing treatments. The tensile residual stresses resulting from laser engraving were reported to enable SCC within two weeks of exposure to MgCl2 (>39 μg/cm2), within corroded areas (Fig. 23c). In addition, transgranular atmospheric-induced SCC was observed after 402 days exposure (Fig. 23d).

Ultimately, the effect of a given laser-induced metallurgical or compositional change on corrosion performance is dependent on both the material and the machining conditions, however large recast layers are broadly detrimental to corrosion resistance. Where recast layers are generated from a machining operation, they are generally removed prior to service, as they strongly affect other failure modes such as fatigue. Routes to improving corrosion resistance include changing the assist gas, depending on the material, and restricting the formation of tensile stresses in the near surface. The latter is influenced by the operational parameters that dictate the heat input into and heat sinkage out of the workpiece. Furthermore, the capability of laser processing to both clad,

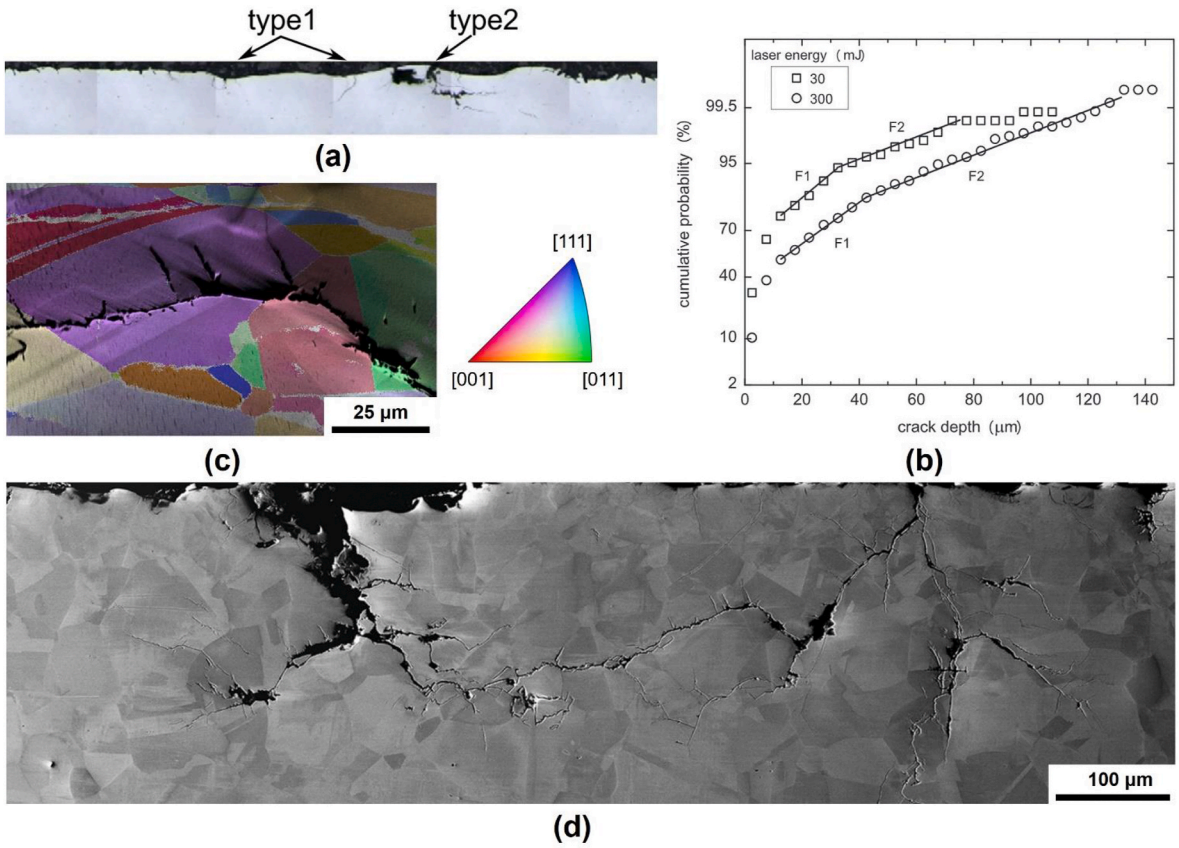

Fig. 23. Stress corrosion cracking (SCC) in laser-processed stainless steels. (a) Type 1 (from surface) and type 2 (from corrosion pits) SCC in 305 stainless steel (synthetic seawater, 1500 h). (b) Crack depth is limited by the extent of tensile residual stress, influenced by laser energy. (c) EBSD map showing transgranular SCC in 316L stainless steel ($MgCl_2$ 3950 μg/cm^2, 402 days). (d) local corrosion and SCC networks in 316L stainless steel. (a)–(b) taken from Eto et al. [149], (c)–(d) taken from Krawcyzk et al. [151].

alloy, and impart repeating microscale surface textures onto materials is a developing aspect of surface finishing (Section 5) that has enormous potential to beneficially affect corrosion resistance of LBM parts.

3.2.2. Influence of chemical machining on the corrosion resistance of the components

Electrochemical machining (ECM) and chemical milling methods remove material in a non-contact manner on an atom-by-atom basis, without thermal input and without altering the stress condition. This

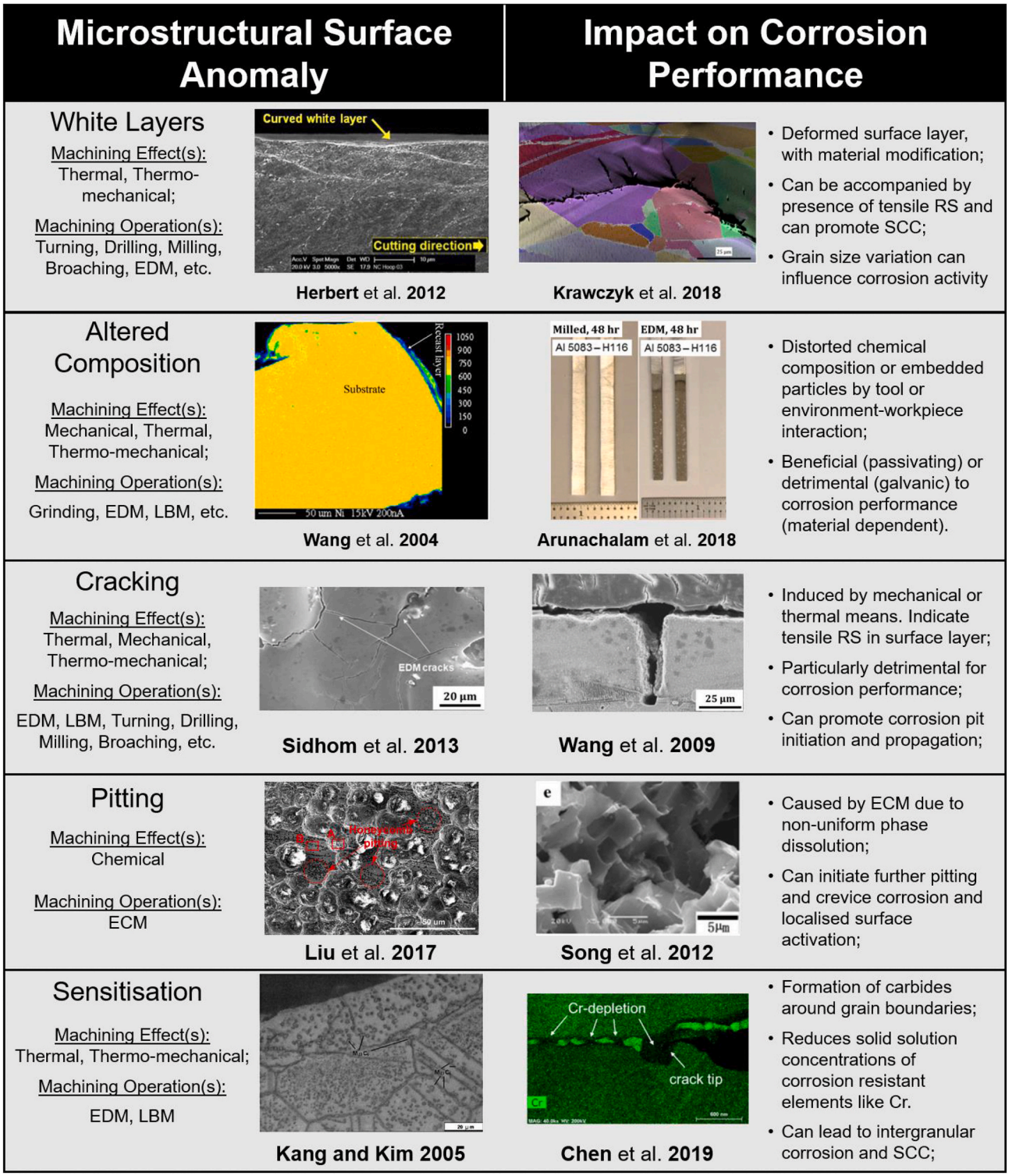

Fig. 24. Examples of surface anomalies and their impact on corrosion resistance. White layers and dragged material: transgranular SCC in machined stainless steel Krawczyk et al. [151]. Altered compositions: Ni-depleted recast layer upon LBM of 305 stainless steel, Wang et al. [148]. Cracking: EDM-induced micro-cracks in 316L stainless steel, Sidhom et al. [129]. Corrosion through-crack of recast layer in Inconel 718, Wang et al. [115]. Pitting: incomplete ECM of TB6 Ti-alloy, Liu et al. [154] Electrochemically machined Al-alloy surface, showing crystallographic pitting, Song et al. [155]. Sensitisation: carbide precipitation at grain boundaries in Hastelloy X after EDM, Kang and Kim [121]. Intergranular SCC though Cr-depleted region, Chen et al. [156].

prevents some key corrosion-enhancing surface integrity effects from occurring, for example the generation of tensile residual stresses during material removal. While surface integrity defects arising from inappropriate ECM parameters, such as pitting [152], localised oxidation, and intergranular attack will undoubtedly diminish corrosion resistance, limited research has been conducted to examine corrosion mechanisms of ECM surfaces. To this end, electrochemical post-processing methods are widely exploited to rectify surface integrity to improve, among other functional properties, corrosion resistance (Section 5).

3.3. Discussion: corrosion-life oriented approaches for machining process design and directions for future research and development

A broad range of machining-induced surface integrity phenomena are understood to influence the corrosion resistance of load-bearing materials. Machining-induced corrosion can manifest in visually apparent states, such as pitting and rust, or it can be more insidious, for example stress corrosion cracking, leaving little trace to the point of failure. In addition, corrosion mechanisms can influence and be influenced by other failure modes, for example fatigue (e.g. corrosion fatigue [136]), and wear (e.g. fretting corrosion [153]). As such, machining-induced surface defects must be considered when selecting processes to machine parts for use in both aggressive chemical environments, and environments that would be considered benign towards the same material with good surface integrity. This is particularly important when combined with elevated temperatures, where chemical reaction kinetics occur at faster rates and where thermodynamic barriers may be overcome, and under applied stress. Fig. 24 indicates different machining-induced microstructural and compositional surface integrity effects and their bearing on the resulting corrosion resistance. Depending on the material and the process in which the machining-induced surface integrity is affected, the resulting effect on the corrosion resistance can be either positive or negative.

WLs (including recast layers) and MD arise from mechanical, thermal, and thermo-mechanical machining processes and the associated microstructural, mechanical, and compositional differences can influence corrosion performance. As previously discussed, mechanical machining methods can lead to nano-crystalline WLs with high strain rates and complex residual stress distributions. The latter is a challenge for aggressive cutting processes and thermal-based machining methods in which the near-surface can be subjected to rapid cooling cycles, which can result in tensile residual stresses in the near-surface material. Tensile residual stresses can lead to surface cracking and depending on the chemical environment to which the part will be exposed, for example stainless steels exposed to chloride, can enable SCC mechanisms. Grain refinement correlated with the nano-crystalline WL and associated increases in near-surface grain boundary and dislocation density can influence the formation and retention of beneficial passive layers, which provide corrosion resistance. However, the relationship between grain size and corrosion resistance is difficult to predict and varies depending on the material and the applied current densities in testing [157]. As such it is a poor indicator of corrosion resistance in isolation.

Distorted near-surface compositions can arise from interactions between the workpiece, the tooling, and the media in which the machining processes are undertaken. For example, the embedding of abrasive material into the near-surface can enable localised micro-galvanic corrosion where the particle remains in contact with the workpiece. In thermal machining processes such as EDM and LBM, compositional contributions to the near-surface can result from the dielectric and any shielding gas, respectively. Again, the effect on the corrosion rates can either be positive or negative depending on the material and the compositional difference. Thermal cycles resulting from mechanical, thermal, and thermo-mechanical machining processes can also change local compositions, for example carbide formation at grain boundary regions, which sensitizes these areas to localised passivation breakdown and increased corrosion rates.

Corrosion resistance can also be influenced by machining-induced topography, for example grind marks from mechanical-based machining, surface cracking from thermal machining, and pitting from chemical machining can have a detrimental effect on performance. Cracking is also indicative of tensile residual stress within the near surface region. Considering machining marks, surface cracks, and pits, feature aspect ratio can influence pitting corrosion, for example high aspect ratios reduce the diffusion flux of oxygen into the crack and acidic corrosion products out of the crack, inhibiting surface passivation and promoting the propagation of active corrosion cells.

Broadly, approaches to reducing corrosion on machined surfaces involve processing strategies or finishing methods to minimise high aspect ratio features such as cracks and pits, and tensile residual stresses. In mechanical machining, less aggressive parameters may reduce the mechanical and thermal loading, while in thermal machining both cracking and tensile residual stresses can be reduced by controlling the cooling rates of the workpiece material. Strategies in chemical machining to reduce the occurrence of surface pits will reduce the propagation of pitting corrosion cells. Ultimately, machining-induced corrosion will benefit from increased understanding of the complex interplay between machining-induced near surface integrity and the different mechanisms of corrosion. This is challenging as corrosion itself tends to be irregular, for example different areas of the same material can simultaneously show active and passive regions, complicating predictions.

4. Influence of surface integrity after machining upon wear behaviour of the components

Wear is a critically important failure process which has a significant economic cost. 23% of the world's total energy consumption originates from tribology contacts, of which the majority is used to overcome friction, and the remainder used to remanufacture worn parts [158]. Economic savings of 1.4% of global GDP have been estimated from successful enhancements to and new technologies in the field of wear and tribology [158]. In addition, a substantial CO_2 emissions saving would be produced by implantation of improved wear technologies. Transportation, power generation and manufacturing all depend on moving parts which have surfaces which interact with each other. Understanding, and mitigating the effect of wear of such surfaces is critical to the reliability and energy and cost efficiency of these services. The main forms of wear which can take place are illustrated in a schematic in Fig. 25.

There are several forms of wear which involve a range of mechanisms. These forms are adhesive wear, abrasive wear, fatigue wear, erosive wear and fretting wear. Fatigue and fretting wear are linked, given fretting fatigue is one mechanism of fretting wear. Adhesive wear, shown in Fig. 25 (a) occurs when high loads, temperatures or pressures cause the asperities on two contacting metal surface in relative motion, to weld together and tear apart. Adhesive wear often occurs in the case of plastic contact between similar materials. Adhesive wear is promoted by two main factors: the tendency of different material to form solid solutions or intermetallic compounds with one another (effectively welding, analogous to the built up edge BUE in machining), and the cleanliness of the surface [159]. If this results in the contact interface having enough adhesive bonding strength to resist relative sliding, a crack is initiated near the contact region and propagates in a tensile and shearing fracture mode, until the crack reaches the contact interface, and wear particle is formed [160]. Surfaces with thick and adherent oxide films have low adhesive wear. Cleaner surfaces are more likely to bond together.

Abrasive wear occurs when material is removed or displaced from a surface by hard particles, or hard protuberances on a counterface, forced against and moving along the surface [161]. Two-body abrasion is caused by hard protuberances on the counterface or hard particles attached to it. In three-body abrasion the hard particles are free to roll

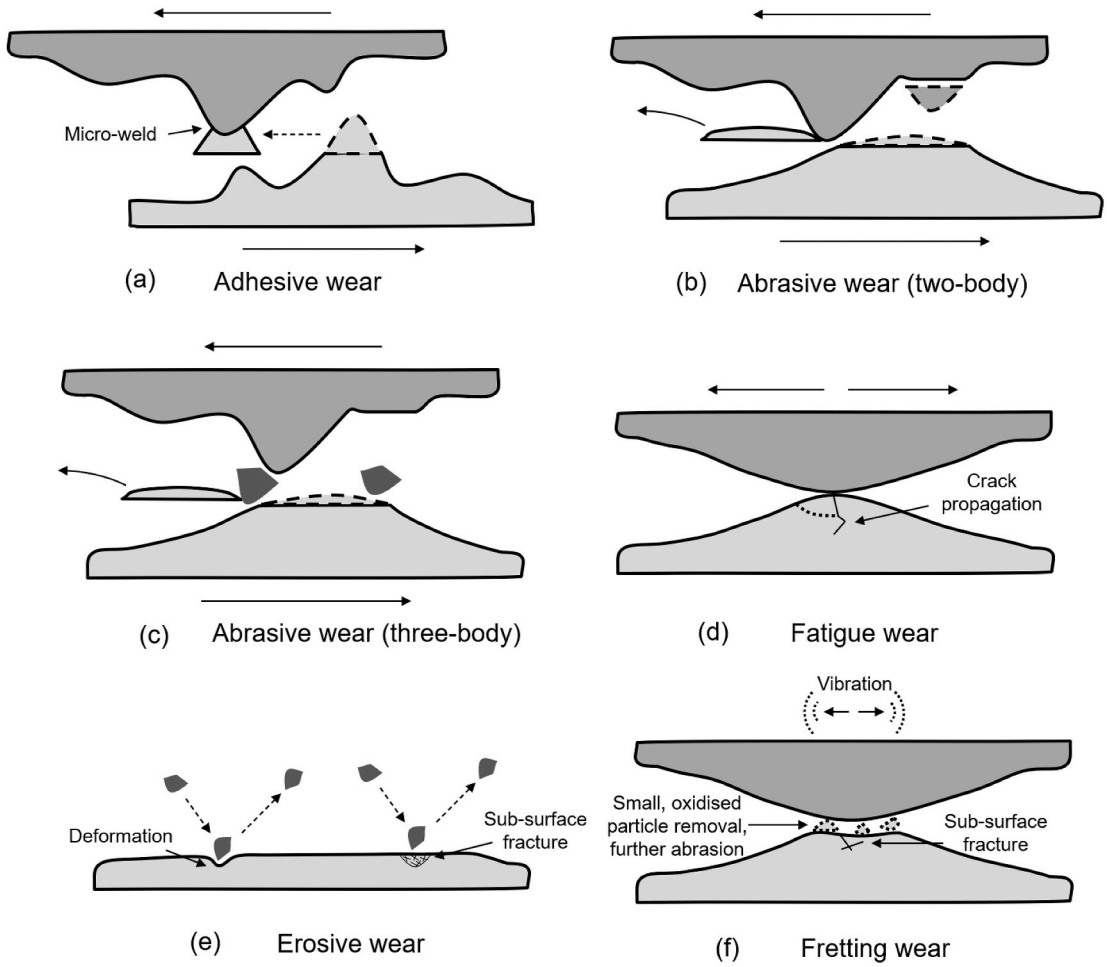

Fig. 25. Main wear mechanisms – (a) Adhesive wear, (b) Two-body abrasive wear, (c) Three-body abrasive wear (d) Fatigue wear (e) Erosive wear and (f) Fretting wear.

and slide between two sliding surfaces. In a single point contact model with a single hard abrasive against a flat surface, a groove is formed by "ploughing", generally displacing material to the side of the track [162]. In the case of the worn material having a more ductile property, a "cutting" mechanism may take place, in which a longer ribbon-like wear particle is generated [162]. In the case of more brittle materials, wear particles are generated by crack propagation and "fragmentation" [162]. For metals, predicted wear volume by abrasive wear is inversely proportional to the worn material's hardness [163]. This relationship is also described as the Archard equation. This is illustrated in Fig. 26 in which relative wear resistance of pure metals is proportional to hardness.

Fatigue wear is caused by cyclic loading between two surfaces. In fatigue wear, repeated contact between the surfaces is essential for the generation of wear particles. In the case of an elastic or elastoplastic contact, accumulation of local plastic strain around points of stress concentration occurs, leading to crack generation and propagation after a certain number of cycles [162]. In the case of plastic contact, plastic flow takes place in an incremental and gradual fashion, resulting in greater deformation wear and ultimately a grooved surface layer on the worn layer after increasing numbers of cycles. Fatigue wear is somewhat linked to fretting wear, another distinct wear process. Fretting wear occurs by the repeated relative motion of two surfaces at small amplitude, of no more than 150 μm [164], down to the order of ~1 μm or lower. This scale of movement can be generally described as vibration. Failure may occur via formation and removal of an oxide layer, and further abrasive action by these oxides, failure of metal-metal adhesive bonds, as well as fatigue crack initiation [164].

Finally, erosive wear is another wear process distinct from all others, in that it occurs by hard particles impacting the surface of the part. Erosion processes and rate of wear depend on the impact angle, impact velocity and relative hardness of the materials and incident particles [165]. Ductile materials show a maximum erosion rate at ~20° impact angle yielding extensive plastic flow around points of impact, with good erosion resistance for impacts at 90° to the surface [165]. However brittle materials show more severe damage under 90° impacts, via crack propagation, while having good wear resistance at low impact angles [165].

Machining processes induce a range of material and morphological changes which can play a role in modifying the wear behaviour. Such changes include the presence of plastic deformation, hardness, fracture toughness, cracking, porosity, recrystallisation, residual stress. The following sections link these specific machining induced defects with their impact on wear behaviour.

4.1. Influence of mechanical machining on wear performance of the components

Mechanical machining induces a white layer on metal surfaces, in which the microstructure is sometimes significantly modified. In addition, cracking can be introduced along with residual stresses. These properties play a key role in the wear behaviour of parts. However, their effect on wear behaviour is complicated and depends on the exact material properties. This means wear behaviour of machined surfaces with

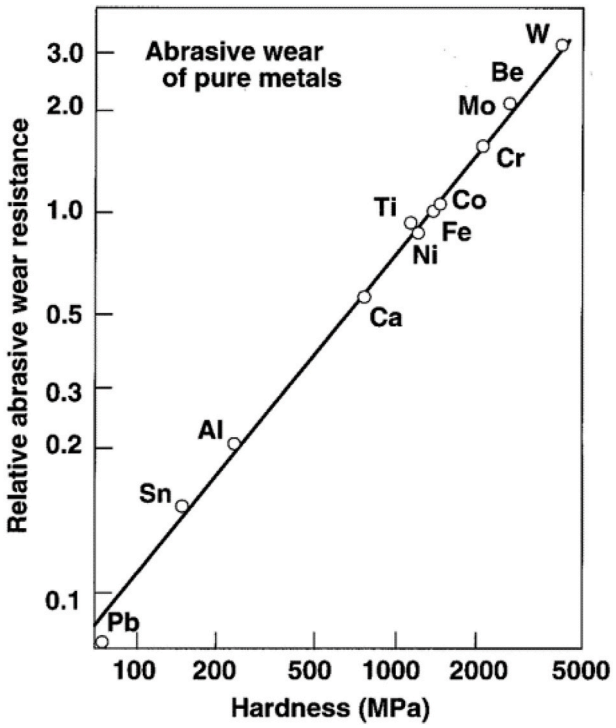

Fig. 26. Relative abrasive wear resistance is proportional to hardness for pure metals [163].

a white layer may either worsen or, in some cases, improve. To demonstrate this phenomenon, some examples in the literature can be used. It is known that the tribological performance of mechanically machined surfaces depends on the method of machining and the tribological conditions. It has been shown that a turned white layer can slightly decrease CoF while a ground white layer can significantly increase CoF under dry conditions [166]. This was explained by the generation of more wear debris in the case of the turned surface, which acts as a solid lubricant. However, this is reversed under lubricated conditions.

In some instances, the white layer is considered to have some advantages in terms of wear resistance. Improvements in wear resistance of machined surfaces are analogous to the burnishing process, which sits somewhere between a machining and a finishing operation. Burnishing is a method of finishing surfaces of revolution or plane surface by plastic deformation under cold working conditions, by application of pressure by a hard ball or a roller. Burnishing has been shown to reduce the specific wear rate of carbon steel by a factor of 6 when burnished against a cemented carbide ball [167]. An increased hardness owing to the 30–50 nm grains produced in the deformed sub-surface layer explained the improved wear behaviour. The smoothened surface was also thought to enhance the wear resistance. This principle is the fundamental basis for cases in which mechanical machining of metals improves their wear behaviour.

Griffiths & Furze showed that a reduction in wear rate could be produced on white layers induced by mechanical machined produced by turning, when tested in block on ring wear mode involving a cyclical wear regime, using loads of 0.6, 1.4 and 3 kg, and two white layer thicknesses of 2 and 7 μm. A 3.3-fold increase in hardness in the white layer compared to the bulk explained the improved tribological behaviour [168]. A study by Yang et al. showed that a white layer produced by mechanical impact yielded reduced wear behaviour in pin on disc testing under a load of 100 g and wear length of 7.6 m. Improved wear behaviour was explained by delamination which was in turn explained by formation of microcracks and voids [169]. Another example of superior sliding wear behaviour was shown in the case of a martensitic steel subject to mechanical machining [170]. A "block--on-cylinder" wear testing set-up was used here. In this case, the dependence of wear on hardness was shown to explain the enhanced wear resistance after machining. The machined surface exhibited a hardened white layer with overtempered martensite. The improvement in wear resistance was generally consistent with the increase in hardness according to the Archard equation. Interestingly here, residual stresses did not have a significant effect on wear performance, likely explained by new residual stresses being induced during the wear process. To summarise the above evidence regarding the impact of mechanical machining on wear, a schematic of the effect of various machining induced phenomena is shown in Fig. 27.

Rolling contact fatigue is a form of material failure or material removal, commonly observed in gears, camshaft mechanisms and rail-wheel contacts, whereby a material is subject to a near-surface alternating stress field. Rolling contacts result in very high contact stresses, which result in either flaking off of the surface material, or the development of cracks below the surface which propagate to the surface causing a pit or spall [171]. The mechanism of failure strongly depends on the level of cleanliness or lubrication. The two main mechanisms for failure by RCF are subsurface originated spalling and surface originated pitting [171]. Which mechanism prevails depends on surface quality as well as lubricant and cleanliness of the lubricant.

There is some evidence regarding the effect of mechanical machining on rolling contact fatigue behaviour. Choi investigated the influence of mechanical machining (CNC lathe using CBN tool) induced white layers on 52100 steel on rolling contact fatigue behaviour [172]. The presence of a white layer reduced crack initiation life and crack propagation life by 75% and 89% respectively, resulting in a reduced fatigue life of 75%. However, the influence of the white layer on these properties reduced with increasing load. The presence of the white layer increased the maximum shear stress at crack initiation depth, but this increase reduced with increasing load. Despite this, under no conditions did the machined sample yield longer fatigue life. A schematic illustrating this behaviour in the context of crack initiation and propagation rate is shown in Fig. 28. Depending on the load during rolling contact fatigue, crack initiation can become shallower or deeper, for high and low stress respectively.

4.2. Influence of thermal machining on wear performance of the components

Both laser and EDM induce defects into the machined surface which are correlated with local changes in mechanical properties and in particular wear performance. The direct wear testing of materials subject to EDM and in particular laser are few, however given the knowledge we have on defect formation in these processes, general comments can be made regarding materials' expected wear performance.

In the case of EDM, components are often machined for use in die, punch and moulding tools for example, in which surface wear is a common problem. For this reason, the impact of EDM in particular on wear of such parts is important to understand. EDM induces significant changes to the microstructure the near-surface of parts, i.e. the recast layer. Typically, the microstructure becomes refined after machining due to rapid cooling after discharge, and the uptake of carbon when machining in oil, can cause carbide formation in steels for example. This can result in increased hardness of the near surface, generally correlated with increased wear resistance. However, the presence of tensile residual stress in EDM recast layers [173], can also have a negative impact on mechanical performance, in particular, wear. The surface and internal morphology of the near-surface also plays a role in wear behaviour. High roughness as well as cracking and porosity generated by intensive machining parameters, can play a key role in reducing potential wear behaviour. Features of cracking and tensile residual stress are also characteristic to both EDM and laser machining. A summary of the surface and sub-surface features introduced by laser and EDM which will

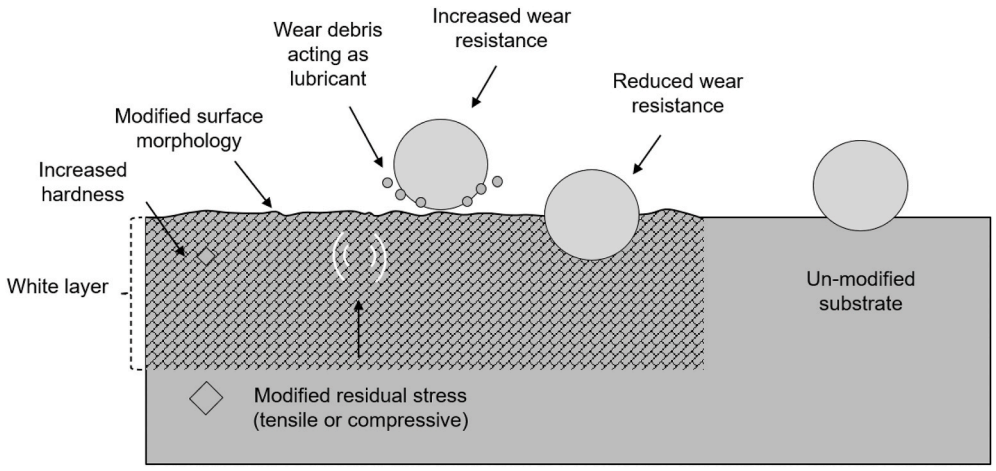

Fig. 27. Positive and negative effects of a mechanical machining induced white layer on wear behaviour in metals.

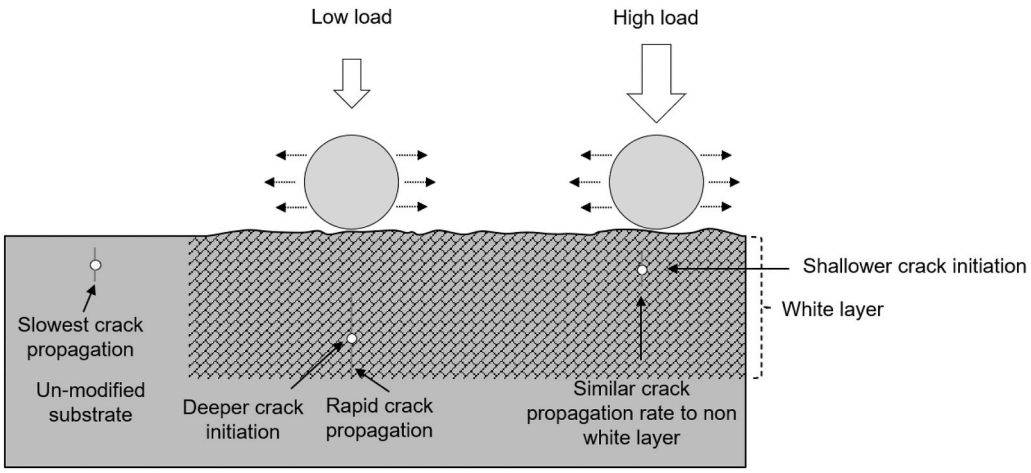

Fig. 28. Schematic of effect of turned white layer on crack initiation depth and propagation rate in rolling contact fatigue of AISI 52100 steel, according to Ref. [172]. The presence of the white layer shortened (worsened) crack initiation and propagation life in all cases. Its effect is substantially reduced at high applied stresses.

impact wear performance are shown in Fig. 29.

The direct assessment of wear performance of EDM'd surfaces has not been extensively researched. Much of the understanding in the literature of the effect of EDM on wear behaviour is from the perspective of tooling type ceramics, with little information available on wear behaviour of EDM'd metals. One example of this is the comparison of the punching wear behaviour of WC-Co punches produced using different surface qualities, including EDM surfaces of between 0.04 and 0.83 μm Ra roughness, and ground surfaces of 0.10–0.11 μm Ra roughness [174]. It was concluded that the different textures made no difference to the change in radii of the punches under this scenario, and hence made no difference to overall wear. In a silicon nitride-titanium nitride ceramic useful for wear resistance at elevated temperatures, wire EDM yielded reduced hardness, higher unlubricated wear rate and a higher

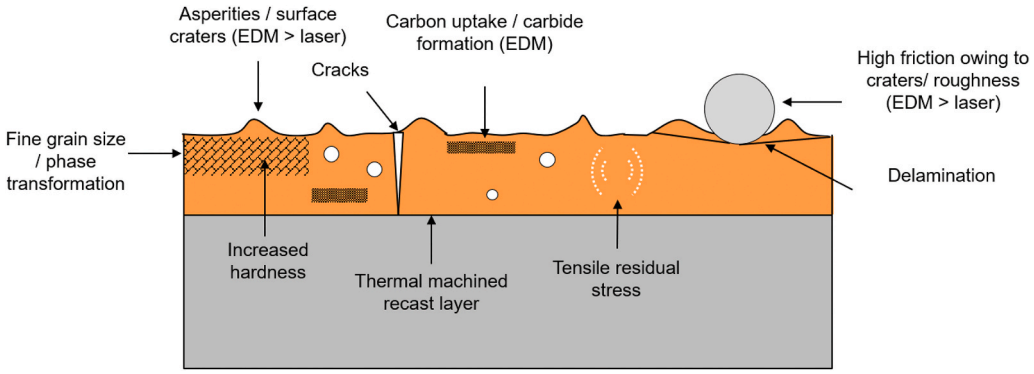

Fig. 29. Effect of EDM or laser machining on layer properties and wear/friction performance. Several properties important to the reduction of wear are worsened, in particular by EDM. These include porosity, asperities, cracks and tensile residual stress.

coefficient of friction [175]. Roughness, porosity, surface craters were hypothesised to contribute to this reduced performance. This behaviour was confirmed in Zirconia based ceramics machined by EDM compared to grinding, whereby increased friction and higher wear rates were produced in the case of EDM [176]. This was exacerbated by more pronounced wear mechanisms, including grain removal, adhesion, abrasion and delamination of wear debris. The inferior wear performance of the EDM surface was also reflected by its lower flexural strength.

In the case of WC and ZrO2 based ceramics, the wire EDM'd surface showed both the highest friction and wear rate, compared to their ground equivalents based on pin on flat testing [177]. A combination of reduced flexural strength and increased surface roughness were used to explain the inferior wear behaviour. A combination of wear mechanisms were revealed which were exacerbated by the presence of the EDM recast layer. These include grain cracking, grain removal, surface binder expulsion, abrasion/adhesion and delamination/spalling. Grain cracking was particularly prevalent on the wire-EDM'd surface, compared to a ground or polished surface. This was explained by the prevalence of pre-existing micro-cracks, induced by EDM acting as notches.

4.3. Discussion: Mitigating the wear of metallic components subject to mechanical and thermal machining

The impact of machining of metals on their wear performance is complex and cannot be summarised simply. In general terms, mechanical as well as thermal machining induce defects into the near-surface of metals which can negatively impact the wear resistance of the component. The defects which effectively in all cases negatively impact such properties are porosity, cracking and high surface roughness.

The concept of producing a mechanically favourable, wear resistant white layer is not new. Furze et al., in 1988 explored the idea of deliberately generating a wear resistant white layer via "abusive" turning [178]. In unlubricated conditions, superior wear resistance was produced on surfaces of 817M40 steel with a "controlled abusive" white layer produced by turning using a tungsten carbide tool. Under the correct conditions, the white layer produced was crack-free with a gradual transition into the bulk, with hardness near the surface higher than the bulk by a factor of between 3 and 4. Under the correct conditions therefore, the negative aspects of surface integrity associated with machined white layers could therefore be avoided, in particular poor fatigue properties, tensile residual stresses and cracks present in the layer. In sliding wear systems, the detachment of material exacerbated by these negative properties results in three-body abrasion and therefore failure. Through manipulation of feed rate and clearance angle, a dense and mechanically favourable white layer can be produced.

It is clear that mechanical machining is likely a better route for the deliberate generation of near-surface layers which are wear resistant, given the difficulty in avoiding more severe defects in the case of thermal machining, such as pores and cracks. In addition, the fundamental removal mechanisms of laser and EDM cause material flow followed by rapid cooling, and uptake of gas/porosity particularly in the case of EDM. Such factors cannot be simply overcome in absolute terms via manipulation of parameters, although some mitigation is possible. In summary, the thermal methods do not offer good potential for wear mitigation without the addition of coating elements, which is discussed in section 5.

5. Advanced post-processing strategies for enhancing the performance of machined surfaces

This review so far has described the impact of machining-induced anomalies on the performance of machined parts which may undergo fatigue, corrosion, stress-corrosion and wear. As also discussed in Part I of this review [1], understanding of the physical mechanisms controlling the in-service behaviour of machined surface layers allows optimisation of machining processes in order to satisfy applicable part life objectives and functional specifications. Despite this, a range of post-processing strategies can be used to achieve targeted performance in machined surfaces by modifying and enhancing their morphological, physical and chemical characteristics. The processes selected and described below are of particular use because their depth of effect in the machined surface is of a similar scale to machined layers. This gives the opportunity to re-modify the machined surface layer without impacting the bulk material or significantly changing geometry of the part. Other techniques which do not fit this remit include physical and chemical vapour deposition and other thin-film coating processes (thin), as well as thermal spray processes including high velocity oxy-fuel and plasma spray techniques (thick).

To be considered as an eligible post-process, the technique should modify at least one of the following: Metallurgical anomalies (microstructure and phase change, severe plastically deformed layer, composition); Geometrical defects (micro-cracking, asperities, pits); Near-surface residual stress field.

As analysed in the previous sections, these three classes of machining-induced surface conditions can be greatly responsible for the environmental behaviour of machined surfaces, especially with respect to their fatigue (Section 2), corrosion and stress corrosion (Section 3) and wear (Section 4) resistance. In this context, depending on the initial machined surface state and on the applicable functional deliverables, a wide range of techniques allow the post-processing of high value machined components, whose key characteristics are summarised in Table 3. Thus, the following sections examine the most relevant enhancement strategies for machined surfaces, whose key traits are discussed in relation to: the surface anomalies to rectify, the possible outcomes in performance, and the research challenges that emerge from the current state-of-the-art. To describe and critically review these enhancement methodologies, this section is written with reference to machining operations and their effect on the workpiece surface prior to treatment. However to discuss the principles of these techniques with sufficient depth, the processes are described generically from their basic mechanisms and their interaction with metal workpieces. Where relevant, the impact of a prior machining operation on the efficacy of the relevant enhancement technique is described.

5.1. Peening approaches for improving the performance of machined parts: Shot peening, laser shock peening & waterjet shock peening

Peening was employed as early as during the 1930s with the primary objective of increasing the fatigue life of critical components (e.g. aircraft structures). A the time, experimental work showed that blasting hard particles into metallic components could significantly increase their fatigue life, but there were no guidelines nor control on the process [179]. Over time, peening evolved with more controlled processing parameters to what now is known as 'shot peening' (SP), plus other peening methods, such as laser shock peening (LSP) and waterjet peening (WJP) have also been developed to enable the same outcome as SP without the need of blasting hard particles, but using other principles instead. In short, peening relies on the use of an energy source (i.e. accelerated particles, water jet stream, laser beam) that is targeted on a surface to produce a subsurface with a compressive residual stress profile. The induced stresses are typically half the value of the yield strength of the bulk material as a minimum [180].

Peening is a widely employed technique for post-processing as-machined components, with the principal aim of improving their functional performance (e.g. fatigue life) by inducing compressive stresses in the machined sub-surface [181]. Peening induces a local and controlled plastic deformation on the machined subsurface to generate a high dislocation density in the crystal lattice. The dislocations in the lattice near the machined surface improve the component's overall performance due to a strain hardening effect induced by the deformation

Table 3
This table discusses the most-widely applied post-processing techniques (colour coded as mechanical, thermal and chemical) for the enhancement of machined surfaces of load-bearing components. Thus, each column considers the nature of the surface modifications induced and their resulting impact on surface performance.

	To improve machined surface metallurgy	To improve machined surface topography	To improve machined surface RS field	Influence on functional performance
Shot peening (SP)	Grain Refinement [177–180] and Strain Hardening [180–182] from cold impacts producing a forest of dislocations	-	Induction of compressive RS. LSP typically achieves greater RS magnitude, followed by SP and WJP [183–185]	Increased fatigue life (SP: [183,186], LSP: [187], WJP: [188]); Better corrosion and corrosion- fatigue resistance (SP: [182,189,190], LSP: [184], WJP: [191]);
Laser shock peening (LSP)		-		
Waterjet peening (WJP)	-	-		
Finish cutting/ polishing	Removal of machined surface layers [192]	Surface smoothening [193]	Removal of tensile RS layers [192]	Increased hardness[193], and fatigue life [192]
Burnishing	Grain refinement [194]	Surface smoothening [194]	Induction of compressive RS [195][196]	Increased hardness [195], fatigue life [195,196], wear [197], and corrosion resistance [194,198]
Laser polishing	Grain refinement [199]	Asperities removed. Down to 0.05 μm Ra roughness [200].	Generally tensile residual stress (e.g. [200]). Compressive RS possible at high powers/beam diameters [201].	Increased hardness (by factor of 1.5-3) [199,200,202] and corrosion resistance [199]
HCPEB	Sub 10nm surface grain size, increasing to 100s nm near to bulk/remelt interface [203]	Fine surface finish, depending on initial roughness. E.g. from 2 to 0.5 μm Sa on SLM steel [204]; from 3.1 to 0.9 μm Sa on EDM'd steel [203].	Tensile residual stress in steel [205]. Compressive RS possible e.g. in zirconium [206], aluminium [207], TiNi [208].	Increased hardness (factor of ~2 [209]); Reduced wear (1-2 orders of magnitude) [207,210–212]; Improved corrosion resistance [206,207,209]
EDM coatings	Replaces recast/white layer. Fine grain size at top (sub 100 nm) larger columnar beneath [213].	EDM-type topography – e.g. 2μm Ra in for TiC. Silicon addition can improve morphology/crack density [214].	Unpublished to date, however tensile RS expected as in EDM recast layers [215].	Hardness (up to 25 GPa with TiC) [214], wear resistance (increased by 1-2 orders of magnitude (TiC on steel)[216,217].
Electropolishing and chemical polishing	Surface layer removal (e.g. recast). Metallurgy tends to bulk on removal.	Asperity and microcrack removal. Mirror finishing (<20 nm Ra).	RS field removal at near surface. RS tends to bulk on removal.	Fatigue (run-out stress increased by factor of 1.1-5) [65,218], corrosion (Cr-enriched layers) [219–221]
Anodization and electrolytic oxidation (EO)	Surface oxidation to stable oxides $<1^0$ μm (anodization); $<10^2$ μm (EO)	Dense/level/hard surfaces with anodization.	EO can impart tensile RS depending on cooling cycles	Wear, corrosion (TiO_2/Al_2O_3 surface layers) [222,223]

[182]. SP (Fig. 30a) is the most employed peening technique in industry and relies on the continuous impact of shots (i.e. round particulates) on the material's surface to induce the plastic deformation [182]. While LSP and WJP are less employed than SP, they are in increasing usage and undergoing in-depth research. LSP (Fig. 30b) induces the compressive stresses in the machined subsurface by using a pulsed laser beam that generates plasma-induced shock waves [183] and WJP (Fig. 30c) does it with the kinetic energy of a water stream and the impingement of water droplets and cavitation on the surface [184].

When it comes to high temperature applications, such as the ones involving heat resistant Ni-base superalloys for safety-critical aerospace components, the most relevant benefits of peening reside in the depth of the strain hardening layer and grain refinement induced by the cold working impacts [185,186]. Compressive RS from peening are in fact quickly redistributed at stress concentration features (such as holes or fillets) if subject to cyclic plastic strains or thermal exposure [187,188]. Thus, compressive stress states can be regarded as beneficial if cyclic stresses are much lower than the monotonic yield stress and the service temperature is low enough to ignore creep. Although peening processes can in fact improve the functional performance of advanced materials after machining, research has shown that unsuitable peening conditions may introduce an opposite effect with reductions in performance, e.g. in terms of reduced LCF endurance [189] and lower ductility under high temperature tensile loading [190]. Therefore, peening strategies need to be carefully optimised to improve the functional performance of advanced materials after material removal, especially when machining Ni-base superalloys for high pressure aero-engine rotors.

The effect of SP on metallic machined components is well understood

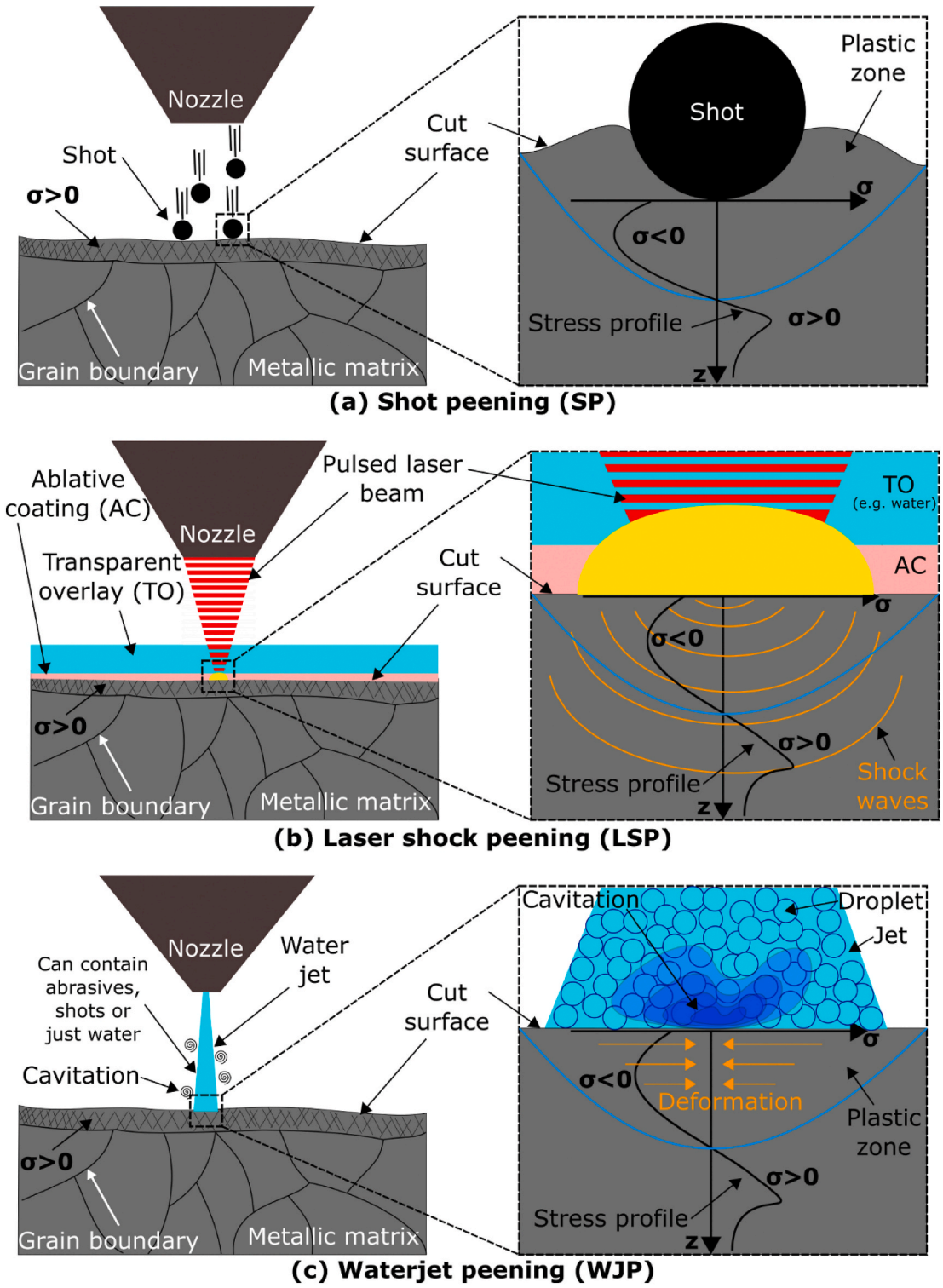

Fig. 30. Mechanisms for inducing compressive stresses in machined surfaces by various peening techniques. (a) Shot peening (SP): continuous impact of shots on the material's surface to induce the plastic deformation. (b) Laser shock peening (LSP): a laser beam generates plasma-induced shock waves. The ablative coating serves as an energy-absorbing media that generates the plasma while the transparent overlay (e.g. water) confines the plasma to the machined surface, thereby controlling the shock wave depth reach. (c) Waterjet peening (WJP): deformation is induced by the impingement of water droplets and cavitation on the surface.

and broadly employed. For example, in Inconel 718, SP can induce a compressive stress of 1200 MPa up to ca. 100 μm beneath the machined surface, which translates into a 38% greater fatigue strength at 10^7 cycles when compared to the non-peened dry milled specimen [191] (see Fig. 31). However, due to the nature of SP, even if it can improve the fatigue life, it can also create an increased surface roughness that could compromise the component's integrity [192]; therefore, extreme caution must be considered for the SP process parameters, and/or follow it with an additional smoothing operation. Regarding this, Xu et al. [193] showed that in general, SP would increase the surface roughness in Ti–6Al–4V after milling, grinding and large area electron beam melting (LAEBM), while it would remain constant following wire

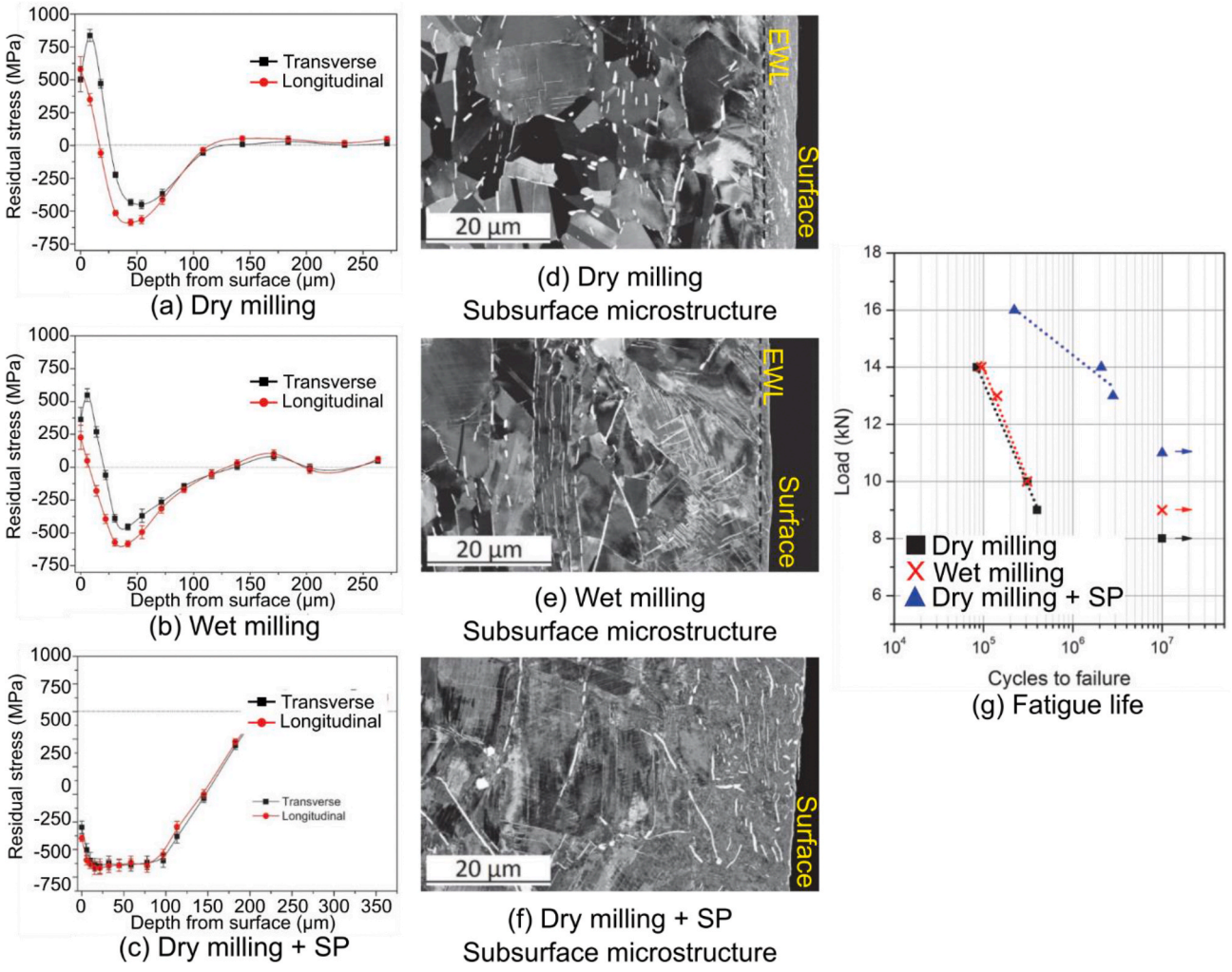

Fig. 31. The effect of SP on the fatigue life of Inconel 718. (a–c) Residual stress profiles of dry-milled, wet-milled and shot-peened surfaces, where the SP process clearly eliminates the occurrence of tensile stresses on the machined surface. (d–f) Electron channelling contrast images corresponding to the specimens from (a–c); note how the white layer is about 5 μm in dry milling, while in wet milling is about 1 μm. (g) HCF results, where significant improvement on the shot-peened component is visible due to the compressive residual stress layer. From Chen et al. [191].

electrical discharge machining (WEDM) and decrease in abrasive waterjet (AWJ) cutting; but no direct relation between surface roughness and fatigue performance was found. However, they showed that regardless of the surface condition before SP, the inducement of compressive stresses in the machined subsurface always resulted in an improved fatigue performance (Fig. 32), with major beneficial effect on AWJ machined surfaces, due to the combined peening effect of the water jet and the SP process itself. Thus, the surface condition before post-processing (i.e. before peening) could play a pivotal role in the fatigue life of metallic components.

LSP could be a good alternative to traditional SP when an increased surface roughness post-peening is not acceptable. In the case of Al 7075-T7451, for instance, using LSP may supersede of SP since the former process is able to create a deeper layer (ca. 2 mm deep) of compressive residual stress with superior surface finish, as opposed to a much thinner compressive layer (ca. 0.26 mm) with rougher surface finish created with SP [192]. However, this is process-dependent, meaning that LSP can achieve superior surface finish and deeper residual stress profile against SP only if the adequate processing parameters are employed. Regardless of the peening method, excessive post-processing (i.e. over-peening) could lead to a detrimental component performance instead, especially in metals with reduced ductility, such as that of magnesium alloys, which are characterized by a hexagonal closely packed crystal lattice.

In FCC crystal structures, the use of LSP has been shown to induce a grain refinement mechanism due to the occurrence of mechanical twins in the surface, which is dependent on the processing parameters (i.e. amount of laser shock impacts). For example, 304 SS has seen a reduction of grain size on the surface from 1-2 μm to 50–200 nm with triangular-shaped grains that are formed due to the appearance of mechanical twins in three different directions, after being exposed to three impacts of laser shock peening (Fig. 33) [194]. Besides amount of shocks, laser power density [195], laser pattern [196] and exposure time [197] are important parameters of this post-processing technique that directly alter the depth and magnitude of the compressive residual stresses and the refined grain layer. However, even if LSP can supersede of SP, other aspects such as the more complex setup (i.e. use of ablative coating, transparent overlay, laser beam) have to be considered due to the process limitations they imply.

Due to the compressive state induced by LSP, crack growth is diminished since the lack of tensile stresses hinder their propagation. For example, AL 7075-T7451, exhibits narrower striation spacing under fatigue loading if laser-shock-peened, extending its fatigue life up to 3 times more than a non-peened surface (Fig. 34) at low values of stress [198]. Similarly, laser shock peened AL 2524-T351 can see a 4-times larger fatigue life with the employment of this technique, since the

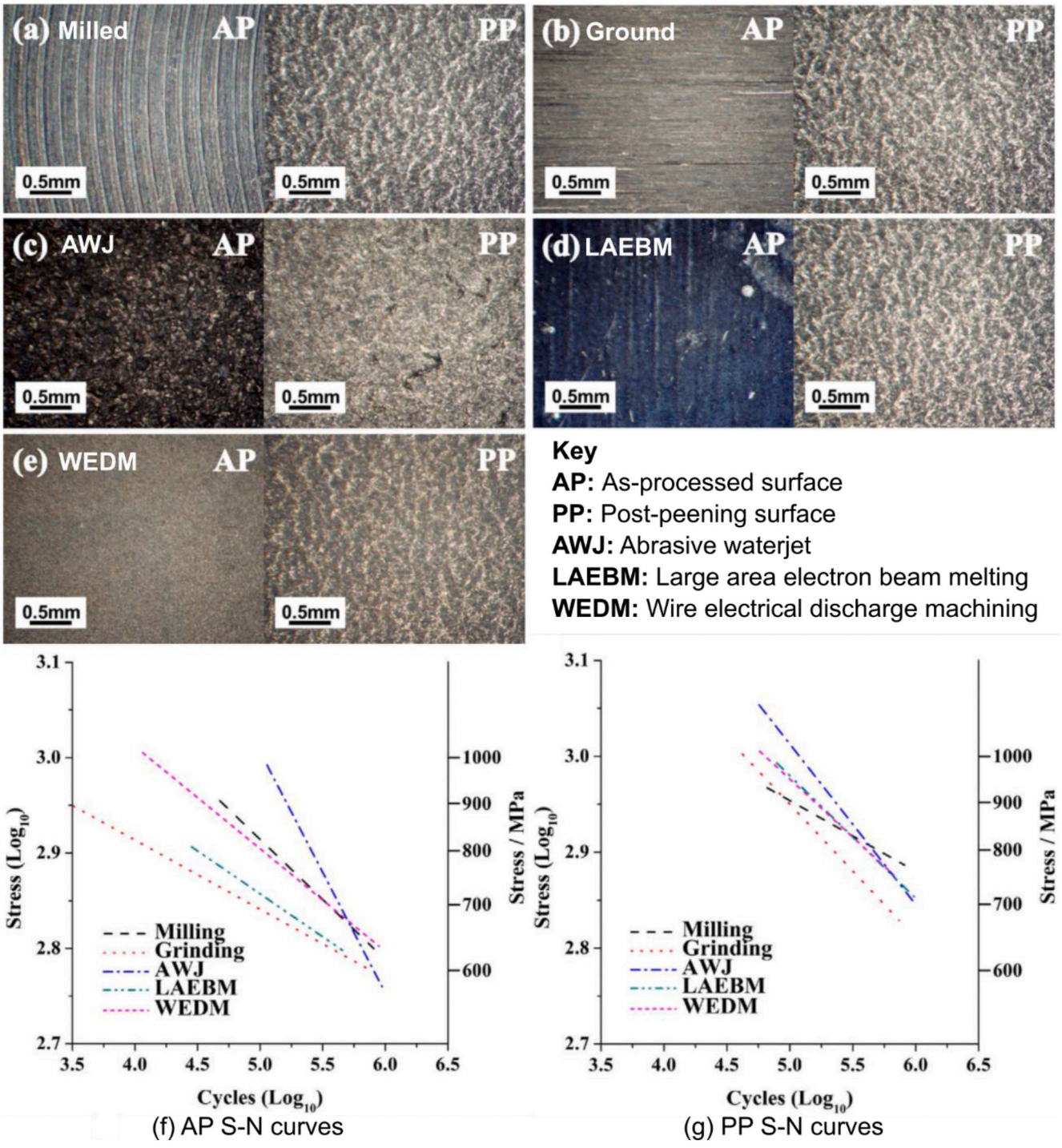

Fig. 32. Comparison of as-processed (AP) and SP post-processed (PP) surfaces of Ti–6Al–4V subjected to different machining processes: (a) milling, (b) grinding, (c) AWJ, (d) LAEBM, (e) WEDBM, with their respective fatigue life (f,g) before and after SP. Note how the SP process induces a very similar surface quality in (a–e), regardless of the as-processed condition. The differences in as-machined components in the S–N curves (f) is easily discernible, but the behaviour after SP (g), besides exhibiting superior performance in all cases, makes the differences between each machining method to narrow down [193].

fatigue crack growth in the peened region is dramatically hindered in the laser shock-peened subsurface [199].

Even if waterjet technology is largely employed for abrasive cutting operations, the standoff distance (i.e. distance from the nozzle to the target) plays a pivotal role in shifting the process from a cutting operation to a peening operation. At small standoff distances, the kinetic energy from the jet is localised in a small surface area, which results in a cutting process by erosion [200]. However, at greater distances, cavitation impacts occur in a larger surface area, thereby creating a peening effect instead of cutting. This is the reason why AWJ results in a compound cutting and peening effect [201]. In fact, this has been addressed by Soyama [200], who proposed the term ‘cavitation peening’ for WJP with small standoff distances, where the peening is driven primarily by cavitation, and suggested to isolate the term ‘waterjet peening’ (WJP) for when the peening is primarily driven by the impingement of water droplets on the surface. However, in the interest of simplicity and to comply with most of the literature, here, the term ‘waterjet peening’ is inclusive of both cavitation- and impingement-driven peening caused by

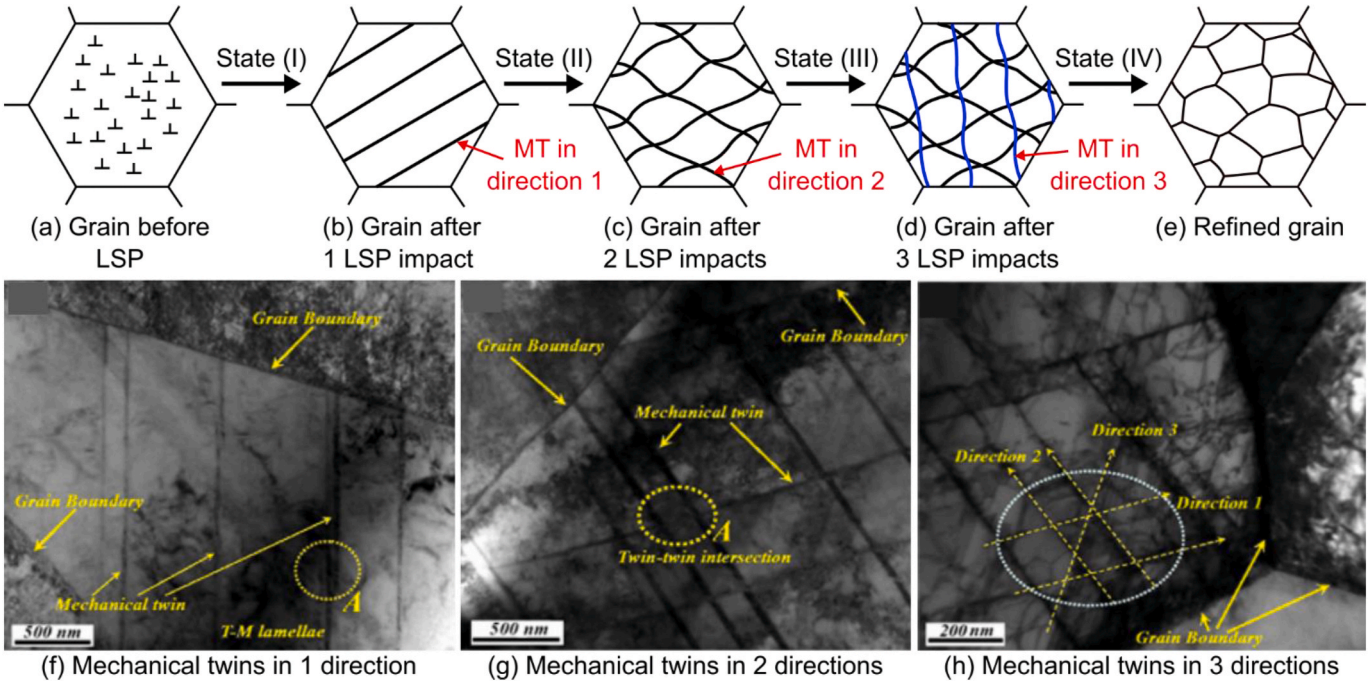

Fig. 33. In their work, Lu et al. [194] **found a twinning mechanism in the crystal lattice of 204 SS that depends on the amount of laser shock impacts.** (a–e) Schematic of the twinning process, in which after a single shock impact, the twins appear in a single direction within a given grain, but after a second and third impact, twinning occurs in other two directions. (f–h) TEM images of 304 SS where a single twinning direction is shown in (f), two directions in (g) and three directions in (h).

the water stream.

WJP usually results in increased surface roughness do to the inherent effect of the water droplets impacting the surface; in fact research on Inconel 718 showed that the surface roughness was higher and the compressive stresses lower when compared to conventional SP [202]. However, an increase in surface roughness is not necessarily a downside. For example, the use of WJP with abrasive particles on orthopaedic implant materials like 304 SS and Ti6Al4V can successfully increase the fatigue life by 10–25% and the increase in surface roughness (i.e. from less than 1 μm to 5–14 μm) could improve the mechanical interlock and aid the surface chemistry that is necessary for an enhanced implant bonding process with the human body [203]. Nevertheless, the addition of abrasive particles could result in particle embedment on the machined surface [203], thereby changing its chemistry and microhardness [204], and/or in mass loss due to erosion. Additionally, mass loss is not limited to the use of abrasives, since it can also occur in conventional WJP if processing parameters are not properly employed (e.g. aggressive jet pressure) [205]. However, regardless of the specific method, if mass loss occurs, then the process is no longer exclusively peening, but a combination of AWJ and WJP.

There are different peening techniques that could be employed in industry but the most suitable one will be defined by the specifications of a given material and its application. In the case of 316L SS, different peening methods have been compared (i.e. cavitation-driven WJP, impingement-driven WJP, LSP, SP) by employing different processing times in each of them and proposing those parameters that yield the maximum fatigue life in the alloy. Soyama [200] showed that at 10^7 cycles the 279 MPa fatigue strength from non-peened 316L SS specimen could be increased to a maximum of 348 MPa, 325 MPa, 303 MPa and 296 MPa if cavitation-driven WJP, SP, LSP or impingement-driven WJP are employed at their optimum processing times, respectively. Additionally, fatigue testing showed that the crack initiation depth was also different for each of the peening methods, depending on the depth of compressive residual stress (Fig. 35).

While the primary objective of using a peening post-processing technique is usually enhancing the fatigue life of metallic alloys, other positive outcomes can also be taken into account, such as improving stress corrosion cracking (SCC) resistance. Since SCC is promoted by near-surface tensile stresses, the use of peening, which induces a compressive layer instead, opposes to this, making crack propagation a less-likely process. For example, while a waterjet shot-peened (i.e. SP with the shots accelerated by water instead of air) ground surface of 316L SS becomes protected from SCC, up to 50 μm cracks can develop from the pitting corrosion sites that appear during the grinding process in a non-peened surface [206]. Similarly, HCF testing under corrosive environment (i.e. chloride) in Al7075-T651 showed that SP can increase the fatigue strength from 85 MPa to 165 MPa ($N_f = 10^7$ cycles) when compared to the non-peened counterpart [181].

Under the adequate processing parameters, peening improves the overall performance of as-machined metallic alloys and the technique is principally employed for improving the fatigue life of structural components. However, most of the findings in the literature are based on observational studies that consist of testing various experimental conditions and recommending the best parameters for an optimum performance (e.g. optimum waterjet pressure for maximum fatigue life). Even though these are quite significant for a mass production and manufacturing environment, there is still lack of in-depth understanding and justification that links the physical phenomena occurring during the peening process that makes a shift in the material's behaviour under different working conditions.

5.2. Mechanical finishing strategies to enhance the performance of machined components: finish cutting, polishing, burnishing

As discussed in section 2, in general the fatigue crack can initiate through topological or metallurgical defects in the machined workpieces. Hence, except introducing compressive residual stress into the superficial layer through peening process, another one of the methods to improve the fatigue performance is to mechanically remove/reduce the surface defect hence to reduce the risk of crack initiation. The commonly this is achieved by low material removal rate process such as grinding, finish cutting, polishing or through surface mechanical modification, e.

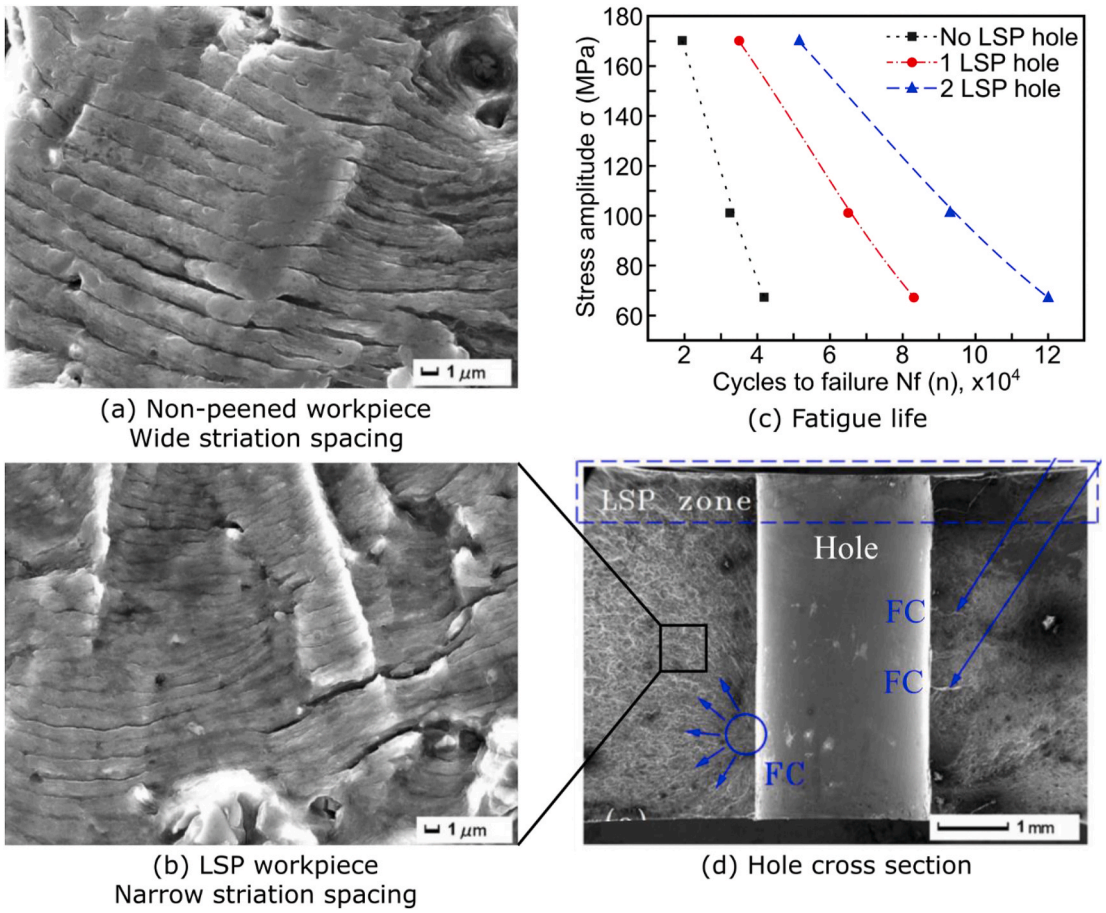

Fig. 34. Local effect of laser shock peening (LSP) on hole fatigue behaviour in AL 7075-T7451 in the vicinity of a 3 mm machined hole. (a) A non-peened sample exhibits wide fatigue striation spacing after a fatigue crack (FC) is created on the hole surface. (b) LSP creates narrower striation bands due to the induction of compressive states. (c) A comparison of fatigue life between these samples, showing that LSP increases fatigue life of the hole significantly under both low and high values of stress. (d) Example of where the striation fatigue bands could be observed in the LSP-worked sample. From Ren et al. [198].

g. burnishing. Fig. 36 shows an example of an improvement of fatigue life of mechanically post processed samples compared to the laser cut results. It was suggested that the metallurgy alternations (i.e. changes from α+β phase to α′ phase on the machined surface) can significantly decrease the fatigue strength due to the higher hardness and lower ductility of this α′-martensite, which has a higher sensitivity for crack initiation and growth. However, a superior fatigue strength was reached for the series with mechanically polished surface (363 MPa) compared to the laser cut surface (235 MPa) [207]. It is also interesting to note that this improvement is also depending on the volume of altered material that has been remove based on the fact that barrel-ground surface has less improvement of the fatigue (351 MPa) as the heat affected zone could be removed only up to 50% by barrel grinding while up to 100% through mechanical polishing [207].

Nevertheless, while most post finishing processes try to remove/reduce the surface defects which may deteriorate the fatigue life, for those components that contain compressive residual stress from initial process the post process may not be advantageous as it may release the original compressive residual stress. In recent research Wu [208] found that while the finish turning process yields high compressive residual stress it also introduces a high plastic deformation layer and surface craters, as shown in Fig. 37. In attempt to remove the surface cavities and plastic deformation through surface circumferential polishing treatment (TCP), a lower compressive residual stress (−86.9 MPa) is accompanied with the post process compared to the as turned sample (231.37 MPa). This surprisingly reduces the fatigue life by 17.5% although the surface defects (cavities and plastic deformation) have been removed. However, when a grinding process is applied on the TCP samples, a comparable compressive residual stress is introduced while the surface defects have been removed. This however leads to increasing fatigue life by 134.2% and 183.7% with oblique grinding (TCPO), and axial grinding (TCPA) respectively.

Burnishing is a post-machining operation in which the surface of the work piece is compressed by the application of a ball or roller to produce a smooth and work-hardened surface by plastic deformation of surface irregularities [209]. Due to the mechanically introduced subsurface plastic deformation and smooth surface the workpiece functional performance (e.g. fatigue) can be significantly improved. As reported by Hua et al. [210], the fatigue life of low plasticity burnishing (LPB) at a pressure of P = 12 MPa (LPB-12), 15 MPa (LPB-15) and 18 MPa (LPB-18) processes is remarkably improved by 37.1%, 62.4% and 82.4% in comparison with the original finish turning (FT) process. This is mainly due to the significantly increased compressive residual stresses that were introduced to the workpiece during the post burnishing process. Moreover, FT specimen is characterized with a single fatigue crack source while the fatigue crack initiate on specimen surface as the maximum equivalent stresses are focused on the specimen surface. However, after LPB processes the fatigue cracks are prone to initiate at surface patches due to the induced surface minimum principal residual stresses which resulted in crack closure during the cyclic loading (Fig. 38) [210].

Besides the improvement of the fatigue life, burnishing can also be adopted to significantly improve the surface quality of materials. This can improve the corrosion resistance and wear resistance of materials. In particular, when burnishing is applied to a machined surface the friction

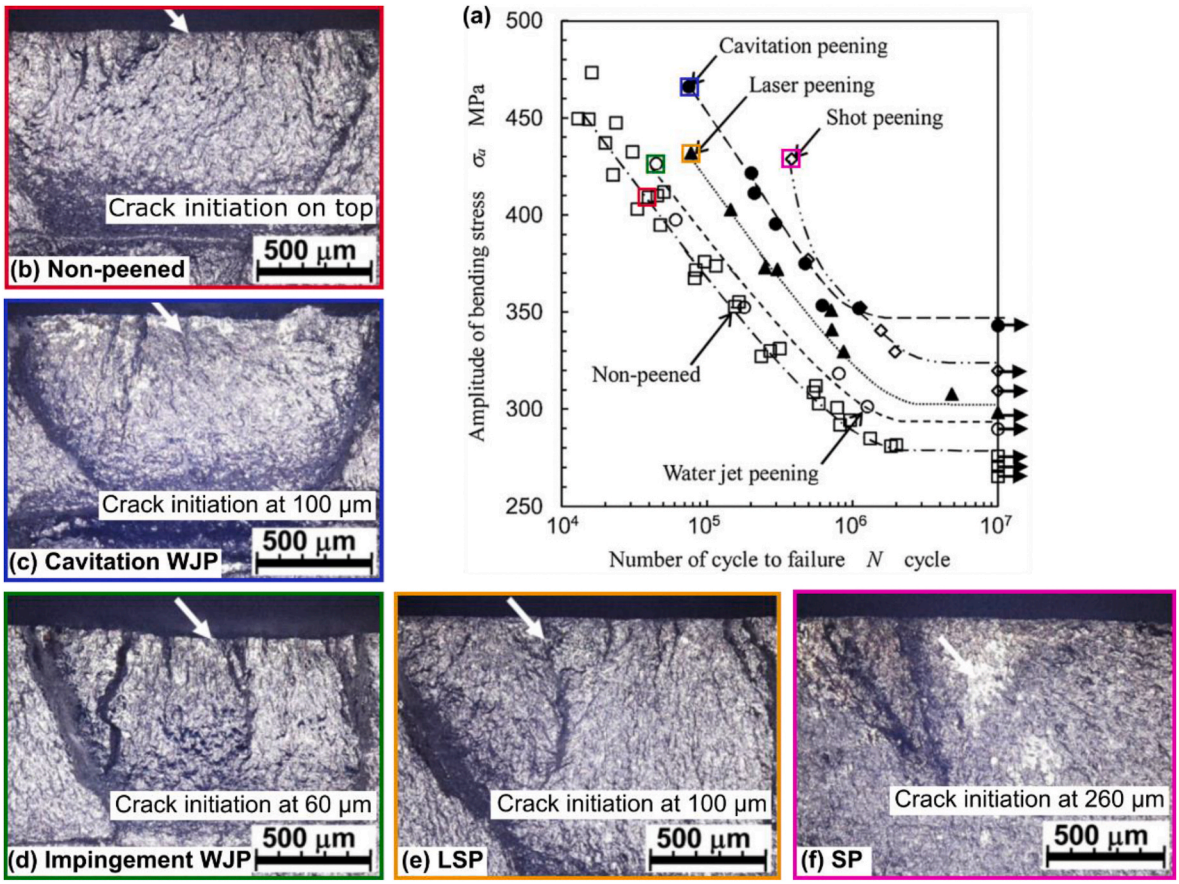

Fig. 35. Comparison of different peening methods on the fatigue life and crack initiation depth of 316L SS, as investigated by Soyama [200]. (a) Fatigue strength curves of all peening techniques. (b–f) Cross sections of the non-peened and peened specimens, where the white arrows show the crack initiation point. (b) Non-peened specimen exhibits crack initiation from the top surface. (c) Cavitation-driven WJP exhibits crack initiation 100 μm below the surface. (d) Impingement-driven WJP exhibits crack initiation 60 μm below the surface. (e) LSP exhibits crack initiation 100 μm below the surface. (f) SP exhibits crack initiation 260 μm below the surface.

coefficient can be reduced up to a critical depth hence improves the wear resistance. This is mainly attributed to the surface work hardening effect with the increased surface hardness and compressive residual stress, that is generated from the severe plastic deformation where condensed grain structure and increased structural homogeneity has been achieved. As shown in Fig. 39 where the wear performance of as turned and subsequently burnished process has been studied [211], the worn surface of the turned specimen showed signs of excessive wear as compared to that of burnished specimen. An in-depth EBSD analysis of the subsurface reveals that the density of sub-grain boundaries and high angle grain boundaries increased due to the high plastic deformation from burnish process, which can lead to dislocation sliding and climbing in the material. The further wear experiment results indicate that the subsurface deformation and work hardening through burnishing can significantly improve the wear resistance as the yielded compressive residual stress and high hardness at the surface layers can hinder the growth of cracks and wear delamination, as shown in Fig. 39 [211].

Burnishing, as a severe plastic deformation (SPD) process, can also generate grain refinement and strong basal texture on the treated surface concurrently hence can remarkably improve the corrosion resistance of the machined workpiece. This is of significance for those materials with poor corrosion resistance, e.g. Mg alloy, with which physical corrosion barriers and smaller grain size can lead to better corrosion resistance. As shown Fig. 40, through burnishing the average grain size on the machined surface of AZ31B Mg alloy can be reduced from 11.9 μm (as ground surface) to 1.4 μm (dry burnished) [212,213]. The corrosion test clearly of as ground AZ31B Mg alloy showed that a relatively large amount of material was lost due to the corrosion effect, wherein large and deep pits are visible all over the surface. However, after burnishing, there are only small pits in some areas of the surface, suggesting much less severe corrosion than in ground specimens. That is, 55% more Mg was corroded from the ground sample than from the burnished ones [212,213] whereby the grain refinement layer can significantly improve its corrosion resistance.

5.3. Beam and spark-based finishing strategies to enhance the performance of machined components

5.3.1. Laser and electron beam

Laser and electron beam finishing processes operate by the remelting of the near-surface of machined metals, with surface tension effects causing flow of what were previously asperities into a smooth remelted surface.

Laser beam polishing induces a remelted layer subject to rapid heating and cooling rates, causing recrystallisation and hardening of the near surface. In case of treatment of machined surfaces, this laser polished region is expected to remelt a significant proportion of it, and hence the laser polished surface properties will likely dominate. A cross-sectional SEM image of a tool steel subject to laser polishing along with an EBSD map of the microstructure is shown in Fig. 41 [214]. In this example, the tool steel was machined by mechanical milling prior to laser polishing, with prior roughness of 0.53 μm, hence this can be considered an example of the effect of laser polishing on a machined surface. The fine cellular structure within much of the laser remelted

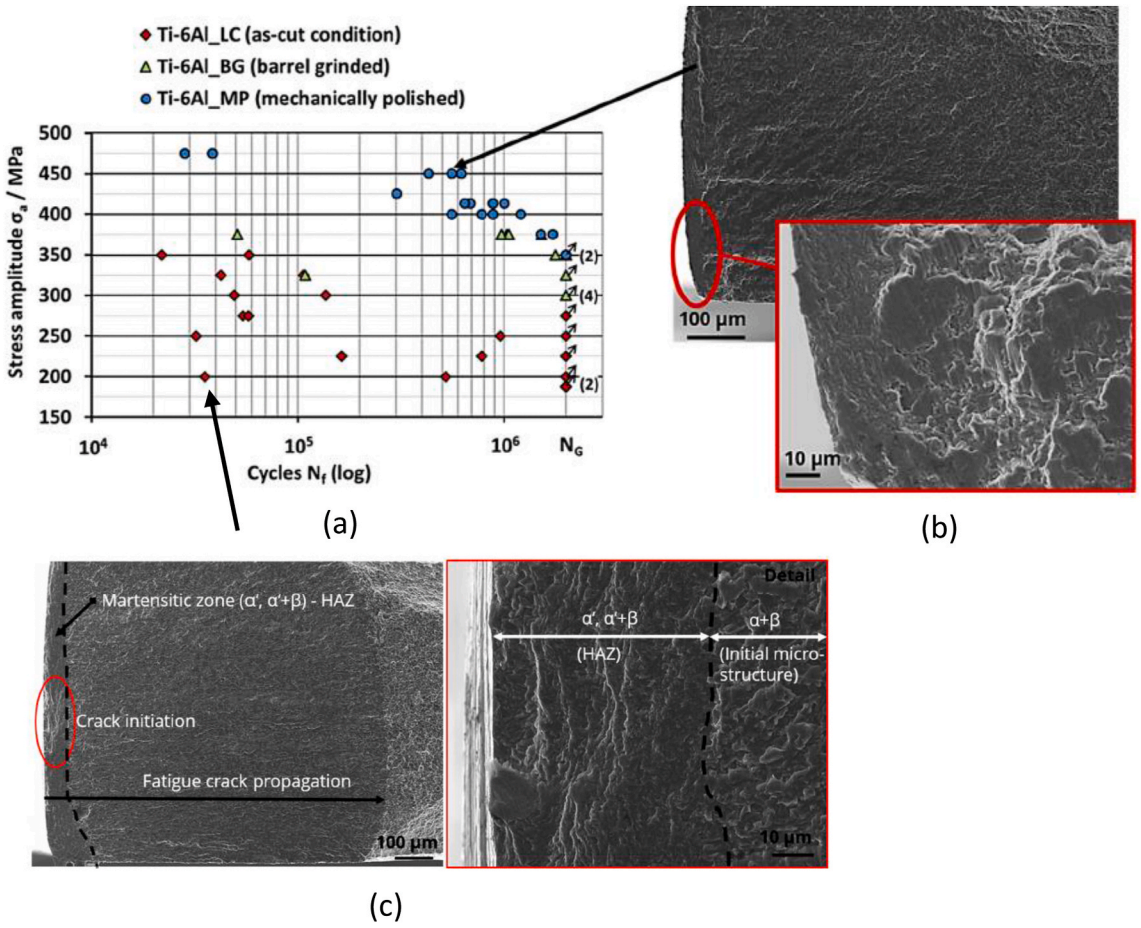

Fig. 36. Fatigue performance of the Ti–6Al–4V-ELI alloy from original laser cutting and post processed by barrel grinding and mechanical polishing. (a) S–N diagram for all three tested sample series; (b) fracture surface with mechanically polished surface conditions and (c) fracture surface of laser cut sample [207].

region is clear.

As discussed and demonstrated in the previous sections, the ability of a process to increase hardness of the near-surface region has significant implications for the enhancement of wear resistance, in particular abrasive wear performance. Hence understanding the effect of laser polishing on hardness is critical to understanding the potential of laser to enhance functional properties. By definition, laser polishing generally reduces surface roughness, eliminating asperities present on the surface, and therefore is particularly applicable to machined surfaces. Some examples of this include a reduction in Ra from 5.01 to 0.44 µm on additive manufactured tool steel [215], and a reduction from 0.53 to 0.05 µm Ra again in tool steel [214], demonstrating the ability of the process to affect and polish multi-scale roughnesses. As is typical in remelting based modification and coating processes, high tensile residual stresses are typically expected within laser polished layers. Up to 926 MPa tensile residual stress has been measured in tool steel subject to laser polishing [214]. In this study interestingly it was observed that stresses in the direction of the remelting tracks were higher than those perpendicular to them, with the latter being explained by partial relief due to plastic deformation. However other work has shown that compressive residual stresses can in be generated, exemplified once again in a tool steel, with a tendency towards compressive when increasing laser beam diameter and laser power as well as number of repetitions via a pre-heating effect [216]. The direction and magnitude of stresses formed and complex and depend on both shrinkage as well as phase transformation.

Several studies have confirmed that laser polishing of various metals induces increased hardness up to 100 µm from the top surface. This effect is exemplified by laser polishing of end-milled Ti6Al4V with an initial characteristic milled surface with roughness 7.3 µm [217], whereby the hardness of the base material is increased from 360 HV to over 450 HV within the top 25 µm of the top surface. The difference was exacerbated in the laser polishing of H11 tool steel (also with a milled surface finish prior to processing) [214], with a hardness dependent on the level of oxygen content in the processing gas atmosphere. It can be noted in the latter study a high tensile residual stress level of up to 926 MPa was measured. Laser polishing of different titanium alloys made by laser additive manufacturing also showed a notable increase in hardness. The refinement of the columnar structure from the additive process, into a fine cellular structure resulted in an increase in hardness from 1.8 to 2.9 GPa. Some examples of the increase in hardness according to cross-sectional depth are shown in Fig. 42.

In the case of laser polished Ti6Al4V increased hardness may be explained by formation of the martensitic phase, as observed by Ma et al. [218]. The increased hardness has shown some evidence of increased wear performance. Ma et al. [218] showed a slight reduction in wear rate for Ti6Al4V and Ti–Al–Mo–Zr–Si of 30–40%, however repeat testing at different loads is needed to clarify this behaviour. However, other work on fretting wear of laser polished stainless steel showed no improvement after laser polishing [219]. Laser polishing has also been demonstrated on additive parts of 316L stainless steel [220]. The refinement of the columnar structure from the additive process, into a fine cellular structure resulted in an increase in hardness from 1.8 to 2.9 GPa. Corrosion behaviour was also improved after laser polishing, explained in somewhat simple terms by a decrease in surface roughness as well as grain refinement, although the exact mechanism behind this improvement requires further investigation.

The schematic in Fig. 43 summarises the enhancements due to laser

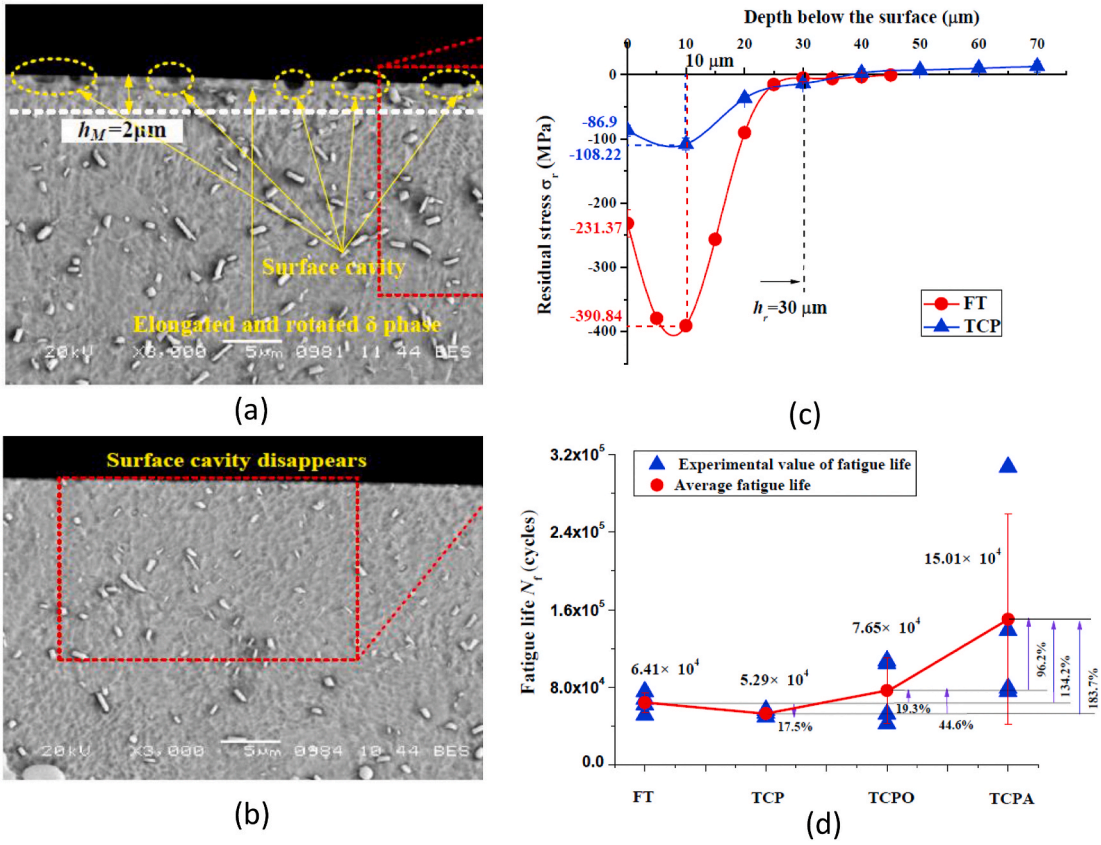

Fig. 37. Microstructures of GH4169 alloy after turning and post-turning polishing treatment. (a) Sample from original finish turning process and (b) subject to post circumferential polishing treatment; (c) Residual stress and (d) average fatigue life of original turning process and different post processes [208].

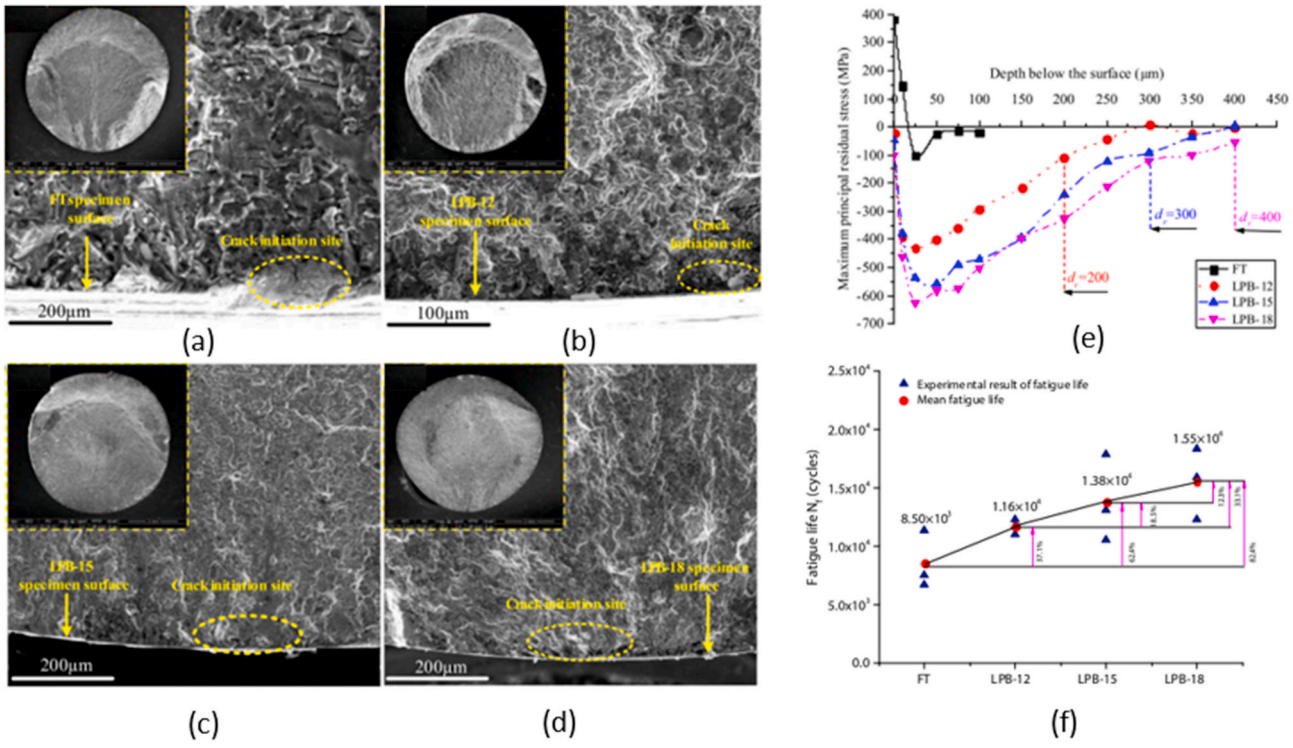

Fig. 38. Fatigue fracture surface morphology after finish turning (FT) and low plasticity burnishing (LPB). (a) FT process, (b) LPB-12 process, (c) LPB-15 process and (d) LPB-18 process; (e) principal residual stress distributions and (f) mean fatigue life after different surface treatments [210].

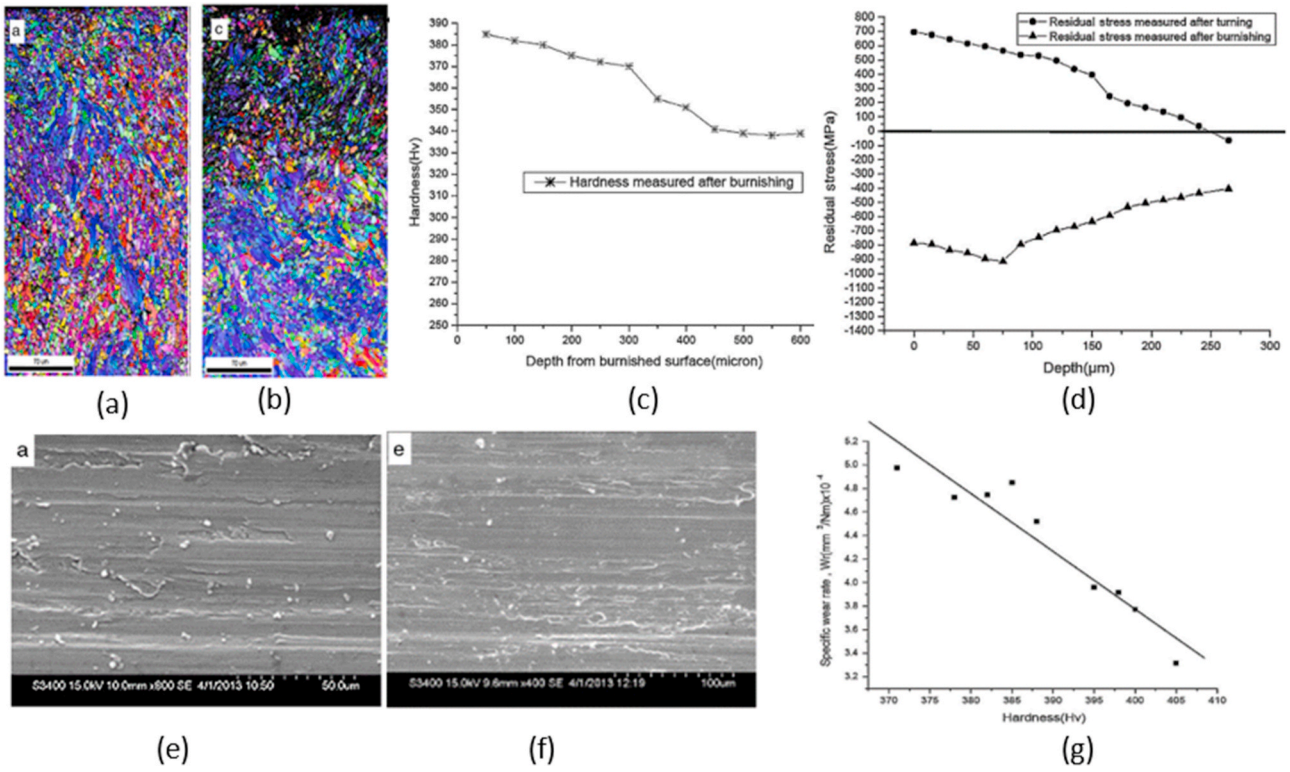

Fig. 39. EBSD orientation maps and surface morphology of Ti–6Al–4V after turning and burnishing. (a) turned and (b) turned & burnished surfaces Ti–6Al–4 V alloy specimens; (c) hardness and (d) residual stress of burnished sample; morphology of worn surfaces of (e) turned and (f) burnished samples; (g) wear rates with hardness of the burnished Ti–6Al–4V alloy [211].

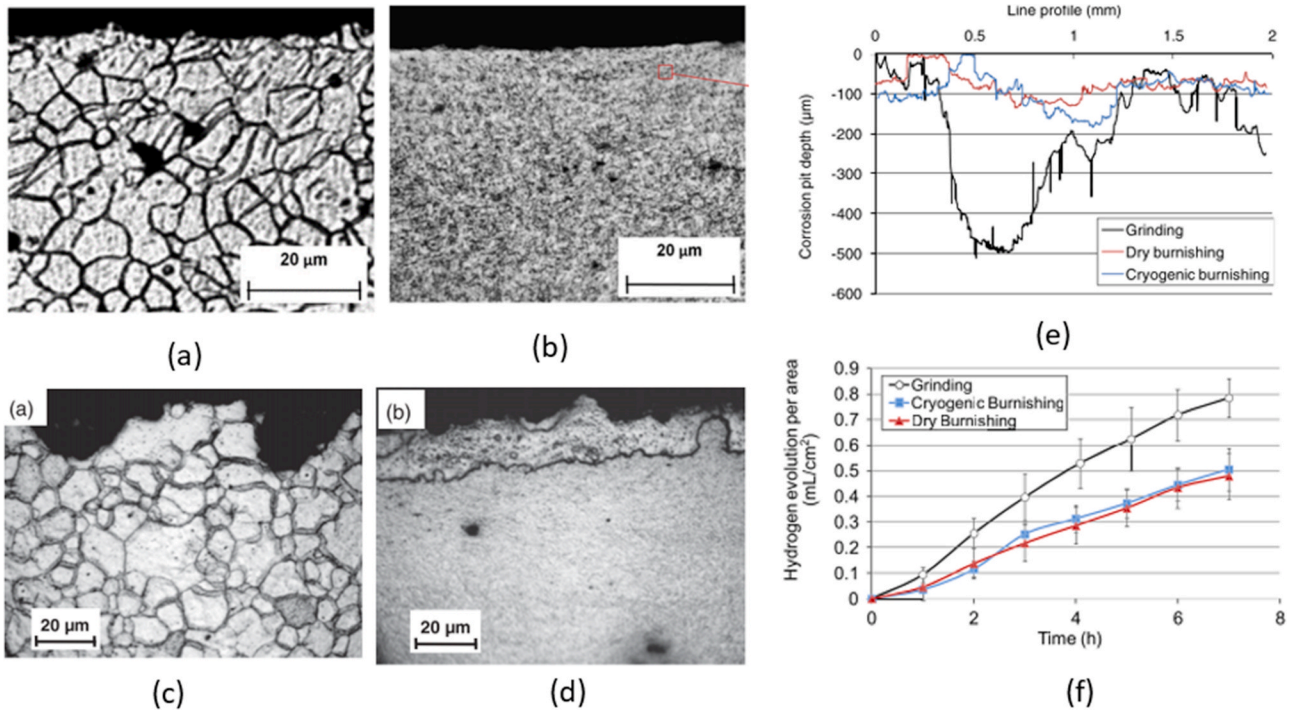

Fig. 40. Machined surface characteristics of AZ31B Mg alloy processed by different machining and post-machining strategies. (a) As ground and (b) post processed by burnishing; corroded surface of (c) as ground and (d) burnished samples; (e) corrosion pit depth profiles; (f) hydrogen evolution of AZ31B samples processed by different treatments [212,213].

polishing which may affect the wear performance of a metal which has been mechanically machined. In summary, laser polishing is expected to yield a fine cellular grain structure in the near-surface region, which will likely be of a smaller scale than the microstructure of a mechanically machined surface layer of a metal. As a result of this, as well as some phase transformations including martensitic phase formation, increased

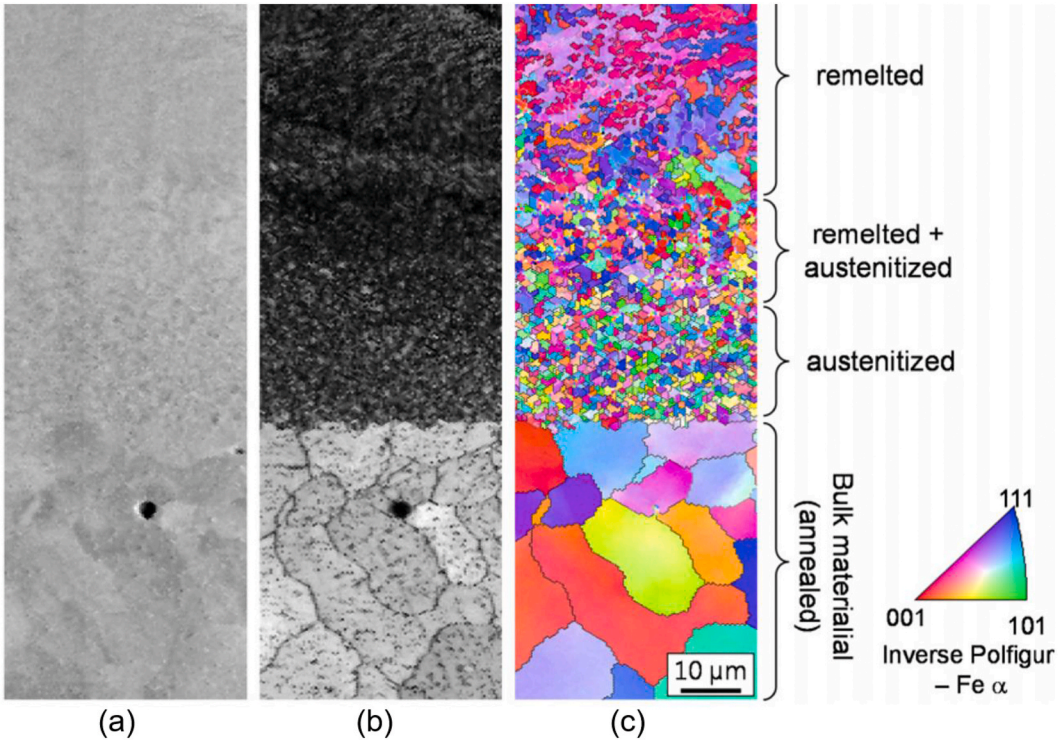

Fig. 41. Microstructural condition of a tool steel subject to a mechanical milling operation prior to laser polishing. (a) SEM, (b) EBSD image quality map and (c) EBSD grain orientation map of the cross-section of a tool steel subject to laser polishing [214].

hardness is expected. Laser polishing smoothens surfaces which exhibit a machining induced roughness, and this tends improve wear resistance. However high tensile residual stresses are expected as a result of contraction of the molten layer upon cooling, which may reverse, or increase in magnitude that residual stress from a machined surface. Such stresses are correlated with increased wear rates. Enhancements to microstructure/density as well as surface finish also show evidence of improving chemical behaviour in a limited case.

High current pulsed electron beam irradiation (HCPEB), despite being a somewhat niche technology, has been subject to a significant research effort to understand its effect on enhancing, in particular, mechanical properties, and the underlying microstructural reasons behind it. The process is particularly applicable to the treatment of machined surfaces, and in particular those of complex shapes, for example produced by EDM or complex milling, given its ability to modify high angle surfaces in a similar manner to those perpendicular to the beam direction [221,222,223]. Its large area (60 mm circle) effect also makes it highly useful for such surfaces. In addition, the scale of the layer modified by this process matches the scale on the fine end of machining induced surface layers, and is an appropriate treatment techniques for such surfaces.

To understand the potential for modifying the properties of machined layers via HCPEB, it is important to understand the hardening modes taking place in a generic sense. Hardening is perhaps the most commonly identified modification induced by HCPEB. HCPEB can act through heating or melting modes. Below the energy density threshold to induce melting, pulsed heating via HCPEB leads to plastic deformation and formation of a non-uniformly hardened zone up to 100 µm depth, with maximum microhardness located at ~20 µm depth [224], using pure iron as an example. Microhardness is correlated with the change in dislocation density with depth. Without reaching the melting threshold, recrystallisation occurs with nucleation at the grain boundaries and this zone typically has a thickness of ~5 µm [225]. When the melting threshold is achieved through an increase in beam parameters, and ultimately energy density, the rapid crystallisation from the melt dominates the microstructure of the surface layer [224]. An increase in melt thickness, caused by an increase in energy density, results in a decrease in melt cooling rate from 10^{10} to 10^{9} K/s. Given the complex heating, cooling and phase transformation phenomena taking place as well as the dynamic intense stress wave induced, residual stresses produced in materials modified by HCPEB are complicated and difficult to predict. Conventionally it would be assumed that tensile stresses are generally produced, but evidence has suggested this can vary between materials. Tensile residual stress over 700 MPa were produced in the modified layer in a tool steel finished by mechanical grinding, from a compressive stress in the virgin material [226]. However in the cases of zirconium [227], aluminium [228] and TiNi [229] compressive residual stresses have been detected. A complex balance of factors including intensive stress wave, shrinkage and phase transformation guide the stress direction and magnitude. In addition, in multi-phase materials the two phases may exhibit two different residual stress levels.

The microstructure formed in metals by HCPEB under melting mode is fairly consistent and predictable. Within the top 100 nm of the surface, the finest grains are produced, typically of a size of 10s of nm [221,230], as represented in Fig. 44. This has been demonstrated in stainless steel subject to electrical discharge machining [221]. Beneath this is a layer of grains on the order of 100 nm. Beneath this is a region of larger grains, which may have preferential orientation [221,230]. Markov & Rotshstein [231] observed a hardened surface zone which could be produced using short pulse (10 µs) electron beams. It was observed that this hardening effect could occur from solidification from the liquid state as well as from the solid state, without transformation of material into liquid, via quench hardening. This general microstructure can have a significant impact on the mechanical as well as corrosive performance of materials subject to HCPEB. In stainless steel, HCPEB has shown to significantly enhance its corrosion resistance, owing to the effective production of a strong, fine grained passive film in the form of the modified layer, and avoidance of pitting corrosion [224]. Passivation data for two stainless steels subject to HCPEB is shown in Fig. 45. Similarly, improved corrosion behaviour was shown in a HCPEB

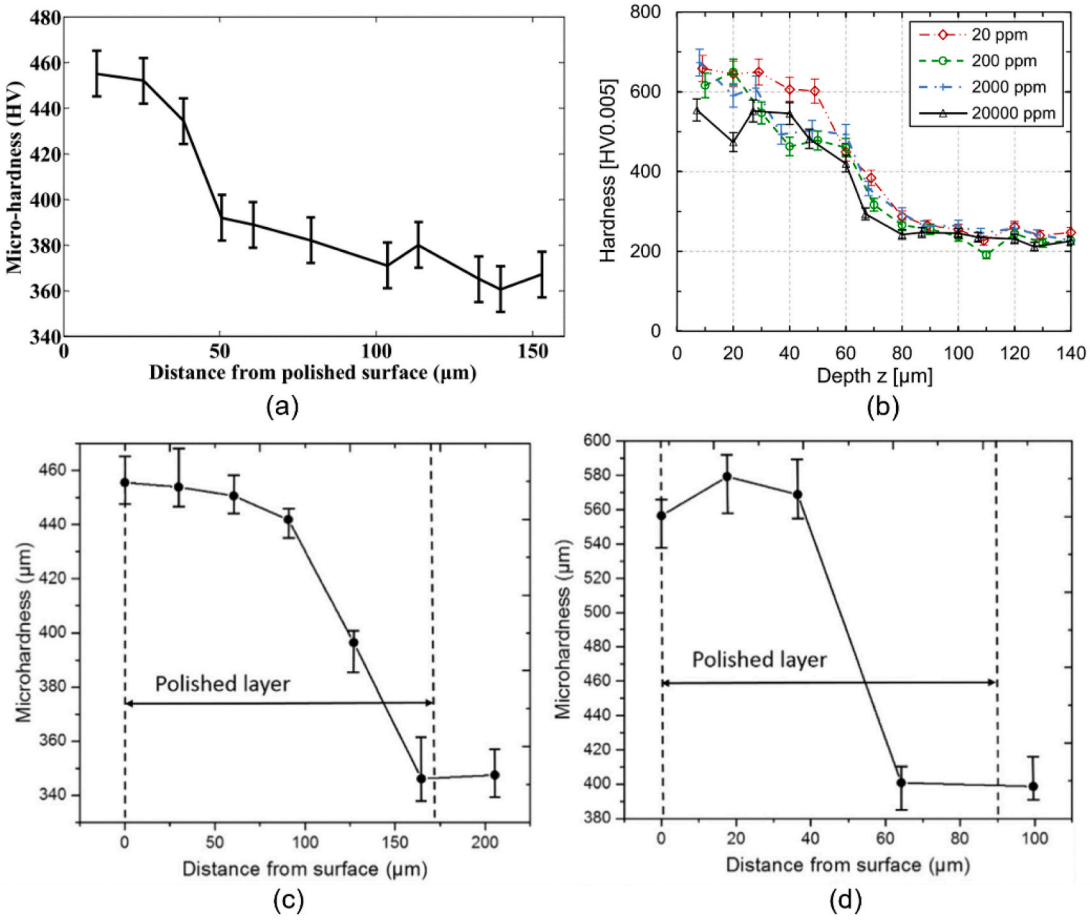

Fig. 42. Examples of increased hardness in the top 100 μm of surfaces after laser polishing of advanced alloys machined through different strategies. (a) Ti6Al4V subject to end-milling with an initial surface roughness of 7.3 μm [217] and (b) in milled H11 tool steel (initial roughness of 0.53 μm), with varying amounts of oxygen in the processing gas atmosphere [214], (c) Ti6Al4V made by laser additive manufacturing [218] and (d) Ti–Al–Mo–Zr–Si made by laser additive manufacturing [218].

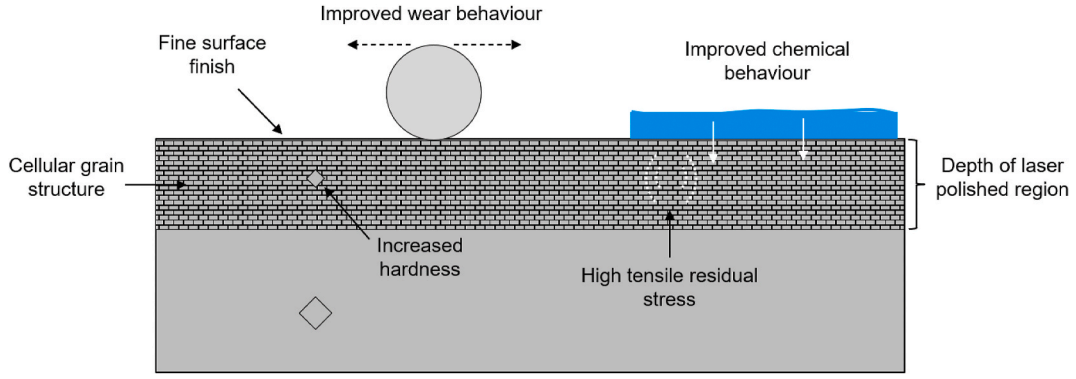

Fig. 43. Effect of laser polishing on mechanical and chemical properties and performance. Increased hardness and wear behaviour are often expected. There is also some evidence of improved corrosion behaviour.

modified titanium material via the creation of a precipitation-free layer via remelting [232]. High pressure corrosion behaviour has also been shown to improve under 500 °C, 10.3 MPa superheated steam in a zirconium alloy, however the reasons for this improvement was multi-faceted, although dissolution of alloying elements was thought to play a key role [227]. It should be noted that in the above cases, the presence of a machined induced surface layer is not expected to play a significant role in the end microstructure of the modified layer and resultant mechanical and corrosive properties, and hence machined surfaces are appropriate workpieces for such modifications.

Given near-surface hardening is universal to materials processed by HCPEB, wear is perhaps the most commonly researched functional property and there is a range of good evidence behind enhancement to wear resistance. Aluminium alloys are of particular research interest, especially Al–Si alloys, given their current use in high wear scenarios such as automotive engine cylinder liners. Some examples of this include the reduction in specific wear rate of up to 66% in an Al–Si A390 alloy treated by HCPEB after mechanical machining to an Ra roughness of

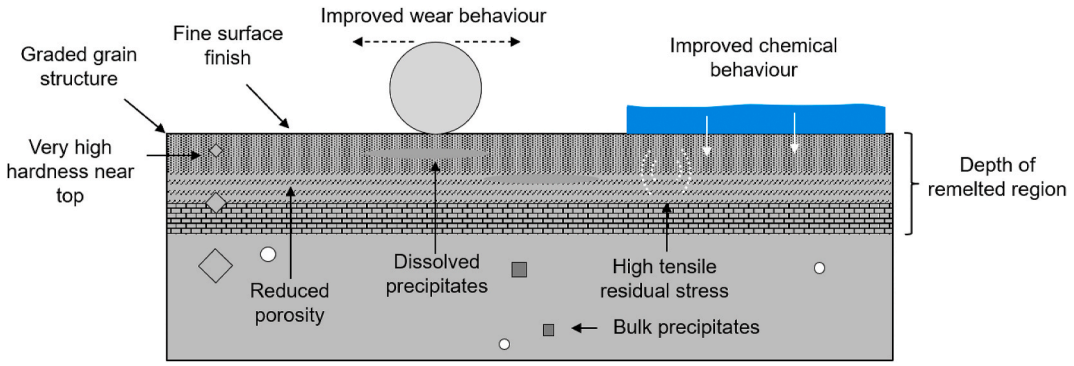

Fig. 44. Effect of HCPEB on structural/mechanical properties and wear and chemical performance.

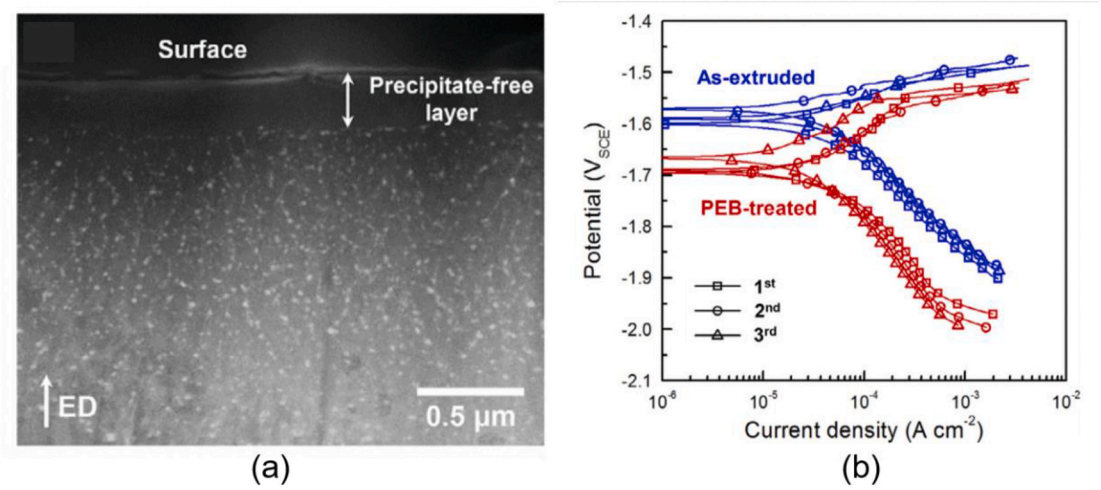

Fig. 45. Surface characteristics induced in magnesium by HCPEB. (a) Precipitate-free layer induced layer in magnesium induced by HCPEB [232] and (b) resultant improved potentiodynamic curves [232].

3.14 μm [234]. In this case the greater tendency to form a beneficial oxidative tribo-layer under dry-sliding wear reduced overall wear rate, despite increased friction. In the case of an Al-11.1%Si alloy, a decrease in specific wear rate by a factor of 18–20 was explained by an increase in microhardness by a factor of 3.2 (from 0.73 to 2.34 GPa) [235]. Improved hardness was explained by the sub-micron grain structure formed in the near-surface [235]. Steels have also shown evidence of improved wear behaviour, for example the surface of Hadfield steel used for long service-life die-inserts subject to pulsed electron irradiation yielded increased micro-hardness as well as enhanced wear resistance owing to the formation of a nano-scale grain structure [236]. The presence of residual stress in both the ferrite and austenite phases of AISI D2 steel has been confirmed [226], whereby after 25 pulses of a mechanically polished surface the austenite phase has a tensile stress value of 700 MPa, and the ferrite is comparable at 730 MPa. Despite the softening effect observed at the top surface of polished 316L steel after irradiation, an increase in hardness and an improvement in wear behaviour were seen, which is thought to be due to work-hardening of the heat-affected zone beneath the remelted layer [237].

Enhanced wear behaviour after HCPEB treatment is also exemplified in harder materials such as WC-Co composites which may be prepared by machining at the final stage. In one study, melting of the near surface by the irradiation process caused melting and fracturing of the WC particles, resulting in a nano-scale grained layer consisting of new phases including $Co_3W_9C_4$ [233], as shown in Fig. 46. A reduction to one eighth of the untreated wear rate was seen, although overuse of HCPEB led to severe surface cracks. Ivanov et al. [238] applied the improvement in surface hardness to the treatment of WC-TiC-Co cutting tools. Again, increased hardness was measured up to depths of about 10 μm and relative wear during cutting tests was also reduced at high cutting speeds. The improved mechanical properties were explained by TEM observations of a fine grain structure in the remelted layer, thereby improving grain boundary strengthening as well as the segregation of nanosized carbide particles, resulting in solid solution strengthening. Achieving nanostructured layers at the surfaces of metals is a research goal in its own right with significant implications for mechanical properties. Therefore, the ability to achieve a uniform layer of nano-structures on large and complex shaped surfaces is highly desirable and applicable to machined surfaces.

5.3.2. *EDM coatings to enhance the performance of machined components*

Electrical discharge coatings (EDC) are particular relevant to this review, as they are effectively formed during a modified machining process. The scale of coating generated matches closely to the scale of machined white layers, and the process has the ability to convert such white layers containing defects into a mechanically favourable layer. The process has attracted interest for its ability to generate hard, wear resistant coatings. EDCs are particularly applicable to EDM'd materials, since the operation can be carried out immediately after machining in the same tool-workpiece setup. However, there is no limitation to the type of surface the process can be applied to, as long as the substrate is electrically conductive. The ability of EDC to deposit hard and high melting point materials such as TiC, as well as the overall typically fine microstructure generated, makes it an attractive adaptation of the EDM process. The wear performance of thin TiC coatings on steel substrates has been investigated in detail by Algodi et al. [239]. As discussed in the

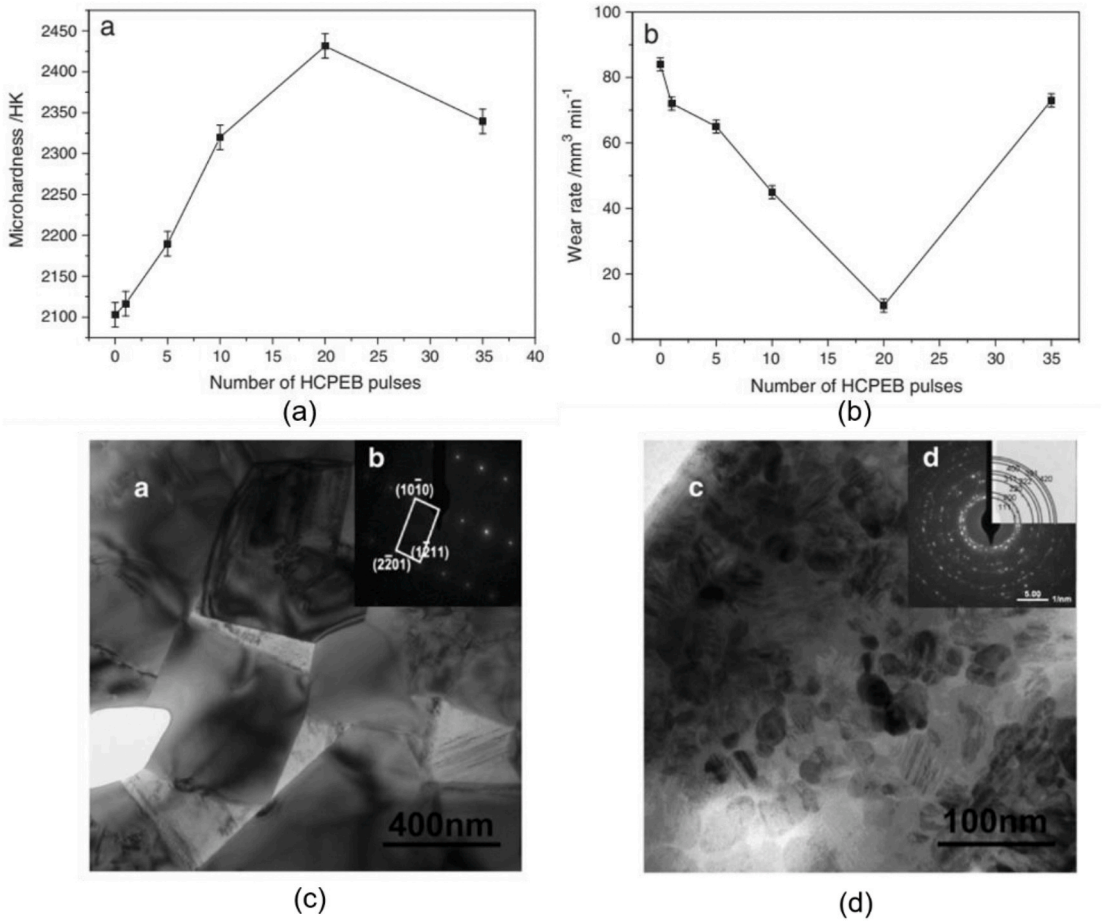

Fig. 46. WC-Co after HCPEB treatment [233]. (a) Microhardness after increasing numbers of pulses, and dry sliding wear rate of the resultant surfaces. (c) and (d) TEM images of the microstructure of the near-surface after 1 and 20 pulses respectively, revealing fine nanostructure in the highly modified surface.

thermal effect section, coatings made via EDC comprise a composite of the deposited material and substrate material drawn into the molten layer. Dry sliding wear rates for two substrates at two different loads are shown in Fig. 47.

The TiC coating, which is effectively a TiC–Fe composite [240], showed superior wear behaviour in the case of deposition on both high speed steel and stainless steel substrates, by factors of approximately 10 and 100 respectively. This trend is for both the 10 and 50 N loads used. Interestingly, the disparity in absolute wear rates between coatings made on the two different substrate materials, also support the concept of EDC as composites comprising substrate and deposited material. In the case of the TiC coating on HSS, wear rates are all notably lower, explained by the higher hardness of the HSS compared to the 304 stainless steel. In effect, the substrate material present between deposited TiC particles plays a role in the load bearing/wear process. It should be noted that in these TiC based coatings, cracking and porosity are sometimes observed and such defects are known to have a strong influence on mechanical properties. However, of particular note is that despite such defects, wear performance was 1–2 orders of magnitude superior to the substrate material alone.

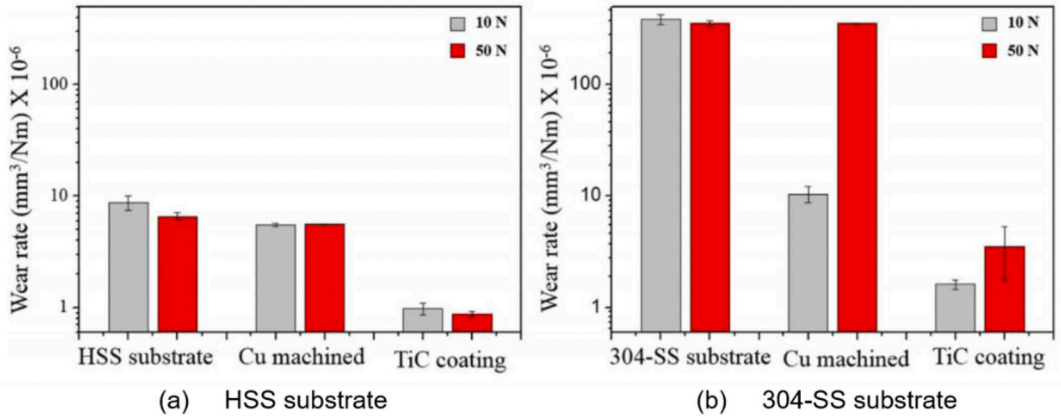

Fig. 47. Reduced specific wear rates under dry-sliding mode of TiC based EDCs compared to two substrate materials on which the coatings were made, and a material machined using a normal EDM copper electrode [239].

An example of a more exotic material combination useful for wear resistance was produced by Li et al. [241], who used a novel method of producing a wear resistant EDC using a titanium electrode combined with a dielectric mixed with reduced graphene oxide nanosheets. The coating's banded microstructure revealed by TEM and dry sliding ball on flat specific wear performance against silicon nitride balls are shown in Fig. 48 (a) and (b) respectively.

Other researchers have noted improved wear behaviour of EDCs, for example coatings from WS_2 and Cu powder electrodes yielded superior wear resistance compared to a mild steel substrate [242]. In this study the initial preparation method for the workpiece prior to coating was not described, however the EDC process is not thought to be particularly sensitive to initial surface roughness/texture. TiCN coatings on polished carbon steel substrates formed from a titanium electrode and nitrogenous oil yielded lower wear than a TiN PVD coating at loads above 30 N [243]. This was explained by an improved microstructure, however a detailed microstructural analysis to directly compare the behaviour was not conducted. A detailed wear study was performed using TiC based coatings from TiC powder metallurgy electrodes deposited onto types of steel substrate [239]. It was shown that due to the composite nature of the coating, the uptake of material from the substrate has a strong influence of the wear performance of the final coating, with coatings on the softer substrate yielding worse wear behaviour. In these TiC based coatings, cracking and porosity are prevalent and such defects are known to have a strong influence of mechanical properties. A schematic representing the features of a ceramic based composite EDC is shown in Fig. 49.

Several attributes illustrated in Fig. 49 are responsible for the good mechanical wear behaviour of ED coatings which are deposited on machined surfaces or coated simultaneous to machining. The composite nature of the coating manufactured using for example TiC as the deposition material, offers hard-facing particles exposed to the adjacent wearing surface. The nature of the manufacturing process results in capillary action of substrate material up to near the surface, surrounding the ceramic particles, in effect offering ductile "cushioning" to the particles deposited in the solid, semi-solid or molten state [244]. This composite structure has good potential for hard-wearing surfaces and this has been well demonstrated. Although porosity is expected to still exist in the EDC surface, so far research has shown quite low levels, perhaps explained by the flow of metal substrate material around the deposited material, and the generally gradual, incremental nature of the coating process. Nevertheless, cracking is evident in coatings made via this process and this will without doubt have some negative effect on ultimate performance.

5.4. Electrochemical/chemical finishing strategies to enhance the performance of machined components

Chemical and electrochemical finishing are widely applied to remove or modify near-surface layers affected by prior machining operations [1]. Removal mechanisms like electropolishing eliminate defects like micro-cracks and inclusions that act as stress concentrators and fatigue crack initiators from machined surfaces, while modification mechanisms such as anodization and plating enable the adaption of near-surface chemical composition. Both types of processes can beneficially affect the functional performance of machined parts.

Chemical and electrochemical polishing (EP) mechanisms after machining remove surface material without imparting stress or thermal energy into the workpiece or modifying surface chemistry. The beneficial effects of chemical and electrochemical finishing on fatigue lives are well understood, wherein the processes chemically remove machining-induced surface defects, inclusions, and microstructural features that are known to act as fatigue crack initiators. For example, EDM is known to generate severe recast layers that can significantly affect the fatigue strength of machined parts (Section 2.4.1). In addition to high cooling rates, the metallurgy of the EDM recast layer can undergo a martensitic phase transformation in Ti-alloys, both of which are associated with increased tensile residual stress at the surface. Janeček et al. [245] showed that electropolishing ED-machined Ti–6Al–4V resulted in high run-out stress (550 MPa) at 10^7 cycles in comparison to the unpolished sample (<100 MPa). The authors reported hundreds of discrete initiation sites in the unpolished material distributed homogeneously around the sample, at the defective surface. Mower [65] investigated finishing surfaces machined with state-of-the-art EDM processing, and also showed that the intrinsic fatigue strength of Ti–6Al–4V alloy could be re-established upon post-processing. Both EP and chemical polishing were shown to improve the fatigue life of EDM parts (10^7 cycles).

Microstructural alteration of 304LN stainless steel has been reported during fatigue testing as a result of EP, leading to a secondary hardening effect [246]. Longer LCF lives of EP specimens led to strain-induced α′-martensite during loading, increasing stress amplitudes in deformation. Gao et al. [247] investigated the effect of different surface finishing methods on the fatigue strength of ground steel specimens (40CrNi2Si2MoVA). The authors reported that EP could improve fatigue limits in comparison to the ground specimen due to a reported decrease in surface toughness, although the improvement in fatigue limit was less than that reported from shot peening, which induced compressive residual stresses at the surface. In addition, the authors reported that hard Cr plating decreased fatigue limits due to the tensile stresses in the plated

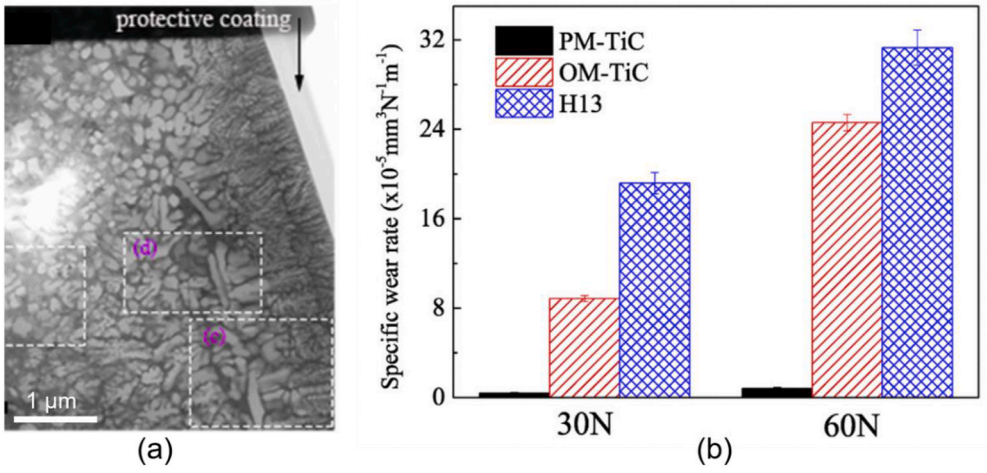

Fig. 48. Surface properties and wear performance of TiC coatings. (a) Microstructure of TiC coating produced using a titanium electrode graphene oxide nanosheets mixed into the dielectric and (b) significantly improved wear behaviour of specific wear rates of TiC made using graphene oxide powder-mixed into the dielectric [241]. The workpiece was prepared prior to coating by mechanical grinding to a roughness of approximately 0.1 μm Ra.

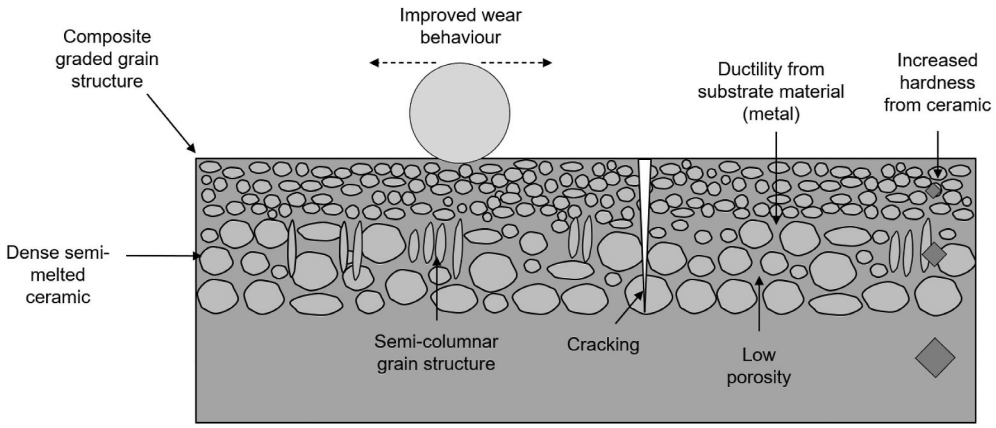

Fig. 49. Main features impacting performance of a ceramic composite ED coating.

layers (Fig. 50a). The residual stress profiles resulting from electro-polishing is shown to be neutralised from that of the ground material, which displayed mild compressive residual stress, due to the removal of the surface layer. Improvements in fatigue performance upon EP have also been reported in 316L stainless steels, compared with ground surfaces, under 3- and 4-point bending fatigue loading conditions [248].

Alternate electrochemical finishing methods, like anodization, modify the composition of near surface layers through a conversion coating mechanism. Anodization processes are generally limited to materials that readily form passivating films such as Al- and Ti-alloys and are industrially applied post-machining in order to improve corrosion resistance. Limited research has been undertaken regarding the influence of anodization treatments on fatigue performance, however it has been reported that such treatments can degrade fatigue strengths in comparison to untreated materials, due to micro-crack propagation to the bulk [250] and tensile residual stresses [251] in the coatings. For example, Shahzhad et al. [249] reported reduced fatigue strength in an anodized 2XXX series Al-alloy. Prior to anodization, the material was treated by chemical pickling, which was shown to create surface pits (Fig. 50b) by preferentially attacking the boundary regions between the alloy and intermetallic particles. The authors showed that these pits presented additional sites for fatigue crack nucleation (Fig. 50c). Fatigue cracking was shown to originate at multiple sites in the anodized coating (Fig. 50d) that propagated through to the bulk material (Fig. 50e).

Electrochemical and chemical finishing processes can affect corrosion resistance after machining, by changing the near surface composition, stress state, and topography of materials. The latter can be associated with the elimination of micro-cracks, or the generation of new topographies that modify the fluid-facing properties of the part. Corrosion behaviour of machined surfaces after EP and chemical finishing is often studied in the chemical environment to which the material would be applied. For example, Ni-alloys and stainless steels exposed to high-temperature environments in aerospace and land-based power generation, and NiTi and Ti-alloys to simulated biological environments.

In aerospace Ni-superalloys, Montero et al. [252] investigated the influence of different surface treatments on the hot corrosion resistance of a single crystal Ni-superalloy (TMS 138), when exposed to hot corrosion environments. The authors reported that in Type I hot corrosion (900 °C, Na_2SO_4 salt deposit, 0.1 vol% SO_2 with synthetic air), the prior EP treatment that promoted modifications to the γ-γ' partition (Fig. 51a) led to greater corrosion depths and TCP formation. In other Ni-alloys, the effect of EP on corrosion resistance in high-temperature water environments has been investigated. Han et al. [253] studied Ni-alloy 600 when exposed to simulated primary water (320 °C, 1–500 h). The authors noted that preferential dissolution of Ni and Fe during prior EP led to the formation of a Cr-enriched inner oxide layer upon exposure to the hot water environment (Fig. 51b). Shim et al. [254]

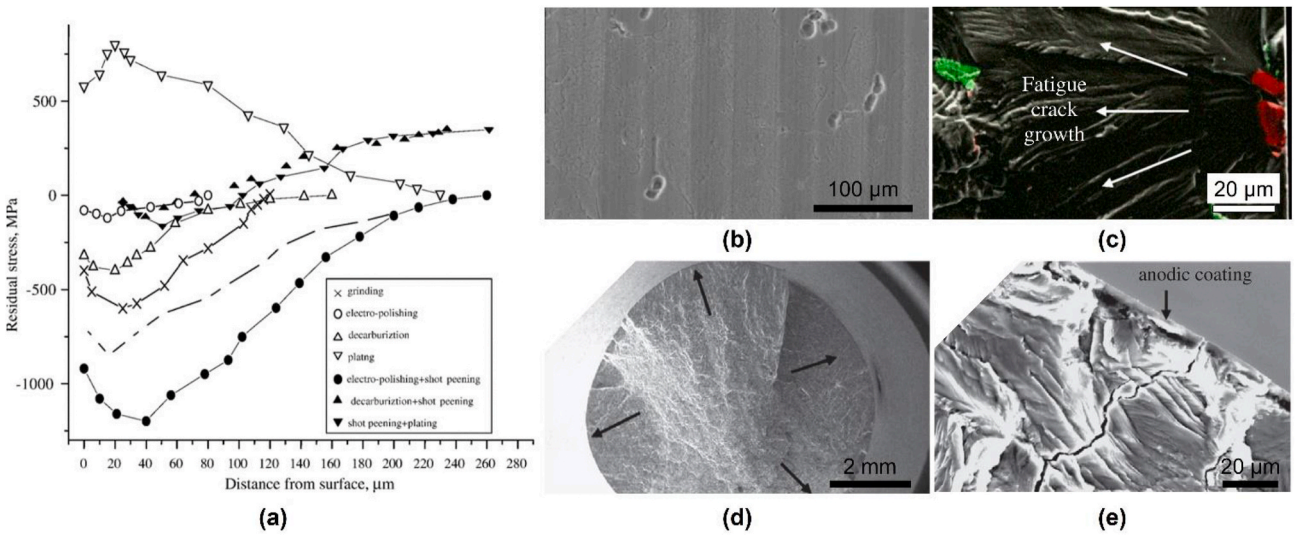

Fig. 50. Effect of chemical and electrochemical finishing on fatigue strength after machining. (a) Residual stress depth profiles resulting from different surface finishing operations after grinding, Gao et al. [247]. (b) Micro-cracking and crevices in unloaded pickled and anodized Al-alloy machined by turning, (c) fatigue cracking from inclusion. (d) Crack initiation from multiple initiation points, (e) at the anodized surface. Shahzhad et al. [249].

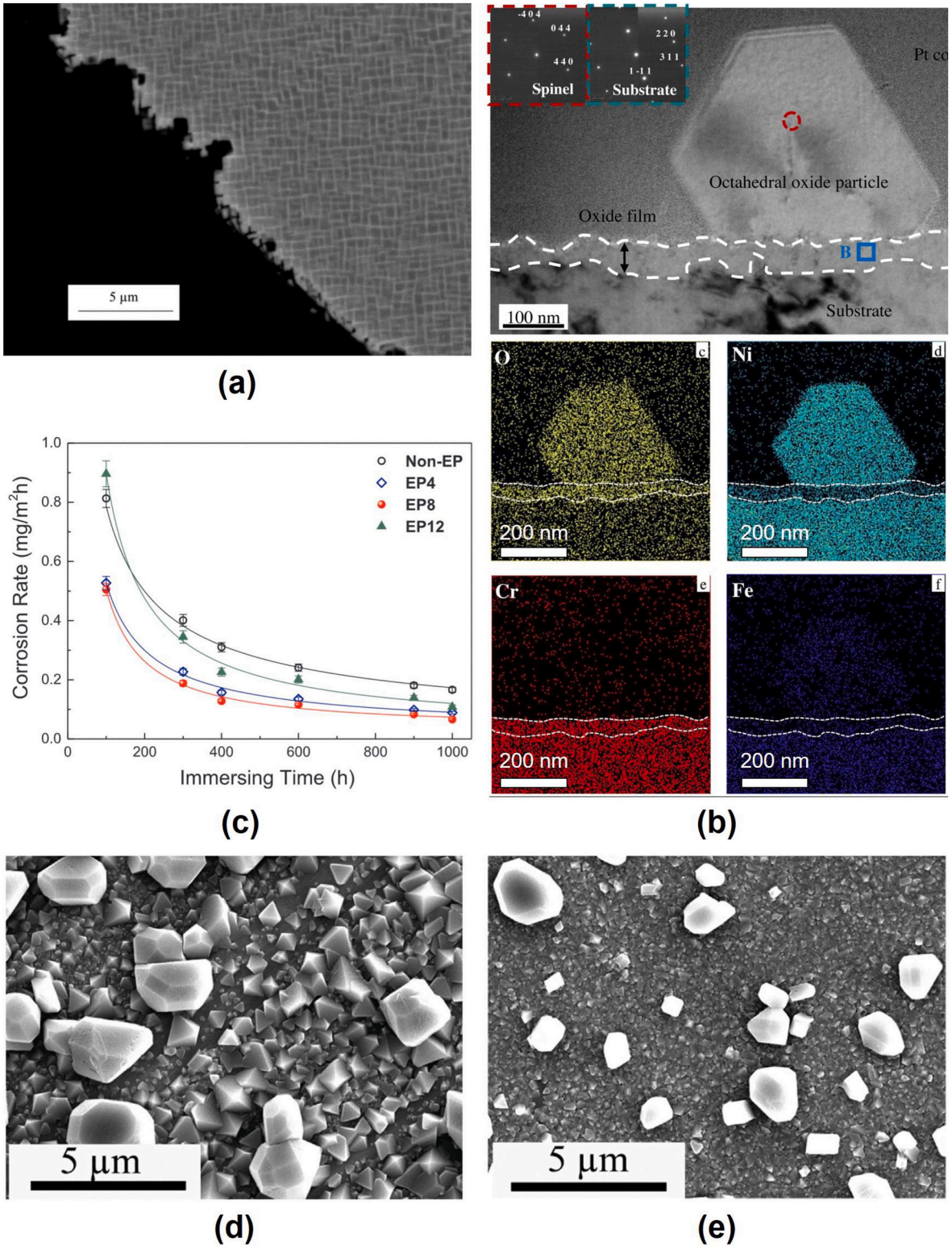

Fig. 51. Electropolishing influences surface oxidation of machined materials at high temperatures. (a) SEM micrograph showing preferential dissolution of γ-matrix resulting from EP, previously machine by EDM. This metallurgical modification affects Type I hot corrosion resistance. Montero et al. [252]. (b) TEM micrograph of the oxide layer of EP alloy-600 after grinding and EP, showing both octahedral outer oxide (spinel group) and inner oxide layer, with EDS maps after EP. Han et al. [253]. (c) Influence of EP time on corrosion rate in alloy 690. Shim et al. [254]. (d) Ground surface and (e) electropolished surface subjected to high temperature water. Fewer large outer-oxide particles are formed on the EP surface, indicative of reduced mass transport of species to the outer layers. Han et al. [255].

studied the influence of EP conditions on the corrosion rates of Ni-alloy 690 in water (330 °C, 100–1000 h). While lower corrosion rates were reported as a result of the elimination of machining marks at low EP times (4–8 min), the authors noted an increase in corrosion rates when EP time was increased to 12 min (Fig. 51c), which was correlated to the formation of dimples around grain boundaries that acted as pathways to atomic diffusion at elevated temperature. The effect of EP on corrosion is therefore determined by the final topography as well as the modified near surface composition.

Similar phenomena have been observed in stainless steels after machining operations such as grinding, where EP-induced compositional modification of passive films has been reported to affect the corrosion resistance. Lee and Lai [256] showed that electropolishing of 316L stainless steel improved corrosion resistance by changing the oxide layer composition from predominantly Fe_2O_3 to Cr_2O_3. This was due to Cr-enrichment of the near surface by EP. Ziemniak et al. [257] showed that the removal of machining-induced surface microstrain through EP reduced the corrosion rates of 304 stainless steel exposed to high temperature water (260 °C, 1000–10,000 h). The authors reported the presence of low porosity, uniform, protective corrosion layer upon EP. This uniformity was correlated with the absence of local high microstrain sites that enabled preferential nucleation of the surface oxides; nucleation was reported to occur across the surface leading to a compact oxide layer. Han et al. [255] exploited prior EP treatments to improve the oxidation resistance of 316L stainless steel when exposed to a simulated water reactor environment (310 °C, 120 and 500 h). The authors observed different oxide size distributions between the ground and EP specimens after exposure (Fig. 51d–e), with the latter dominated by a thicker compact layer, which led to increased oxidation resistance. This was attributed to fewer nucleation sites and slower cation diffusion through Cr-rich oxides in the EP specimens, preventing the larger grained oxide formation.

In NiTi-alloys exposed to simulated physiological environments, finishing with EP after machining can improve the corrosion resistance and reduce the Ni-release rate by forming passive TiO_2 layer on the surface in comparison to the non-EP material [258]. Chu et al. [259] demonstrated that the thin (10 nm) TiO_2-dominated surface phase contained no detectable Ni. The authors showed that prior EP mitigated the out-diffusion of Ni ions in comparison to chemical polishing. Milošev and Kapun [260] investigated the surface compositions resulting from ground NiTi surfaces and those resulting from EP and chemical etching. The authors reported that while grinding depleted surface Ni concentrations enriching the surface with Ti and Ti-oxides, EP enriched the surfaces with metallic Ni and Ti by preferentially removing hard Ti-oxide asperities. This composition, and the smoother topography was reported to improve corrosion resistance in simulated physiological solutions. Similar EP-induced surface oxides (e.g. Al_2O_3) have been reported to improve the corrosion resistance of Al-alloys after EP in aqueous and non-aqueous electrolytes [261], which could reduce machining-induced corrosion. Altering the fluid-facing properties by electrochemical surface processing after machining has been shown to adapt corrosion resistance. For example, the formation of superhydrophobic surface by electrochemical etching on material machined by EDM prevents wetting by trapping air to prevent corrosion induced charge transfer [262].

The effect of EP as a post-processing method on wear rates after machining operations has been the subject of limited investigation, however comparative studies with other finishing processes have indicated differences in resulting tribological performance. For example, Zeng et al. [263] compared prior EP with mechanical polishing (MP) of a CoCrMo-alloy, showing that the specific wear rate of the EP specimen was less than that of MP. The authors reported the absence of mechanical deformation and recessed carbides in the near surface after EP, and protruding carbides and significant deformation after MP. Alternate electrochemical finishing methods have been applied to improve wear performance after machining processes. Anodization and spark anodization (plasma electrolytic oxidation) are exploited as conversion coating mechanisms to generate hardwearing, well adhered, and chemically stable ceramic-type layers onto appropriate passivating metals. Both techniques have been applied to improve the corrosion and wear resistance of Al-alloys (Al_2O_3 surface layers) [264], and Ti-alloys (TiO_2 surface layers) [265]. This is not always the case, despite oxide-based coating materials generally being more thermodynamically stable and possessing high hardness compared with metals. This is due to the presence of cracking and porosity that can exist after some electrolytic oxidation treatments, which can influence fatigue strength and corrosion resistance. In addition, differences in thermal expansion coefficients between the bulk and the coating can lead to cracking in service, depending on the thermal cycle. As such, care must be taken when selecting oxidation methods with the intention of creating hardwearing surfaces. Plating methods are industrially applied to improve wear and corrosion resistance of machined parts. Electroplated coatings can either be metallic or co-deposits with harder materials, like SiC [266], and those like graphene and graphene oxide that can refine coating microstructures and reduce friction [267].

Chemical and electrochemical finishing processes are widely employed industrially to improve the functional performance of machined parts. However, an understanding of the interplay between different failure modes and the final application is necessary given that surface processing to improve one performance aspect may detrimentally affect others. For example, anodization can improve wear resistance and near-surface hardness, however it can in some cases degrade fatigue and corrosion performance. In addition, not all chemical and electrochemical treatments can be applied towards all metals and alloys. Therefore, knowledge of the ultimate loading condition is vital to applying appropriate finishing methods.

6. Conclusion and future challenges

This review represents the second more applied instalment of a comprehensive assessment of surface integrity and how manufacturing technologies have a bearing upon this. In Part II the characteristics of process deployment for surface integrity enhancement has been considered alongside considering engineering functionality of the resultant surface. From the observations made within the literature it is now possible to identify opportunities for further research which spans both laboratory scale experimentation but necessitates enhanced engagement between the materials processing specialist and the component designer.

- Fatigue performance is dependent upon heterogeneous systems of microstructural and micro-geometrical alterations that can be induced to machined surface layers, whose behaviour under cyclic loading is dependent on their micro and nanoscale properties. Significant progress has been made on researching the influence of single anomalies (e.g. white layers, material drag, micro-cracks, etc.) on fatigue performance, which has been highly supported by adoption of advanced material analysis techniques. However, as multiple machining-induced anomalies often coexist, further scientific effort should be directed to understanding their combined effect and interaction from a material perspective, when machined surfaces are subject to alternating stress cycles.
- Due to the hindered oxygen delivery into the narrow machining grooves, machined surfaces with increased roughness will be more sensitive to pitting corrosion (and stress corrosion cracking as a consequence). Intermetallic compounds (i.e. machining-induced) will act as pitting corrosion sites due to their cathodic behaviour relative to the metallic matrix. The combination of tensile residual stresses on the machined sub-surface and a corrosive working environment will promote stress corrosion cracking, thereby facilitating early-stage failures. However, these can be improved with a post-processing technique, such as peening, to induce a compressive

residual stress profile. In general, a finer grain surface (i.e. a machined surface with large grain boundary density), as opposed to a coarse-grain surface, will possess an enhanced corrosion resistance due to the increased reactivity of the grain boundaries, which promotes the passivation process of the metal, easing the formation of the protective oxide film.

- The evolution of microstructure, metallurgy and composition that mechanical, thermal, and chemical machining processes can induce in the near-surface regions of processed materials can significantly alter the resistance to different forms of corrosion. Ultimately, the resistance to corrosion can be maintained where the prevalence of surface cracking and high aspect ratio surface features can be minimised. This is often related to inappropriate cooling cycles in thermal machining, severe plastic deformation and deep grooves in mechanical machining, and pitting in electrochemical machining. Rapid cooling from machining operations can also induce metallurgical changes like sensitisation, and tensile surface stresses at the near surface, the latter of which can enable forms of corrosion such as stress corrosion cracking in otherwise benign chemical environments. The literature regarding machining-induced corrosion phenomena will benefit from more application-specific corrosion testing, for example under thermal and mechanical loading as well as fundamental research towards understand how surface anomalies associated with specific machining processes affect how materials passivate and actively dissolve within corrosive environments. This will provide the key to designing processes to reduce or inhibit corrosion at the near surface.
- Machined surface defects including residual stress, cracking and porosity, as well as increased surface roughness, decrease the in-service performance of machined parts by accelerating the associated wear mechanisms. In the case of EDM, there has been no evidence that wear performance can be enhanced by the presence of the EDM induced recast layer. In the case of mechanical machining however, there is some evidence that under controlled conditions, the increased hardness associated with machined white layers can offer a mechanically favourable wear resistant layer.
- Machining parameters and tools should be optimised in order to control the machining-induced physical effects and produce high levels of surface integrity, with limited strain hardening and tensile residual stresses. In addition, minimising surface roughness is also beneficial as micro-notches from machining grooves induce localised stress concentrations. Thus, if good surface integrity is produced during machining, fatigue life, damage tolerance (ability to tolerate scratches & dents) life and corrosion-fatigue life can be maximised by careful optimisation of post-machining strategies, e.g. by identification of optimal shot peening parameters. In fact, shot peening is also beneficial to machined parts as it extends the number of cycles to develop fatigue cracks from surface defects or inclusions as a result of strain hardening and compressive residual stress states. In addition, peened surfaces also provide damage tolerance from undetected handling damage during manufacture or from foreign object damage in service.
- Laser, electron beam and electrical discharge-based surface modification methods offer practical methods of improving the surface integrity of materials subject to machining. Laser polishing and high-current electron beam irradiation are capable of re-melting the top few microns of machined material, into a dense, fine grained zone, which offers enhanced hardness and wear performance, absent of machining induced defects.
- Chemical and electrochemical surface finishing methods are widely applied industrially to eliminate the machining-induced surface integrity defects that are understood to influence fatigue, corrosion, and wear performance. They are often considered to provide the *gold* standard in surface integrity. Electropolishing and chemical etching methods have been used for many decades to finish machined parts, which is a testament to the stress-free nature of material removal and the generation of smooth and relatively defect-free surfaces upon appropriate finishing. However, surface treatments improving certain aspects of surface integrity can detrimentally affect other aspects. For example, anodization and electrolytic oxidation can improve the corrosion and wear characteristics of machined surfaces, however in some studies these methods have been shown to reduce fatigue strengths of machined components due to the presence of near-surface porosity and cracking. Accordingly, studies to understand the interrelationships between various aspects of surface integrity after chemical and electrochemical finishing operations will represent important additions to the literature. Furthermore, investigations towards detoxifying this area of finishing, where it is not uncommon to exploit chemicals such as Cr(VI) and hydrofluoric acid to finish advanced engineering materials should be undertaken.

In compiling this literature review the authors have had the privilege of exploring contributions from numerous scholars and charting the course of an exciting and dynamic research field which can trace its heritage back to the industrial revolution and the characteristics of the first machines. As our desire to extend the service life and safety of engineered components the shortcomings of machined surfaces have come to the fore as a performance limiting characteristic. Despite a rich (and growing) body of literature challenges remain to define economical material removal processes which provide appropriate surface conditions. However, the requirements imposed by designers on engineering surfaces become ever more complex. The advent of more complex materials which do not obey 'convention', for example super elastic materials (e.g. NiTi alloy), high entropy alloys or metal and ceramic matrix composites also challenge our understanding of surface integrity and invite us to devise appropriate methods of material processing. The interplay between material-process-function will be increasingly important with regard to surface integrity for these materials and will present technical challenges for their usage.

Development of models to investigate the microstructural surface condition induced by machining operations also represents a fundamental direction of development for the surface integrity community. In this context, advancement in modelling approaches studying the small-scale mechanisms of surface modification in machining will provide key support to the understanding and control of the in-service component performance of machined parts.

New manufacturing methods also provide significant challenges to the scholar intent on understanding resulting surface integrity. Fabrication methods (e.g. Friction Stir Welding), additive manufacturing (e.g. laser powder bed fusion) and multi-material methods (e.g. Metal Injection Moulding) will all require machining methods to achieve net shape based on the current state-of-the-art. Hence, there will be a need for processes capable of delivering surface conditions which are consistent with the bulk performance of material properties associated with these techniques.

Surface integrity resulting from additive manufacturing processes also presents a rich pasture for the scholar of surface integrity. Since components produced by these techniques are effectively composites in their 'non-normalised' state their machinability is location specific and hence obtaining a uniform surface integrity is not without difficulties.

In identifying opportunities for further research perhaps it is also useful to consider emergent changes to industry which will be driven low carbon initiatives. Legislative changes, reduced availability of high-octane hydrocarbons and changes to materials supply [268] will increase usage of electrical machines for transport and transduction alongside technologies for energy storage. As such the requirements for manufacturing processes associated with energy storage materials and electrically/magnetically active materials will be of increased importance. An emergent area worthy of further attention.

Historically, the first use of the term 'surface integrity' has been attributed by DeGarmo et al. [269] to Field and Kahles [270] in 1964. In their formative work the relationship between process and resulting

surface integrity is defined as "the inherent or enhanced condition of a surface produced in a machining or other surface generation operation". Little has changed in how we might describe surface integrity in the 56 years since Field and Kahles explored the topic but the tools available to characterise it have developed rapidly. We are now able to visualise microstructure at sub μm level detail using SEM, characterised stress fields in minutes using X-ray diffraction and identify with high precision the chemical composition of surfaces using an array electron interaction phenomena. Hence our ability to observe near surface phenomena and augment process technology and materials science to accommodate these permits express innovation. As such the authors (and the reader) are challenged to contemplate the state-of-the-art in 2077 in surface integrity of manufacturing processes.

Credit author statement

Andrea la Monaca, Methodology, Investigation, Writing – original draft, Writing – review & editing. James W. Murray, Investigation, Writing – original draft, Writing – review & editing. Zhirong Liao, Investigation, Writing – original draft, Writing – review & editing. Alistair Speidel, Investigation, Writing – original draft, Writing – review & editing. Jose A. Robles-Linares, Investigation; Writing – original draft, Writing – review & editing. Dragos A. Axinte, Methodology, Supervision, Writing – review & editing. Mark C. Hardy, Investigation, Writing – original draft, Writing – review & editing. Adam T. Clare, Methodology, Investigation, Supervision, Writing – original draft, Writing – review & editing.

Declaration of competing interest

The authors declare that they have no known competing financial interests or personal relationships that could have appeared to influence the work reported in this paper.

Acknowledgement

This study was supported by EPSRC through the DTP 2018–19 University of Nottingham (No: EP/R513283/1), NanoPrime (No: EP/R025282/1) and Rolls-Royce CASE award scheme (No: 19000151). The authors would like to thank the support from the Nottingham research fellowship programme. A.T. Clare would like to acknowledge the generous support of the Royal Academy of Engineering which supports his Research Chair (RCSRF1920\9\27).

References

[1] Z. Liao, A. la Monaca, J. Murray, A. Speidel, D. Ushmaev, A. Clare, D. Axinte, R. M'Saoubi, Surface integrity in metal machining - Part I: fundamentals of surface characteristics and formation mechanisms, Int. J. Mach. Tool Manufact. 162 (2021) 103687, https://doi.org/10.1016/j.ijmachtools.2020.103687.
[2] A.F. El-Sayed, Aircraft Propulsion and Gas Turbine Engines, CRC Press, 2017.
[3] A.I. Hovorun, T P, K.V. Berladir, V.I. Pererva, S.G. Rudenko, Martynov, Modern Materials for Automotive Industry, 2017.
[4] F.S. Rad Hr, M.H. Idris, M.R. Kadir, Microstructure analysis and corrosion behavior of biodegradable Mg–Ca implant alloys, Mater. Des. 33 (2012) 88–97.
[5] Z. Liao, D. Xu, D. Axinte, R. M'Saoubi, J. Thelin, A. Wretland, Novel cutting inserts with multi-channel irrigation at the chip-tool interface: modelling, design and experiments, CIRP Ann (2020) 7–10, https://doi.org/10.1016/j.cirp.2020.04.028, 4000.
[6] A. la Monaca, Z. Liao, D. Axinte, A digital approach to automatically assess the machining-induced microstructural surface integrity, J. Mater. Process. Technol. 282 (2020) 116703, https://doi.org/10.1016/j.jmatprotec.2020.116703.
[7] D. Cha, D. Axinte, J. Billingham, Geometrical modelling of pulsed laser ablation of high performance metallic alloys, Int. J. Mach. Tool Manufact. 141 (2019) 78–88, https://doi.org/10.1016/j.ijmachtools.2019.04.004.
[8] J. Schijve, Fatigue of structures and materials in the 20th century and the state of the art, Int. J. Fatig. 25 (2003) 679–702, https://doi.org/10.1016/S0142-1123(03)00051-3.
[9] W.J.M. Rankine, On the causes of the unexpected breakage of the journals of railway axles; and on the mean of preventing such accidents by observing the law of continuity in their construction, J. Franklin Inst. 36 (1843) 178–180, https://doi.org/10.1016/S0016-0032(43)91062-2.
[10] J.A. Ewing, J.C.W. Humfreym, The fracture of metals under repeated alternations of stress, Philos. Trans. R. Soc. Lond. - Ser. A Contain. Pap. a Math. or Phys. Character 200 (1903) 241–250, https://doi.org/10.1098/rsta.1903.0006.
[11] A.A. Griffith, The phenomena of rupture and flow in solids, Philos. Trans. R. Soc. Lond. - Ser. A Contain. Pap. a Math. or Phys. Character 221 (1921) 163–198, https://doi.org/10.1098/rsta.1921.0006.
[12] P. Paris, F. Erdogan, A critical analysis of crack propagation laws, J. Basic Eng. 85 (1963) 528–533, https://doi.org/10.1115/1.3656900.
[13] P.A. Withey, Fatigue failure of the de Havilland comet I, Eng. Fail. Anal. 4 (1997) 147–154, https://doi.org/10.1016/S1350-6307(97)00005-8.
[14] M.C. Hardy, C.R.J. Herbert, J. Kwong, W. Li, D.A. Axinte, A.R.C. Sharman, A. Encinas-Oropesa, P.J. Withers, Characterising the integrity of machined surfaces in a powder nickel alloy used in aircraft engines, Procedia CIRP 13 (2014) 411–416, https://doi.org/10.1016/j.procir.2014.04.070.
[15] S. Ghosh, V. Kain, Microstructural changes in AISI 304L stainless steel due to surface machining: effect on its susceptibility to chloride stress corrosion cracking, J. Nucl. Mater. 403 (2010) 62–67, https://doi.org/10.1016/j.jnucmat.2010.05.028.
[16] X. Guan, J. He, Life time extension of turbine rotating components under risk constraints: a state-of-the-art review and case study, Int. J. Fatig. 129 (2019) 104799, https://doi.org/10.1016/j.ijfatigue.2018.08.003.
[17] T. Makino, H. Sakai, C. Kozuka, Y. Yamazaki, M. Yamamoto, K. Minoshima, Overview of fatigue damage evaluation rule for railway axles in Japan and fatigue property of railway axle made of medium carbon steel, Int. J. Fatig. 132 (2020) 105361, https://doi.org/10.1016/j.ijfatigue.2019.105361.
[18] D. Novovic, R.C. Dewes, D.K. Aspinwall, W. Voice, P. Bowen, The effect of machined topography and integrity on fatigue life, Int. J. Mach. Tool Manufact. (2004), https://doi.org/10.1016/j.ijmachtools.2003.10.018.
[19] D. Arola, C.L. Williams, Estimating the fatigue stress concentration factor of machined surfaces, Int. J. Fatig. 24 (2002) 923–930, https://doi.org/10.1016/S0142-1123(02)00012-9.
[20] F. Hashimoto, Y.B. Guo, A.W. Warren, Surface integrity difference between hard turned and ground surfaces and its impact on fatigue life, CIRP Ann. - Manuf. Technol. 55 (2006) 81–84, https://doi.org/10.1016/S0007-8506(07)60371-0.
[21] Y. Matsumoto, D. Magda, D.W. Hoeppner, T.Y. Kim, Effect of machining processes on the fatigue strength of hardened AISI 4340 steel, J. Manuf. Sci. Eng. Trans. ASME. 113 (1991) 154–159, https://doi.org/10.1115/1.2899672.
[22] A. Thakur, S. Gangopadhyay, State-of-the-art in surface integrity in machining of nickel-based super alloys, Int. J. Mach. Tool Manufact. 100 (2016) 25–54, https://doi.org/10.1016/j.ijmachtools.2015.10.001.
[23] H. Sasahara, The effect on fatigue life of residual stress and surface hardness resulting from different cutting conditions of 0.45%C steel, Int. J. Mach. Tool Manufact. 45 (2005) 131–136, https://doi.org/10.1016/j.ijmachtools.2004.08.002.
[24] Y. Choi, A study on the effects of machining-induced residual stress on rolling contact fatigue, Int. J. Fatig. 31 (2009) 1517–1523, https://doi.org/10.1016/j.ijfatigue.2009.05.001.
[25] Y. Choi, Influence of tool flank wear on performance of finish hard machined surfaces in rolling contact, Int. J. Fatig. 32 (2010) 390–397, https://doi.org/10.1016/j.ijfatigue.2009.07.014.
[26] I.S. Jawahir, E. Brinksmeier, R. M'Saoubi, D.K. Aspinwall, J.C. Outeiro, D. Meyer, D. Umbrello, A.D. Jayal, Surface integrity in material removal processes: recent advances, CIRP Ann. - Manuf. Technol. 60 (2011) 603–626, https://doi.org/10.1016/j.cirp.2011.05.002.
[27] Z. Liao, M. Polyakov, O.G. Diaz, D. Axinte, G. Mohanty, X. Maeder, J. Michler, M. Hardy, Grain refinement mechanism of nickel-based superalloy by severe plastic deformation - mechanical machining case, Acta Mater. 180 (2019) 2–14, https://doi.org/10.1016/j.actamat.2019.08.059.
[28] A.M. Wusatowska-Sarnek, B. Dubiel, A. Czyrska-Filemonowicz, P.R. Bhowal, N. Ben Salah, J.E. Klemberg-Sapieha, Microstructural characterization of the white etching layer in nickel-based superalloy, Metall. Mater. Trans. A Phys. Metall. Mater. Sci. 42 (2011) 3813–3825, https://doi.org/10.1007/s11661-011-0779-8.
[29] C. Herbert, D.A. Axinte, M. Hardy, P. Withers, Influence of surface anomalies following hole making operations on the fatigue performance for a nickel-based superalloy, J. Manuf. Sci. Eng. Trans. ASME. 136 (2014) 1–9, https://doi.org/10.1115/1.4027619.
[30] M.C. Hardy, M. Detrois, E.T. McDevitt, C. Argyrakis, V. Saraf, P.D. Jablonski, J. A. Hawk, R.C. Buckingham, H.S. Kitaguchi, S. Tin, Solving recent challenges for wrought Ni-base superalloys, Metall. Mater. Trans. (2020), https://doi.org/10.1007/s11661-020-05773-6.
[31] R. M'Saoubi, D. Axinte, S.L. Soo, C. Nobel, H. Attia, G. Kappmeyer, S. Engin, W. M. Sim, High performance cutting of advanced aerospace alloys and composite materials, CIRP Ann. - Manuf. Technol. 64 (2015) 557–580, https://doi.org/10.1016/j.cirp.2015.05.002.
[32] T. Connolley, M.J. Starink, P.A.S. Reed, Effect of broaching on high-temperature fatigue behavior in notched specimens of INCONEL 718, Metall. Mater. Trans. A Phys. Metall. Mater. Sci. 35 (2004) 771–783, https://doi.org/10.1007/s11661-004-0005-z.
[33] M.C. Hardy, B. Zirbel, G. Shen, R. Shenkar, Developing damage tolerance and creep resistance in a high strength nickel alloy for disc applications, in: Superalloys 2004, Tenth Int. Symp., TMS, 2004, pp. 83–90, https://doi.org/10.7449/2004/Superalloys_2004_83_90.
[34] R. M'Saoubi, D. Axinte, C. Herbert, M. Hardy, P. Salmon, Surface integrity of nickel-based alloys subjected to severe plastic deformation by abusive drilling,

CIRP Ann. - Manuf. Technol. 63 (2014) 61–64, https://doi.org/10.1016/j.cirp.2014.03.067.
[35] S.L. Soo, R. Hood, D.K. Aspinwall, W.E. Voice, C. Sage, Machinability and surface integrity of RR1000 nickel based superalloy, CIRP Ann. - Manuf. Technol. 60 (2011) 89–92, https://doi.org/10.1016/j.cirp.2011.03.094.
[36] C.R.J. Herbert, J. Kwong, M.C. Kong, D.A. Axinte, M.C. Hardy, P.J. Withers, An evaluation of the evolution of workpiece surface integrity in hole making operations for a nickel-based superalloy, J. Mater. Process. Technol. 212 (2012) 1723–1730, https://doi.org/10.1016/j.jmatprotec.2012.03.014.
[37] D. Xu, Z. Liao, D. Axinte, J.A. Sarasua, R. M'Saoubi, A. Wretland, Investigation of surface integrity in laser-assisted machining of nickel based superalloy, Mater. Des. (2020) 108851, https://doi.org/10.1016/j.matdes.2020.108851.
[38] Z. Shang, Z. Liao, J.A. Sarasua, J. Billingham, D. Axinte, On modelling of laser assisted machining: forward and inverse problems for heat placement control, Int. J. Mach. Tool Manufact. (2019), https://doi.org/10.1016/j.ijmachtools.2018.12.001.
[39] S.A. Niknam, R. Khettabi, V. Songmene, Machinability and machining of titanium alloys: a review, in: J.P. Davim (Ed.), Mach. Titan. Alloy., Springer Berlin Heidelberg, Berlin, Heidelberg, 2014, pp. 1–30, https://doi.org/10.1007/978-3-662-43902-9_1.
[40] P. Crawforth, B. Wynne, S. Turner, M. Jackson, Subsurface deformation during precision turning of a near-alpha titanium alloy, Scripta Mater. 67 (2012) 842–845, https://doi.org/10.1016/j.scriptamat.2012.08.001.
[41] Q. Wang, Z. Liu, Plastic deformation induced nano-scale twins in Ti-6Al-4V machined surface with high speed machining, Mater. Sci. Eng. 675 (2016) 271–279, https://doi.org/10.1016/j.msea.2016.08.076.
[42] C.H. Che-Haron, A. Jawaid, The effect of machining on surface integrity of titanium alloy Ti-6% Al-4% v, J. Mater. Process. Technol. 166 (2005) 188–192, https://doi.org/10.1016/j.jmatprotec.2004.08.012.
[43] A. Cox, S. Herbert, J.P. Villain-Chastre, S. Turner, M. Jackson, The effect of machining and induced surface deformation on the fatigue performance of a high strength metastable β titanium alloy, Int. J. Fatig. 124 (2019) 26–33, https://doi.org/10.1016/j.ijfatigue.2019.02.033.
[44] K. Kothari, R. Radhakrishnan, N.M. Wereley, Advances in gamma titanium aluminides and their manufacturing techniques, Prog. Aero. Sci. 55 (2012) 1–16, https://doi.org/10.1016/j.paerosci.2012.04.001.
[45] A.L. Mantle, D.K. Aspinwall, Surface integrity and fatigue life of turned gamma titanium aluminide, J. Mater. Process. Technol. 72 (1997) 413–420, https://doi.org/10.1016/S0924-0136(97)00204-5.
[46] G.R. Dickinson, Influence of Machining on the Performance of Ultra High Strength Steels, ASME Pap, 1970.
[47] A. Javidi, U. Rieger, W. Eichlseder, The effect of machining on the surface integrity and fatigue life, Int. J. Fatig. 30 (2008) 2050–2055, https://doi.org/10.1016/j.ijfatigue.2008.01.005.
[48] S. Smith, S.N. Melkote, E. Lara-Curzio, T.R. Watkins, L. Allard, L. Riester, Effect of surface integrity of hard turned AISI 52100 steel on fatigue performance, Mater. Sci. Eng. 459 (2007) 337–346, https://doi.org/10.1016/j.msea.2007.01.011.
[49] J. Ajaja, W. Jomaa, P. Bocher, R.R. Chromik, M. Brochu, High cycle fatigue behavior of hard turned 300 M ultra-high strength steel, Int. J. Fatig. 131 (2019) 105380, https://doi.org/10.1016/j.ijfatigue.2019.105380.
[50] A. Rasti, M.H. Sadeghi, S.S. Farshi, An investigation into the effect of surface integrity on the fatigue failure of AISI 4340 steel in different drilling strategies, Eng. Fail. Anal. 95 (2019) 66–81, https://doi.org/10.1016/j.engfailanal.2018.08.022.
[51] S. Hasunuma, S. Oki, K. Motomatsu, T. Ogawa, Fatigue life prediction of carbon steel with machined surface layer under low-cycle fatigue, Int. J. Fatig. 123 (2019) 255–267, https://doi.org/10.1016/j.ijfatigue.2019.02.017.
[52] Y. Choi, Influence of rake angle on surface integrity and fatigue performance of machined surfaces, Int. J. Fatig. 94 (2017) 81–88, https://doi.org/10.1016/j.ijfatigue.2016.09.013.
[53] X. Zhang, Y. Chen, J. Hu, Recent advances in the development of aerospace materials, Prog. Aero. Sci. 97 (2018) 22–34, https://doi.org/10.1016/j.paerosci.2018.01.001.
[54] M. Suraratchai, J. Limido, C. Mabru, R. Chieragatti, Modelling the influence of machined surface roughness on the fatigue life of aluminium alloy, Int. J. Fatig. 30 (2008) 2119–2126, https://doi.org/10.1016/j.ijfatigue.2008.06.003.
[55] F. Abroug, E. Pessard, G. Germain, F. Morel, A probabilistic approach to study the effect of machined surface states on HCF behavior of a AA7050 alloy, Int. J. Fatig. 116 (2018) 473–489, https://doi.org/10.1016/j.ijfatigue.2018.06.048.
[56] G. Rotella, Effect of surface integrity induced by machining on high cycle fatigue life of 7075-T6 aluminum alloy, J. Manuf. Process. 41 (2019) 83–91, https://doi.org/10.1016/j.jmapro.2019.03.031.
[57] K.H. Ho, S.T. Newman, State of the art electrical discharge machining (EDM), Int. J. Mach. Tool Manufact. 43 (2003) 1287–1300, https://doi.org/10.1016/S0890-6955(03)00162-7.
[58] D. Ulutan, T. Ozel, Machining induced surface integrity in titanium and nickel alloys: a review, Int. J. Mach. Tool Manufact. 51 (2011) 250–280, https://doi.org/10.1016/j.ijmachtools.2010.11.003.
[59] T.R. Newton, S.N. Melkote, T.R. Watkins, R.M. Trejo, L. Reister, Investigation of the effect of process parameters on the formation and characteristics of recast layer in wire-EDM of Inconel 718, Mater. Sci. Eng. (2009) 513–514, https://doi.org/10.1016/j.msea.2009.01.061, 208–215.
[60] J.F. Liu, Y.B. Guo, T.M. Butler, M.L. Weaver, Crystallography, compositions, and properties of white layer by wire electrical discharge machining of nitinol shape memory alloy, Mater. Des. (2016), https://doi.org/10.1016/j.matdes.2016.07.063.
[61] M. Anthony Xavior, P. Ashwath, Fatigue life and fracture morphology of Inconel 718 machined by spark EDM process, Procedia Manuf 30 (2019) 292–299, https://doi.org/10.1016/j.promfg.2019.02.042.
[62] M.T. Antar, S.L. Soo, D.K. Aspinwall, C. Sage, M. Cuttell, R. Perez, A.J. Winn, Fatigue response of Udimet 720 following minimum damage wire electrical discharge machining, Mater. Des. 42 (2012) 295–300, https://doi.org/10.1016/j.matdes.2012.06.003.
[63] I. Ayesta, B. Izquierdo, O. Flaño, J.A. Sánchez, J. Albizuri, R. Avilés, Influence of the WEDM process on the fatigue behavior of Inconel® 718, Int. J. Fatig. 92 (2016) 220–233, https://doi.org/10.1016/j.ijfatigue.2016.07.011.
[64] A. Pramanik, A.K. Basak, Effect of wire electric discharge machining (EDM) parameters on fatigue life of Ti-6Al-4V alloy, Int. J. Fatig. 128 (2019) 105186, https://doi.org/10.1016/j.ijfatigue.2019.105186.
[65] T.M. Mower, Degradation of titanium 6Al-4V fatigue strength due to electrical discharge machining, Int. J. Fatig. 64 (2014) 84–96, https://doi.org/10.1016/j.ijfatigue.2014.02.018.
[66] T.Y. Tai, S.J. Lu, Improving the fatigue life of electro-discharge-machined SDK11 tool steel via the suppression of surface cracks, Int. J. Fatig. 31 (2009) 433–438, https://doi.org/10.1016/j.ijfatigue.2008.07.013.
[67] O.A.A. Zeid, On the effect of electrodischarge machining parameters on the fatigue life of AISI D6 tool steel, J. Mater. Process. Technol. 68 (1997) 27–32, https://doi.org/10.1016/b978-008042140-7/50010-x.
[68] D.J. Thomas, Optimising laser cut-edge durability for steel structures in high stress applications, J. Constr. Steel Res. 121 (2016) 40–49, https://doi.org/10.1016/j.jcsr.2016.01.013.
[69] D.F. Pessoa, P. Herwig, A. Wetzig, M. Zimmermann, Influence of surface condition due to laser beam cutting on the fatigue behavior of metastable austenitic stainless steel AISI 304, Eng. Fract. Mech. 185 (2017) 227–240, https://doi.org/10.1016/j.engfracmech.2017.05.040.
[70] A. Reck, A.T. Zeuner, M. Zimmermann, Fatigue behavior of non-optimized laser-cut medical grade Ti-6Al-4V-ELI sheets and the effects of mechanical post-processing, Metals 9 (2019) 843, https://doi.org/10.3390/met9080843.
[71] D. Cha, O.G. Diaz, Z. Liao, D. Gilbert, D. Axinte, J. Kell, A. Norton, M. O'Key, M. R. Osborne, D. Main, Development of a novel system for in-situ repair of aeroengine airfoil via pulsed laser ablation, J. Manuf. Syst. 55 (2020) 126–131, https://doi.org/10.1016/j.jmsy.2020.03.001.
[72] K.K. Saxena, J. Qian, D. Reynaerts, A review on process capabilities of electrochemical micromachining and its hybrid variants, Int. J. Mach. Tool Manufact. 127 (2018) 28–56, https://doi.org/10.1016/j.ijmachtools.2018.01.004.
[73] T. Paczkowski, J. Zdrojewski, Monitoring and control of the electrochemical machining process under the conditions of a vibrating tool electrode, J. Mater. Process. Technol. 244 (2017) 204–214, https://doi.org/10.1016/j.jmatprotec.2017.01.023.
[74] D. Clifton, A.R. Mount, D.J. Jardine, R. Roth, Electrochemical machining of gamma titanium aluminide intermetallics, J. Mater. Process. Technol. 108 (2001) 338–348, https://doi.org/10.1016/S0924-0136(00)00739-1.
[75] F. Klocke, A. Klink, D. Veselovac, D.K. Aspinwall, S.L. Soo, M. Schmidt, J. Schilp, G. Levy, J.P. Kruth, Turbomachinery component manufacture by application of electrochemical, electro-physical and photonic processes, CIRP Ann. - Manuf. Technol. 63 (2014) 703–726, https://doi.org/10.1016/j.cirp.2014.05.004.
[76] A.D. Spear, A.R. Ingraffea, Effect of chemical milling on low-cycle fatigue behavior of an Al-Mg-Si alloy, Corrosion Sci. 68 (2013) 144–153, https://doi.org/10.1016/j.corsci.2012.11.006.
[77] B. Sefer, R. Gaddam, J.J. Roa, A. Mateo, M.L. Antti, R. Pederson, Chemical milling effect on the low cycle fatigue properties of cast Ti–6Al–2Sn–4Zr–2Mo alloy, Int. J. Fatig. 92 (2016) 193–202, https://doi.org/10.1016/j.ijfatigue.2016.07.003.
[78] A.R.C. Sharman, D.K. Aspinwall, R.C. Dewes, D. Clifton, P. Bowen, The effects of machined workpiece surface integrity on the fatigue life of γ-titanium aluminide, Int. J. Mach. Tool Manufact. 41 (2001) 1681–1685, https://doi.org/10.1016/S0890-6955(01)00034-7.
[79] S.B. Hosseini, U. Klement, Y. Yao, K. Ryttberg, Formation mechanisms of white layers induced by hard turning of AISI 52100 steel, Acta Mater. 89 (2015) 258–267, https://doi.org/10.1016/j.actamat.2015.01.075.
[80] S. Sadek, et al., The probability of HCF – Surface and sub-surface models, Int. J. Fatigue (2016), https://doi.org/10.1016/j.ijfatigue.2016.06.021.
[81] J.T. Staley, Corrosion of aluminum aerospace alloys, Mater. Sci. Forum 877 (2017) 485–491, https://doi.org/10.4028/www.scientific.net/MSF.877.485.
[82] Y. Sueishi, A. Kohyama, H. Kinoshita, M. Narui, K. Fukumoto, Microstructure and nano-hardness analyses of stress corrosion cracking, utilizing 316L core shroud of BWR power reactors, Fusion Eng. Des. 81 (2006) 1099–1103, https://doi.org/10.1016/j.fusengdes.2005.09.065.
[83] H. Mansoori, R. Mirzaee, F. Esmaeilzadeh, A. Vojood, A.S. Dowrani, Pitting corrosion failure analysis of a wet gas pipeline, Eng. Fail. Anal. 82 (2017) 16–25, https://doi.org/10.1016/j.engfailanal.2017.08.012.
[84] M.K. Hsieh, D.A. Dzombak, R.D. Vidic, Effect of tolyltriazole on the corrosion protection of copper against ammonia and disinfectants in cooling systems, Ind. Eng. Chem. Res. 49 (2010) 7313–7322, https://doi.org/10.1021/ie100384d.
[85] N.S. More, N. Diomidis, S.N. Paul, M. Roy, S. Mischler, Tribocorrosion behavior of β titanium alloys in physiological solutions containing synovial components, Mater. Sci. Eng. C 31 (2011) 400–408, https://doi.org/10.1016/j.msec.2010.10.021.
[86] D. Wang, G.P. Bierwagen, Sol-gel coatings on metals for corrosion protection, Prog. Org. Coating 64 (2009) 327–338, https://doi.org/10.1016/j.porgcoat.2008.08.010.

[87] B. Liu, X. Zhang, X. Zhou, T. Hashimoto, J. Wang, The corrosion behaviour of machined AA7150-T651 aluminium alloy, Corrosion Sci. 126 (2017) 265–271, https://doi.org/10.1016/j.corsci.2017.07.008.
[88] Y. Wan, Z. Wang, Z. Liu, Z. Jiang, D. Zhang, Stress influence on corrosion resistance of aluminum alloy surface, Adv. Mater. Res. 1017 (2014) 287–291, https://doi.org/10.4028/www.scientific.net/AMR.1017.287.
[89] J. Liu, K. Zhao, M. Yu, S. Li, Effect of surface abrasion on pitting corrosion of Al-Li alloy, Corrosion Sci. 138 (2018) 75–84, https://doi.org/10.1016/j.corsci.2018.04.010.
[90] R. Grilli, M.A. Baker, J.E. Castle, B. Dunn, J.F. Watts, Localized corrosion of a 2219 aluminium alloy exposed to a 3.5% NaCl solution, Corrosion Sci. 52 (2010) 2855–2866, https://doi.org/10.1016/j.corsci.2010.04.035.
[91] K.D. Ralston, N. Birbilis, Effect of grain size on corrosion: a review, Corrosion 66 (2010) 750051–7500513, https://doi.org/10.5006/1.3462912.
[92] W. Deng, P. Lin, Q. Li, G. Mo, Ultrafine-grained copper produced by machining and its unusual electrochemical corrosion resistance in acidic chloride pickling solutions, Corrosion Sci. 74 (2013) 44–49, https://doi.org/10.1016/j.corsci.2013.04.007.
[93] K.D. Ralston, D. Fabijanic, N. Birbilis, Effect of grain size on corrosion of high purity aluminium, Electrochim. Acta 56 (2011) 1729–1736, https://doi.org/10.1016/j.electacta.2010.09.023.
[94] Z. Pu, O.W. Dillon, I.S. Jawahir, D.A. Puleo, Microstructural changes of AZ31 magnesium alloys induced by cryogenic machining and its influence on corrosion resistance in simulated body fluid for biomedical applications, ASME 2010 Int. Manuf. Sci. Eng. Conf. MSEC 1 (2010) 271–277, https://doi.org/10.1115/MSEC2010-34234, 2010.
[95] Z. Pu, D.A. Puleo, O.W. Dillon, I.S. Jawahir, Controlling the biodegradation rate of magnesium-based implants through surface nanocrystallization induced by cryogenic machining implants through surface nanocrystallization induced by cryogenic machining, Magnes. Technol. (2011) 635–642, https://doi.org/10.1002/9781118062029.ch116, 2011.
[96] Z. Pu, J.C. Outeiro, A.C. Batista, O.W. Dillon, D.A. Puleo, I.S. Jawahir, Surface integrity in dry and cryogenic machining of AZ31B Mg alloy with varying cutting edge radius tools, Procedia Eng 19 (2011) 282–287, https://doi.org/10.1016/j.proeng.2011.11.113.
[97] V. Vignal, S. Bissey-Breton, J.B. Coudert, Mechanical properties and corrosion behaviour of low carbon martensitic stainless steel after machining, Int. J. Mach. Mach. Mater. 15 (2014) 36–53, https://doi.org/10.1504/IJMMM.2014.059186.
[98] A.M. Elhoud, N.C. Renton, W.F. Deans, The effect of manufacturing variables on the corrosion resistance of a super duplex stainless steel, Int. J. Adv. Manuf. Technol. 52 (2011) 451–461, https://doi.org/10.1007/s00170-010-2756-6.
[99] S. Wang, Y. Hu, K. Fang, W. Zhang, X. Wang, Effect of surface machining on the corrosion behaviour of 316 austenitic stainless steel in simulated PWR water, Corrosion Sci. 126 (2017) 104–120, https://doi.org/10.1016/j.corsci.2017.06.019.
[100] T. Terachi, T. Yamada, T. Miyamoto, K. Arioka, K. Fukuya, Corrosion behavior of stainless steels in simulated PWR primary water—effect of chromium content in alloys and dissolved hydrogen—, J. Nucl. Sci. Technol. 45 (2008) 975–984, https://doi.org/10.1080/18811248.2008.9711883.
[101] I.S. Harrison, T.R. Kurfess, E.J. Oles, P.M. Singh, Inspection of white layer in hard turned components using electrochemical methods, J. Manuf. Sci. Eng. Trans. ASME. 129 (2007) 447–452, https://doi.org/10.1115/1.2540655.
[102] A. Turnbull, K. Mingard, J.D. Lord, B. Roebuck, D.R. Tice, K.J. Mottershead, N. D. Fairweather, A.K. Bradbury, Sensitivity of stress corrosion cracking of stainless steel to surface machining and grinding procedure, Corrosion Sci. 53 (2011) 3398–3415, https://doi.org/10.1016/j.corsci.2011.06.020.
[103] W. Zhang, K. Fang, Y. Hu, S. Wang, X. Wang, Effect of machining-induced surface residual stress on initiation of stress corrosion cracking in 316 austenitic stainless steel, Corrosion Sci. 108 (2016) 173–184, https://doi.org/10.1016/j.corsci.2016.03.008.
[104] J. Rajaguru, N. Arunachalam, Investigation on machining induced surface and subsurface modifications on the stress corrosion crack growth behaviour of super duplex stainless steel, Corrosion Sci. 141 (2018) 230–242, https://doi.org/10.1016/j.corsci.2018.07.012.
[105] S. Ghosh, V. Kain, Effect of surface machining and cold working on the ambient temperature chloride stress corrosion cracking susceptibility of AISI 304L stainless steel, Mater. Sci. Eng. 527 (2010) 679–683, https://doi.org/10.1016/j.msea.2009.08.039.
[106] S. Ghosh, V.P.S. Rana, V. Kain, V. Mittal, S.K. Baveja, Role of residual stresses induced by industrial fabrication on stress corrosion cracking susceptibility of austenitic stainless steel, Mater. Des. 32 (2011) 3823–3831, https://doi.org/10.1016/j.matdes.2011.03.012.
[107] L. Chang, L. Volpe, Y.L. Wang, M.G. Burke, A. Maurotto, D. Tice, S. Lozano-Perez, F. Scenini, Effect of machining on stress corrosion crack initiation in warm-forged type 304L stainless steel in high temperature water, Acta Mater. 165 (2019) 203–214, https://doi.org/10.1016/j.actamat.2018.11.046.
[108] L. Chang, M.G. Burke, F. Scenini, Stress corrosion crack initiation in machined type 316L austenitic stainless steel in simulated pressurized water reactor primary water, Corrosion Sci. 138 (2018) 54–65, https://doi.org/10.1016/j.corsci.2018.04.003.
[109] A.K. Dubey, V. Yadava, Laser beam machining-A review, Int. J. Mach. Tool Manufact. 48 (2008) 609–628.
[110] P. Bleys, J.-P. Kruth, B. Lauwers, B. Schacht, V. Balasubramanian, L. Froyen, J. Van Humbeeck, Surface and sub-surface quality of steel after EDM, Adv. Eng. Mater. 8 (2006) 15–25, https://doi.org/10.1002/adem.200500211.
[111] G. Cusanelli, A. Hessler-Wyser, F. Bobard, R. Demellayer, R. Perez, R. Flükiger, Microstructure at submicron scale of the white layer produced by EDM technique, J. Mater. Process. Technol. 149 (2004) 289–295.
[112] J. Soltis, Passivity breakdown, pit initiation and propagation of pits in metallic materials – Review, Corrosion Sci. 90 (2015) 5–22, https://doi.org/10.1016/j.corsci.2014.10.006.
[113] S.R. Arunachalam, S.E. Galyon Dorman, R.T. Buckley, N.A. Conrad, S.A. Fawaz, Effect of electrical discharge machining on corrosion and corrosion fatigue behavior of aluminum alloys, Int. J. Fatig. 111 (2018) 44–53, https://doi.org/10.1016/j.ijfatigue.2018.02.005.
[114] H. Obara, H. Satou, M. Hatano, Fundamental study on corrosion of cemented carbide during wire EDM, J. Mater. Process. Technol. 149 (2004) 370–375, https://doi.org/10.1016/j.jmatprotec.2003.10.045.
[115] C.-C. Wang, H.-M. Chow, L.-D. Yang, C.-T. Lu, Recast layer removal after electrical discharge machining via Taguchi analysis: a feasibility study, J. Mater. Process. Technol. 209 (2009) 4134–4140, https://doi.org/10.1016/j.jmatprotec.2008.10.012.
[116] B. Hertweck, A.-C.L. Kimmel, T.G. Steigerwald, N.S.A. Alt, E. Schlücker, Electro discharge machining - a suitable fabrication process for high-pressure/high-temperature equipment, Chem. Eng. Technol. 41 (2018) 994–1002, https://doi.org/10.1002/ceat.201700680.
[117] Y. Sato, K. Watanabe, T. Shoji, Simulation of stress corrosion cracking behavior in a tube-shaped specimen of nickel-based alloy 600, Nucl. Eng. Des. 238 (2008) 1–7, https://doi.org/10.1016/j.nucengdes.2007.06.009.
[118] C.-Y. Bai, Effects of electrical discharge surface modification of superalloy Haynes 230 with aluminum and molybdenum on oxidation behavior, Corrosion Sci. 49 (2007) 3889–3904, https://doi.org/10.1016/j.corsci.2007.05.009.
[119] Z. Wen, H. Pei, C. Zhang, B. Wang, Analysis of surface quality of multi-film cooling holes in nickel-based single crystal superalloy, Mater. Sci. Technol. 32 (2016) 1845–1854, https://doi.org/10.1080/02670836.2016.1149277.
[120] C. Li, X. Xu, Y. Li, H. Tong, S. Ding, Q. Kong, L. Zhao, J. Ding, Effects of dielectric fluids on surface integrity for the recast layer in high speed EDM drilling of nickel alloy, J. Alloys Compd. 783 (2019) 95–102, https://doi.org/10.1016/j.jallcom.2018.12.283.
[121] S.H. Kang, D.E. Kim, Effect of electrical discharge machining process on crack susceptibility of nickel based heat resistant alloy, Mater. Sci. Technol. 21 (2005) 817–823, https://doi.org/10.1179/174328405X36601.
[122] A. Mandal, A.R. Dixit, S. Chattopadhyaya, A. Paramanik, S. Hloch, G. Królczyk, Improvement of surface integrity of Nimonic C 263 super alloy produced by WEDM through various post-processing techniques, Int. J. Adv. Manuf. Technol. 93 (2017) 433–443, https://doi.org/10.1007/s00170-017-9993-x.
[123] N. Eliaz, G. Shemesh, R.M. Latanision, Hot corrosion in gas turbine components, Eng. Fail. Anal. 9 (2002) 31–43, https://doi.org/10.1016/S1350-6307(00)00035-2.
[124] A. Ntasi, W.D. Mueller, G. Eliades, S. Zinelis, The effect of Electro Discharge Machining (EDM) on the corrosion resistance of dental alloys, Dent. Mater. 26 (2010) 237–245, https://doi.org/10.1016/j.dental.2010.08.001.
[125] S. Zinelis, Y.S. Al Jabbari, A. Thomas, N. Silikas, G. Eliades, Multitechnique characterization of CPTi surfaces after electro discharge machining (EDM), Clin. Oral Invest. 18 (2014) 67–75, https://doi.org/10.1007/s00784-013-0962-y.
[126] C. Prakash, M.S. Uddin, Surface modification of β-phase Ti implant by hydroaxyapatite mixed electric discharge machining to enhance the corrosion resistance and in-vitro bioactivity, Surf. Coating. Technol. 326 (2017) 134–145, https://doi.org/10.1016/j.surfcoat.2017.07.040.
[127] B. Jabbaripour, M.H. Sadeghi, M.R. Shabgard, H. Faraji, Investigating surface roughness, material removal rate and corrosion resistance in PMEDM of γ-TiAl intermetallic, J. Manuf. Process. 15 (2013) 56–68, https://doi.org/10.1016/j.jmapro.2012.09.016.
[128] Y. Uno, A. Okada, K. Uemura, P. Raharjo, T. Furukawa, K. Karato, High-efficiency finishing process for metal mold by large-area electron beam irradiation, Precis. Eng. 29 (2005) 449–455.
[129] H. Sidhom, F. Ghanem, T. Amadou, G. Gonzalez, C. Braham, Effect of electro discharge machining (EDM) on the AISI316L SS white layer microstructure and corrosion resistance, Int. J. Adv. Manuf. Technol. 65 (2013) 141–153, https://doi.org/10.1007/s00170-012-4156-6.
[130] S. Bhattacharya, G.J. Abraham, A. Mishra, V. Kain, G.K. Dey, Corrosion behavior of wire electrical discharge machined surfaces of P91 steel, J. Mater. Eng. Perform. 27 (2018) 4561–4570, https://doi.org/10.1007/s11665-018-3558-5.
[131] S.R. Pujari, R. Koona, S. Beela, Surface integrity of wire EDMed aluminum alloy: a comprehensive experimental investigation, J. King Saud Univ. - Eng. Sci. 30 (2018) 368–376, https://doi.org/10.1016/j.jksues.2016.12.001.
[132] K. Stambekova, H.-M. Lin, J.-Y. Uan, Microstructural and corrosion characteristics of alloying modified layer on 5083 Al alloy by electrical discharge alloying process with pure silicon electrode, Mater. Trans. 53 (2012) 1436–1442, https://doi.org/10.2320/matertrans.M2012131.
[133] Q. Feng, Y.N. Picard, H. Liu, S.M. Yalisove, G. Mourou, T.M. Pollock, Femtosecond laser micromachining of a single-crystal superalloy, Scripta Mater. 53 (2005) 511–516, https://doi.org/10.1016/j.scriptamat.2005.05.006.
[134] A.K. Dubey, V. Yadava, Laser beam machining—a review, Int. J. Mach. Tool Manufact. 48 (2008) 609–628, https://doi.org/10.1016/j.ijmachtools.2007.10.017.
[135] B.T. Rao, R. Kaul, P. Tiwari, A.K. Nath, Inert gas cutting of titanium sheet with pulsed mode CO2 laser, Optic Laser. Eng. 43 (2005) 1330–1348, https://doi.org/10.1016/j.optlaseng.2004.12.009.
[136] N. Morar, R. Roy, J. Mehnen, J.R. Nicholls, S. Gray, The effect of trepanning speed of laser drilled acute angled cooling holes on the high temperature low cycle

corrosion fatigue performance of CMSX-4 at 850 °C, Int. J. Fatig. 102 (2017) 112–120, https://doi.org/10.1016/j.ijfatigue.2017.04.017.
[137] K.E.C. Vidyasagar, A. Rana, D. Kalyanasundaram, Optimization of laser parameters for improved corrosion resistance of nitinol, Mater. Manuf. Process. (2020) 1–9, https://doi.org/10.1080/10426914.2020.1784926.
[138] H. Man, Z. Cui, T. Yue, Corrosion properties of laser surface melted NiTi shape memory alloy, Scripta Mater. 45 (2001) 1447–1453, https://doi.org/10.1016/S1359-6462(01)01182-4.
[139] A. Michael, A. Pequegnat, J. Wang, Y.N. Zhou, M.I. Khan, Corrosion performance of medical grade NiTi after laser processing, Surf. Coating. Technol. 324 (2017) 478–485, https://doi.org/10.1016/j.surfcoat.2017.05.092.
[140] L. Shanjin, W. Yang, An investigation of pulsed laser cutting of titanium alloy sheet, Optic Laser. Eng. 44 (2006) 1067–1077, https://doi.org/10.1016/j.optlaseng.2005.09.003.
[141] Z. Sun, I. Annergren, D. Pan, T.A. Mai, Effect of laser surface remelting on the corrosion behavior of commercially pure titanium sheet, Mater. Sci. Eng. 345 (2003) 293–300, https://doi.org/10.1016/S0921-5093(02)00477-X.
[142] F.J. Gil, L. Delgado, E. Espinar, J.M. Llamas, Corrosion and corrosion-fatigue behavior of cp-Ti and Ti–6Al–4V laser-marked biomaterials, J. Mater. Sci. Mater. Med. 23 (2012) 885–890, https://doi.org/10.1007/s10856-012-4572-z.
[143] T. Yue, L. Yan, C. Chan, C. Dong, H. Man, G.K. Pang, Excimer laser surface treatment of aluminum alloy AA7075 to improve corrosion resistance, Surf. Coating. Technol. 179 (2004) 158–164, https://doi.org/10.1016/S0257-8972(03)00850-8.
[144] W.L. Xu, T.M. Yue, H.C. Man, Nd:YAG laser surface melting of aluminium alloy 6013 for improving pitting corrosion fatigue resistance, J. Mater. Sci. 43 (2008) 942–951, https://doi.org/10.1007/s10853-007-2208-3.
[145] S. Valette, P. Steyer, L. Richard, B. Forest, C. Donnet, E. Audouard, Influence of femtosecond laser marking on the corrosion resistance of stainless steels, Appl. Surf. Sci. 252 (2006) 4696–4701, https://doi.org/10.1016/j.apsusc.2005.07.161.
[146] E.F. Pieretti, S.M. Manhabosco, L.F.P. Dick, S. Hinder, I. Costa, Localized corrosion evaluation of the ASTM F139 stainless steel marked by laser using scanning vibrating electrode technique, X-ray photoelectron spectroscopy and Mott–Schottky techniques, Electrochim. Acta 124 (2014) 150–155, https://doi.org/10.1016/j.electacta.2013.10.137.
[147] M. Švantner, M. Kučera, E. Smazalová, Š. Houdková, R. Čerstvý, Thermal effects of laser marking on microstructure and corrosion properties of stainless steel, Appl. Optic. 55 (2016) D35, https://doi.org/10.1364/AO.55.000D35.
[148] X.Y. Wang, G.K.L. Ng, Z. Liu, L. Li, L. Bradley, EPMA microanalysis of recast layers produced during laser drilling of type 305 stainless steel, Thin Solid Films 453 (2004) 84–88, https://doi.org/10.1016/j.tsf.2003.11.158.
[149] S. Eto, Y. Miura, J. Tani, T. Fujii, Effect of residual stress induced by pulsed-laser irradiation on initiation of chloride stress corrosion cracking in stainless steel, Mater. Sci. Eng. 590 (2014) 433–439, https://doi.org/10.1016/j.msea.2013.10.066.
[150] R.K. Gupta, A. Kumar, D.C. Nagpure, S.K. Rai, M.K. Singh, A. Khooha, A.K. Singh, A. Singh, M.K. Tiwari, P. Ganesh, R. Kaul, B. Singh, Comparison of stress corrosion cracking susceptibility of laser machined and milled 304 L stainless steel, Lasers Manuf. Mater. Process. 3 (2016) 191–203, https://doi.org/10.1007/s40516-016-0030-y.
[151] B. Krawczyk, P. Cook, J. Hobbs, D.L. Engelberg, Atmospheric chloride-induced stress corrosion cracking of laser engraved type 316L stainless steel, Corrosion Sci. 142 (2018) 93–101, https://doi.org/10.1016/j.corsci.2018.07.016.
[152] F. Klocke, S. Harst, L. Ehle, M. Zeis, A. Klink, Surface integrity in electrochemical machining processes: an analysis on material modifications occurring during electrochemical machining, Proc. Inst. Mech. Eng. Part B J. Eng. Manuf. 232 (2018) 578–585, https://doi.org/10.1177/0954405417703422.
[153] Z. Cai, Z. Li, M. Yin, M. Zhu, Z. Zhou, A review of fretting study on nuclear power equipment, Tribol. Int. 144 (2020) 106095, https://doi.org/10.1016/j.triboint.2019.106095.
[154] W. Liu, S. Ao, Y. Li, Z. Liu, H. Zhang, S.M. Manladan, Z. Luo, Z. Wang, Effect of anodic behavior on electrochemical machining of TB6 titanium alloy, Electrochim. Acta 233 (2017) 190–200, https://doi.org/10.1016/j.electacta.2017.03.025.
[155] J. Song, W. Xu, X. Liu, Y. Lu, J. Sun, Electrochemical machining of super-hydrophobic Al surfaces and effect of processing parameters on wettability, Appl. Phys. A 108 (2012) 559–568, https://doi.org/10.1007/s00339-012-6927-1.
[156] K. Chen, J. Wang, D. Du, X. Guo, L. Zhang, Characterizing the effects of in-situ sensitization on stress corrosion cracking of austenitic steels in supercritical water, Scripta Mater. 158 (2019) 66–70, https://doi.org/10.1016/j.scriptamat.2018.08.041.
[157] K.D. Ralston, N. Birbilis, C.H.J. Davies, Revealing the relationship between grain size and corrosion rate of metals, Scripta Mater. 63 (2010) 1201–1204, https://doi.org/10.1016/j.scriptamat.2010.08.035.
[158] K. Holmberg, A. Erdemir, Influence of tribology on global energy consumption, costs and emissions, Friction 5 (2017) 263–284, https://doi.org/10.1007/s40544-017-0183-5.
[159] W.F. Gale, T.C. Totemeier, Friction and Wear, 2004, https://doi.org/10.1016/B978-075067509-3/50028-2, 25–1.
[160] J.R. Laguna-Camacho, L.A. Cruz-Mendoza, J.C. Anzelmetti-Zaragoza, A. Marquina-Chávez, M. Vite-Torres, J. Martínez-Trinidad, Solid particle erosion on coatings employed to protect die casting molds, Prog. Org. Coating 74 (2012) 750–757, https://doi.org/10.1016/j.porgcoat.2011.09.022.
[161] I. Hutchings, Tribology: Friction and Wear of Engineering Materials, Elsevier Science, 1992.
[162] K. Kato, K. Adachi, Wear mechanisms, in: Mod. Tribol. Handb. Vol. One Princ. Tribol., CRC Press, 2000, pp. 273–300, https://doi.org/10.1007/978-3-662-53120-4_6415.
[163] M. Khruschov, Resistance of metal to wear by abrasion as related to hardness, in: Conf. Lubr. Wear, Institution of Mechanical Engineers, London, 1957, pp. 655–659.
[164] W.F. Gale, T.C. Toemeier, Smithells Metals Reference Book, eighth ed., 2004.
[165] A.-E. Jiménez, M.-D. Bermúdez, 2 - friction and wear, in: J.P.B. Davim (Ed.), Tribol. Eng. A Pract. Guid., Woodhead Publishing, 2011, pp. 33–63, https://doi.org/10.1533/9780857091444.33.
[166] Y.B. Guo, R.A. Waikar, An experimental study on the effect of machining-induced white layer on frictional and wear performance at dry and lubricated sliding contact, Tribol. Trans. 53 (2010) 127–136, https://doi.org/10.1080/10402000903283250.
[167] H. Kato, H. Ueki, K. Yamamoto, K. Yasunaga, Wear resistance improvement by nanostructured surface layer produced by burnishing, in: Mater. Sci. Forum, Trans Tech Publications Ltd, 2018, pp. 231–235, https://doi.org/10.4028/www.scientific.net/MSF.917.231.
[168] B.J. Griffiths, D.C. Furze, Tribological advantages of white layers produced by machining, J. Tribol. 109 (1987) 338–342, https://doi.org/10.1115/1.3261363.
[169] Y.Y. Yang, H.S. Fang, W.G. Huang, A Study on Wear Resistance of the White Layer, 1996.
[170] B.B. Bartha, J. Zawadzki, S. Chandrasekar, T.N. Farris, Wear of hard-turned AISI 52100 steel, Metall. Mater. Trans. A Phys. Metall. Mater. Sci. 36 (2005) 1417–1425, https://doi.org/10.1007/s11661-005-0234-9.
[171] B. Jalalahmadi, T.S. Slack, N. Raje, N.K. Arakere, A Review of Rolling Contact Fatigue, 2009, https://doi.org/10.1115/1.3209132.
[172] Y. Choi, Influence of a white layer on the performance of hard machined surfaces in rolling contact, Proc. Inst. Mech. Eng. Part B J. Eng. Manuf. 224 (2010) 1207–1215, https://doi.org/10.1243/09544054JEM1847.
[173] B. Ekmekci, Residual stresses and white layer in electric discharge machining (EDM), Appl. Surf. Sci. 253 (2007) 9234–9240, https://doi.org/10.1016/j.apsusc.2007.05.078.
[174] B. Lauwers, J.-P. Kruth, W. Eeraerts, Wear Behaviour and Tool Life of Wire-EDM-Ed and Ground Carbide Punches, n.d.
[175] V.P. Srinivasan, P.K. Palani, Surface integrity, fatigue performance and dry sliding wear behaviour of Si3N4–TiN after wire-electro discharge machining, Ceram. Int. (2020) 1–6, https://doi.org/10.1016/j.ceramint.2020.01.082.
[176] K. Bonny, Y. Perez, J. Van Wittenberghe, P. De Baets, J. Vleugels, B. Lauwers, Effect of Surface Finishing on Tribological Properties of ZrO 2-based Composites, n.d.
[177] Y. Perez Delgado, K. Bonny, P. De Baets, P.D. Neis, O. Malek, J. Vleugels, B. Lauwers, Impact of wire-EDM on dry sliding friction and wear of WC-based and ZrO2-based composites, Wear 271 (2011) 1951–1961, https://doi.org/10.1016/j.wear.2010.12.068.
[178] D.C. Furze, B.J. Griffiths, G.P. Bertolotti, Engineering the surface characteristics of wear resistant white layers with reference to the design of tribosystems, J. FUELS Lubr. 97 (1988) 746–755.
[179] J. Champaigne, History of shot peening specifications, Shot Peen 20 (2006) 12–38.
[180] E.J. Hearn, Contact stress, residual stress and stress concentrations, in: Mech. Mater., vol. 2, Elsevier, 1997, pp. 381–442, https://doi.org/10.1016/B978-075063266-9/50011-1.
[181] U. Zupanc, J. Grum, Effect of pitting corrosion on fatigue performance of shot-peened aluminium alloy 7075-T651, J. Mater. Process. Technol. 210 (2010) 1197–1202.
[182] S.B. Mahagaonkar, P.K. Brahmankar, C.Y. Seemikeri, Effect on fatigue performance of shot peened components: an analysis using DOE technique, Int. J. Fatig. 31 (2009) 693–702, https://doi.org/10.1016/j.ijfatigue.2008.03.020.
[183] C.S. Montross, T. Wei, L. Ye, G. Clark, Y.W. Mai, Laser shock processing and its effects on microstructure and properties of metal alloys: a review, Int. J. Fatig. 24 (2002) 1021–1036, https://doi.org/10.1016/S0142-1123(02)00022-1.
[184] M. Srivastava, R. Tripathi, S. Hloch, S. Chattopadhyaya, A.R. Dixit, Potential of using water jet peening as a surface treatment process for welded joints, Procedia Eng 149 (2016) 472–480, https://doi.org/10.1016/j.proeng.2016.06.694.
[185] D.J. Child, et al., Assessment of surface hardening effects from shot peening on a Ni-based alloy using electron backscatter diffraction techniques, Acta Mater. (2011), https://doi.org/10.1016/j.actamat.2011.04.025.
[186] Messé, et al., Characterization of plastic deformation induced by shot- peening in a Ni-base superalloy, JOM (2014), https://doi.org/10.1007/s11837-014-1184-8.
[187] Gibson, et al., Influence of shot peening on high-temperature corrosion and corrosion-fatigue of nickel based superalloy 720Li, Mater. High Temp. (2016), https://doi.org/10.1080/09603409.2016.1161945.
[188] Kim, et al., Stress relaxation of shot-peened UDIMET 720Li under solely elevated-temperature exposure and under isothermal fatigue, Metall. Mater. Trans. A (2005), https://doi.org/10.1007/s11661-005-0076-5.
[189] M. Tufft, Shot Peen Impact on Life, Part 1: Designed Experiment Using Rene 88DT, ICSP 7 7 Th Int. Conf. Shot Peen. (1999) 244–253.
[190] Jackson, et al., The Effect of shot peening on the ductility and tensile strength of nickel-based superalloy alloy 720Li, in: S. Tin, et al. (Eds.), Superalloys 2020. The Minerals, Metals & Materials Series., Springer, Cham, 2020, https://doi.org/10.1007/978-3-030- 51834-9_52.
[191] Z. Chen, R.L. Peng, J. Moverare, O. Widman, Effect of cooling and shot peening on residual stresses and fatigue performance of milled Inconel 718, Residual Stress 2 (2017) 13–18, https://doi.org/10.21741/9781945291173-3, 2016.

[192] Y.K. Gao, Improvement of fatigue property in 7050-T7451 aluminum alloy by laser peening and shot peening, Mater. Sci. Eng. 528 (2011) 3823–3828, https://doi.org/10.1016/j.msea.2011.01.077.
[193] Z. Xu, J. Dunleavey, M. Antar, R. Hood, S.L. Soo, G. Kucukturk, C.J. Hyde, A. T. Clare, The influence of shot peening on the fatigue response of Ti-6Al-4V surfaces subject to different machining processes, Int. J. Fatig. 111 (2018) 196–207, https://doi.org/10.1016/j.ijfatigue.2018.02.022.
[194] J.Z. Lu, K.Y. Luo, Y.K. Zhang, G.F. Sun, Y.Y. Gu, J.Z. Zhou, X.D. Ren, X.C. Zhang, L.F. Zhang, K.M. Chen, C.Y. Cui, Y.F. Jiang, A.X. Feng, L. Zhang, Grain refinement mechanism of multiple laser shock processing impacts on ANSI 304 stainless steel, Acta Mater. 58 (2010) 5354–5362, https://doi.org/10.1016/j.actamat.2010.06.010.
[195] A.S. Gill, Z. Zhou, U. Lienert, J. Almer, D.F. Lahrman, S.R. Mannava, D. Qian, V. K. Vasudevan, High spatial resolution, high energy synchrotron x-ray diffraction characterization of residual strains and stresses in laser shock peened Inconel 718SPF alloy, J. Appl. Phys. 111 (2012), https://doi.org/10.1063/1.3702890.
[196] S.D. Cuellar, M.R. Hill, A.T. Dewald, J.E. Rankin, Residual stress and fatigue life in laser shock peened open hole samples, Int. J. Fatig. 44 (2012) 8–13, https://doi.org/10.1016/j.ijfatigue.2012.06.011.
[197] X.D. Ren, Q.B. Zhan, S.Q. Yuan, J.Z. Zhou, Y. Wang, N.F. Ren, G.F. Sun, L. M. Zheng, F.Z. Dai, H.M. Yang, W.J. Dai, A finite element analysis of thermal relaxation of residual stress in laser shock processing Ni-based alloy GH4169, Mater. Des. 54 (2014) 708–711, https://doi.org/10.1016/j.matdes.2013.08.054.
[198] X.D. Ren, Q.B. Zhan, H.M. Yang, F.Z. Dai, C.Y. Cui, G.F. Sun, L. Ruan, The effects of residual stress on fatigue behavior and crack propagation from laser shock processing-worked hole, Mater. Des. 44 (2013) 149–154, https://doi.org/10.1016/j.matdes.2012.07.024.
[199] M. Pavan, D. Furfari, B. Ahmad, M.A. Gharghouri, M.E. Fitzpatrick, Fatigue crack growth in a laser shock peened residual stress field, Int. J. Fatig. 123 (2019) 157–167, https://doi.org/10.1016/j.ijfatigue.2019.01.020.
[200] H. Soyama, Comparison between the improvements made to the fatigue strength of stainless steel by cavitation peening, water jet peening, shot peening and laser peening, J. Mater. Process. Technol. 269 (2019) 65–78, https://doi.org/10.1016/j.jmatprotec.2019.01.030.
[201] Z. Liao, I. Sanchez, D. Xu, D. Axinte, G. Augustinavicius, A. Wretland, Dual-processing by abrasive waterjet machining–A method for machining and surface modification of nickel-based superalloy, J. Mater. Process. Technol. (2020) 116768.
[202] J. Holmberg, A. Wretland, J. Berglund, T. Beno, Surface integrity after post processing of EDM processed Inconel 718 shaft, Int. J. Adv. Manuf. Technol. 95 (2018) 2325–2337, https://doi.org/10.1007/s00170-017-1342-6.
[203] D. Arola, A.E. Alade, W. Weber, Improving fatigue strength of metals using abrasive waterjet peening, Mach. Sci. Technol. 10 (2006) 197–218.
[204] X. He, M. Song, Y. Du, Y. Shi, B.A. Johnson, K.F. Ehmann, Y.W. Chung, Q.J. Wang, Surface hardening of metals at room temperature by nanoparticle-laden cavitating waterjets, J. Mater. Process. Technol. 275 (2020) 116316, https://doi.org/10.1016/j.jmatprotec.2019.116316.
[205] M. Lieblich, S. Barriuso, J. Ibáñez, L. Ruiz-de-Lara, M. Díaz, J.L. Ocaña, A. Alberdi, J.L. González-Carrasco, On the fatigue behavior of medical Ti6Al4V roughened by grit blasting and abrasiveless waterjet peening, J. Mech. Behav. Biomed. Mater. 63 (2016) 390–398, https://doi.org/10.1016/j.jmbbm.2016.07.011.
[206] A. Naito, O. Takakuwa, H. Soyama, Development of peening technique using recirculating shot accelerated by water jet, Mater. Sci. Technol. 28 (2012) 234–239, https://doi.org/10.1179/1743284711Y.0000000027.
[207] A. Reck, A.T. Zeuner, M. Zimmermann, Fatigue behavior of non-optimized laser-cut medical grade ti-6AL-4V-ELI sheets and the effects of mechanical post-processing, Metals 9 (2019) 843, https://doi.org/10.3390/met9080843.
[208] D. Wu, D. Zhang, C. Yao, Effect of turning and surface polishing treatments on surface integrity and fatigue performance of nickel-based alloy GH4169, Metals 8 (2018), https://doi.org/10.3390/met8070549.
[209] P.S. Prevéy, J. Cammett, Low cost corrosion damage mitigation and improved fatigue performance of low plasticity burnished 7075-T6, J. Mater. Eng. Perform. 10 (2001) 548–555, https://doi.org/10.1361/105994901770344692.
[210] Y. Hua, Z. Liu, B. Wang, X. Hou, Surface modification through combination of finish turning with low plasticity burnishing and its effect on fatigue performance for Inconel 718, Surf. Coating. Technol. 375 (2019) 508–517, https://doi.org/10.1016/j.surfcoat.2019.07.057.
[211] G.D. Revankar, R. Shetty, S.S. Rao, V.N. Gaitonde, Wear resistance enhancement of titanium alloy (Ti-6Al-4V) by ball burnishing process, J. Mater. Res. Technol. 6 (2017) 13–32, https://doi.org/10.1016/j.jmrt.2016.03.007.
[212] Z. Pu, G.L. Song, S. Yang, J.C. Outeiro, O.W. Dillon, D.A. Puleo, I.S. Jawahir, Grain refined and basal textured surface produced by burnishing for improved corrosion performance of AZ31B Mg alloy, Corrosion Sci. 57 (2012) 192–201, https://doi.org/10.1016/j.corsci.2011.12.018.
[213] Z. Pu, O.W. Dillon, D.A. Puelo, I.S. Jawahir, Cryogenic Machining and Burnishing of Magnesium Alloys to Improve in Vivo Corrosion Resistance, 2015, https://doi.org/10.1016/B978-1-78242-078-1.00005-0.
[214] A. Temmler, D. Liu, J. Preußner, S. Oeser, J. Luo, R. Poprawe, J.H. Schleifenbaum, Influence of laser polishing on surface roughness and microstructural properties of the remelted surface boundary layer of tool steel H11, Mater. Des. 192 (2020) 108689, https://doi.org/10.1016/j.matdes.2020.108689.
[215] K.C. Yung, S.S. Zhang, L. Duan, H.S. Choy, Z.X. Cai, Laser polishing of additive manufactured tool steel components using pulsed or continuous-wave lasers, Int. J. Adv. Manuf. Technol. 105 (2019) 425–440, https://doi.org/10.1007/s00170-019-04205-z.
[216] J. Preußner, S. Oeser, W. Pfeiffer, A. Temmler, E. Willenborg, Microstructure and residual stresses of laser remelted surfaces of a hot work tool steel, Int. J. Mater. Res. 105 (2014) 328–336, https://doi.org/10.3139/146.111027.
[217] J. Zhou, C. Liao, H. Shen, X. Ding, Surface and Property Characterization of Laser Polished Ti6Al4V, 2019, https://doi.org/10.1016/j.surfcoat.2019.125016.
[218] C.P. Ma, Y.C. Guan, W. Zhou, Laser polishing of additive manufactured Ti alloys, Optic Laser. Eng. 93 (2017) 171–177, https://doi.org/10.1016/j.optlaseng.2017.02.005.
[219] B. Raeymaekers, F.E. Talke, The effect of laser polishing on fretting wear between a hemisphere and a flat plate, Wear 269 (2010) 416–423, https://doi.org/10.1016/j.wear.2010.04.027.
[220] L. Chen, B. Richter, X. Zhang, X. Ren, F.E. Pfefferkorn, Modification of surface characteristics and electrochemical corrosion behavior of laser powder bed fused stainless-steel 316L after laser polishing, Addit. Manuf. 32 (2020) 101013, https://doi.org/10.1016/j.addma.2019.101013.
[221] J.W. Murray, J.C. Walker, A.T. Clare, Nanostructures in austenitic steel after EDM and pulsed electron beam irradiation, Surf. Coating. Technol. 259 (2014) 465–472, https://doi.org/10.1016/j.surfcoat.2014.10.045.
[222] J.W. Murray, A.T. Clare, Repair of EDM induced surface cracks by pulsed electron beam irradiation, J. Mater. Process. Technol. 212 (2012) 2642–2651, https://doi.org/10.1016/j.jmatprotec.2012.07.018.
[223] Y. Uno, A. Okada, Y. Okamoto, Y. Uno A. Okada, Y. Okamoto, Surface modification of EDMed surface by wide-area electron beam irradiation, J. Japan Soc. Eng. Educ. 51 (2003) 58–61.
[224] D.I. Proskurovsky, V.P. Rotshtein, G.E. Ozur, Y.F. Ivanov, A.B. Markov, Physical foundations for surface treatment of materials with low energy, high current electron beams, Surf. Coating. Technol. 125 (2000) 49–56, https://doi.org/10.1016/S0257-8972(99)00604-0.
[225] D.I. Proskurovsky, V.P. Rotshtein, G.E. Ozur, A.B. Markov, D.S. Nazarov, V. A. Shulov, Y.F. Ivanov, R.G. Buchheit, Pulsed electron-beam technology for surface modification of metallic materials, J. Vac. Sci. Technol. A Vacuum, Surfaces, Film. 16 (1998) 2480–2488, https://doi.org/10.1116/1.581369.
[226] K.M. Zhang, J.X. Zou, B. Bolle, T. Grosdidier, Evolution of residual stress states in surface layers of an AISI D2 steel treated by low energy high current pulsed electron beam, Vacuum 87 (2013) 60–68, https://doi.org/10.1016/j.vacuum.2012.03.061.
[227] S. Yang, Z. Guo, L. Zhao, L. Zhao, Q. Guan, Y. Liu, Surface Microstructures and High-Temperature High-Pressure Corrosion Behavior of N18 Zirconium Alloy Induced by High Current Pulsed Electron Beam Irradiation, 2019, https://doi.org/10.1016/j.apsusc.2019.04.124.
[228] F. Guo, W. Jiang, G. Tang, Z. Xie, H. Dai, E. Wang, Y. Chen, L. Liu, Enhancing anti-wear and anti-corrosion performance of cold spraying aluminum coating by high current pulsed electron beam irradiation, Vacuum 182 (2020) 109772, https://doi.org/10.1016/j.vacuum.2020.109772.
[229] L.L. Meisner, V.O. Semin, Y.P. Mironov, S.N. Meisner, F.A. D'yachenko, Cross-sectional Analysis of the Graded Microstructure and Residual Stress Distribution in a TiNi Alloy Treated with Low Energy High-Current Pulsed Electron Beam, 2018, https://doi.org/10.1016/j.mtcomm.2018.08.018.
[230] D.I. Proskurovsky, V.P. Rotshtein, G.E. Ozur, Use of low-energy, high-current electron beams for surface treatment of materials, Surf. Coating. Technol. 96 (1997) 117–122, https://doi.org/10.1016/S0257-8972(97)00093-5.
[231] A.B. Markov, V.P. Rotshtein, Calculation and experimental determination of dimensions of hardening and tempering zones in quenched U7A steel irradiated with a pulsed electron beam, Nucl. Instrum. Methods Phys. Res. Sect. B Beam Interact. Mater. Atoms 132 (1997) 79–86, https://doi.org/10.1016/S0168-583X(97)00416-3.
[232] D. Lee, B. Kim, S.M. Baek, J. Kim, H.W. Park, J.G. Lee, S.S. Park, Microstructure and corrosion resistance of a Mg2Sn-dispersed Mg alloy subjected to pulsed electron beam treatment, J. Magnes. Alloy. 8 (2020) 345–351, https://doi.org/10.1016/j.jma.2020.02.005.
[233] S. Hao, Y. Xu, Y. Zhang, L. Zhao, Improvement of surface microhardness and wear resistance of WC/Co hard alloy by high current pulsed electron beam irradiation, Int. J. Refract. Metals Hard Mater. 41 (2013) 553–557, https://doi.org/10.1016/j.ijrmhm.2013.07.006.
[234] J. Walker, J. Murray, S. Narania, A. Clare, Dry sliding friction and wear behaviour of an electron beam melted hypereutectic Al–Si alloy, Tribol. Lett. (2011) 1–10, https://doi.org/10.1007/s11249-011-9865-8.
[235] D. Zaguliaev, S. Konovalov, Y. Ivanov, V. Gromov, E. Petrikova, Microstructure and Mechanical Properties of Doped and Electron-Beam Treated Surface of Hypereutectic Al-11.1%Si Alloy, 2019, https://doi.org/10.1016/j.jmrt.2019.06.045.
[236] S. Gnyusov, S. Tarasov, Y. Ivanov, V. Rothstein, The effect of pulsed electron beam melting on microstructure, friction and wear of WC–Hadfield steel hard metal, Wear 257 (2004) 97–103, https://doi.org/10.1016/j.wear.2003.10.011.
[237] J.X. Zou, K.M. Zhang, S.Z. Hao, C. Dong, T. Grosdidier, Mechanisms of hardening, wear and corrosion improvement of 316 L stainless steel by low energy high current pulsed electron beam surface treatment, Thin Solid Films 519 (2010) 1404–1415.
[238] Y.F. Ivanov, V.P. Rotshtein, D.I. Proskurovsky, P. V Orlov, K.N. Polestchenko, G. E. Ozur, I.M. Goncharenko, Pulsed electron-beam treatment of WC–TiC–Co hard-alloy cutting tools: wear resistance and microstructural evolution, Surf. Coating. Technol. 125 (2000) 251–256, https://doi.org/10.1016/S0257-8972(99)00569-1.
[239] S.J. Algodi, J.W. Murray, P.D. Brown, A.T. Clare, Wear performance of TiC/Fe cermet electrical discharge coatings, Wear (2018) 402–403, https://doi.org/10.1016/j.wear.2018.02.007, 109–123.

[240] J.W. Murray, R.B. Cook, N. Senin, S.J. Algodi, A.T. Clare, N. Senin, S.J. Algodi, A. T. Clare, Defect-free TiC/Si multi-layer electrical discharge coatings, Mater. Des. 155 (2018) 352–365, https://doi.org/10.1016/j.matdes.2018.06.019.
[241] S.L. Li, Y.J. Mai, M.Y. Huang, X.H. Jie, Anti-wear hierarchical TiC enhanced cermet coating obtained via electrical discharge coating using a reduced graphene oxide nanosheets mixed dielectric, Ceram. Int. (2020), https://doi.org/10.1016/j.ceramint.2020.01.231.
[242] R. Tyagi, A.K. Das, A. Mandal, Electrical discharge coating using WS2 and Cu powder mixture for solid lubrication and enhanced tribological performance, Tribol. Int. 120 (2018) 80–92, https://doi.org/10.1016/j.triboint.2017.12.023.
[243] Z. Zeng, H. Xiao, X. Jie, Y. Zhang, Friction and wear behaviors of TiCN coating based on electrical discharge coating, Trans. Nonferrous Metals Soc. China 25 (2015) 3716–3722, https://doi.org/10.1016/S1003-6326(15)64013-4.
[244] J.W. Murray, S.J. Algodi, M.W. Fay, P.D. Brown, A.T. Clare, Formation mechanism of electrical discharge TiC-Fe composite coatings, J. Mater. Process. Technol. 243 (2017) 143–151, https://doi.org/10.1016/j.jmatprotec.2016.12.011.
[245] M. Janeček, F. Nový, J. Stráský, P. Harcuba, L. Wagner, Fatigue endurance of Ti-6Al-4V alloy with electro-eroded surface for improved bone in-growth, J. Mech. Behav. Biomed. Mater. 4 (2011) 417–422, https://doi.org/10.1016/j.jmbbm.2010.12.001.
[246] S. Ganesh Sundara Raman, K.A. Padmanabhan, Effect of electropolishing on the room-temperature low-cycle fatigue behaviour of AISl 304LN stainless steel, Int. J. Fatig. 17 (1995) 179–182, https://doi.org/10.1016/0142-1123(95)98938-Y.
[247] Y. Gao, X. Li, Q. Yang, M. Yao, Influence of surface integrity on fatigue strength of 40CrNi2Si2MoVA steel, Mater. Lett. 61 (2007) 466–469, https://doi.org/10.1016/j.matlet.2006.04.089.
[248] A. Laamouri, H. Sidhom, C. Braham, Evaluation of residual stress relaxation and its effect on fatigue strength of AISI 316L stainless steel ground surfaces: experimental and numerical approaches, Int. J. Fatig. 48 (2013) 109–121, https://doi.org/10.1016/j.ijfatigue.2012.10.008.
[249] M. Shahzad, M. Chaussumier, R. Chieragatti, C. Mabru, F. Rezai-Aria, Effect of sealed anodic film on fatigue performance of 2214-T6 aluminum alloy, Surf. Coating. Technol. 206 (2012) 2733–2739, https://doi.org/10.1016/j.surfcoat.2011.10.033.
[250] R. Sadeler, Effect of a commercial hard anodizing on the fatigue property of a 2014-T6 aluminium alloy, J. Mater. Sci. 41 (2006) 5803–5809, https://doi.org/10.1007/s10853-006-0725-0.
[251] J.A.M. de Camargo, H.J. Cornelis, V.M.O.H. Cioffi, M.Y.P. Costa, Coating residual stress effects on fatigue performance of 7050-T7451 aluminum alloy, Surf. Coating. Technol. 201 (2007) 9448–9455, https://doi.org/10.1016/j.surfcoat.2007.03.032.
[252] X. Montero, A. Ishida, T.M. Meißner, H. Murakami, M.C. Galetz, Effect of surface treatment and crystal orientation on hot corrosion of a Ni-based single-crystal superalloy, Corrosion Sci. 166 (2020) 108472, https://doi.org/10.1016/j.corsci.2020.108472.
[253] Y. Han, J. Mei, Q. Peng, E.-H. Han, W. Ke, Effect of electropolishing on corrosion of Alloy 600 in high temperature water, Corrosion Sci. 98 (2015) 72–80, https://doi.org/10.1016/j.corsci.2015.05.026.
[254] H.S. Shim, M.J. Seo, D.H. Hur, Effect of electropolishing on general corrosion of Alloy 690TT tubes in simulated primary coolant of pressurized water reactors, Appl. Surf. Sci. (2019) 467–468, https://doi.org/10.1016/j.apsusc.2018.10.178, 467–476.
[255] G. Han, Z. Lu, X. Ru, J. Chen, Q. Xiao, Y. Tian, Improving the oxidation resistance of 316L stainless steel in simulated pressurized water reactor primary water by electropolishing treatment, J. Nucl. Mater. 467 (2015) 194–204, https://doi.org/10.1016/j.jnucmat.2015.09.029.
[256] S.-J. Lee, J.-J. Lai, The effects of electropolishing (EP) process parameters on corrosion resistance of 316L stainless steel, J. Mater. Process. Technol. 140 (2003) 206–210, https://doi.org/10.1016/S0924-0136(03)00785-4.
[257] S.E. Ziemniak, M. Hanson, P.C. Sander, Electropolishing effects on corrosion behavior of 304 stainless steel in high temperature, hydrogenated water, Corrosion Sci. 50 (2008) 2465–2477, https://doi.org/10.1016/j.corsci.2008.06.032.
[258] W. Simka, M. Kaczmarek, A. Baron-Wiecheć, G. Nawrat, J. Marciniak, J. Żak, Electropolishing and passivation of NiTi shape memory alloy, Electrochim. Acta 55 (2010) 2437–2441, https://doi.org/10.1016/j.electacta.2009.11.097.
[259] C.L. Chu, R.M. Wang, T. Hu, L.H. Yin, Y.P. Pu, P.H. Lin, S.L. Wu, C.Y. Chung, K.W. K. Yeung, P.K. Chu, Surface structure and biomedical properties of chemically polished and electropolished NiTi shape memory alloys, Mater. Sci. Eng. C 28 (2008) 1430–1434, https://doi.org/10.1016/j.msec.2008.03.009.
[260] I. Milošev, B. Kapun, The corrosion resistance of Nitinol alloy in simulated physiological solutions, Mater. Sci. Eng. C 32 (2012) 1087–1096, https://doi.org/10.1016/j.msec.2011.11.007.
[261] Y. Hou, R. Li, J. Liang, P. Su, P. Ju, Electropolishing of Al and Al alloys in AlCl 3/trimethylamine hydrochloride ionic liquid, Surf. Coating. Technol. 335 (2018) 72–79, https://doi.org/10.1016/j.surfcoat.2017.12.028.
[262] H. Wang, G. Chi, Y. Wang, F. Yu, Z. Wang, Fabrication of superhydrophobic metallic surface on the electrical discharge machining basement, Appl. Surf. Sci. 478 (2019) 110–118, https://doi.org/10.1016/j.apsusc.2019.01.102.
[263] P. Zeng, A. Rana, R. Thompson, W. Rainforth, Subsurface characterisation of wear on mechanically polished and electro-polished biomedical grade CoCrMo, Wear 332–333 (2015) 650–661, https://doi.org/10.1016/j.wear.2015.02.007.
[264] J.A. Picas, A. Forn, E. Rupérez, M.T. Baile, E. Martín, Hard anodizing of aluminium matrix composite A6061/(Al2O3)p for wear and corrosion resistance improvement, Plasma Process. Polym. 4 (2007) S579–S583, https://doi.org/10.1002/ppap.200731409.
[265] S. Wu, S. Wang, W. Liu, X. Yu, G. Wang, Z. Chang, D. Wen, Microstructure and properties of TiO2 nanotube coatings on bone plate surface fabrication by anodic oxidation, Surf. Coating. Technol. 374 (2019) 362–373, https://doi.org/10.1016/j.surfcoat.2019.06.019.
[266] M.R. Vaezi, S.K. Sadrnezhaad, L. Nikzad, Electrodeposition of Ni–SiC nano-composite coatings and evaluation of wear and corrosion resistance and electroplating characteristics, Colloids Surfaces A Physicochem. Eng. Asp. 315 (2008) 176–182, https://doi.org/10.1016/j.colsurfa.2007.07.027.
[267] C. Liu, F. Su, J. Liang, Producing cobalt–graphene composite coating by pulse electrodeposition with excellent wear and corrosion resistance, Appl. Surf. Sci. 351 (2015) 889–896, https://doi.org/10.1016/j.apsusc.2015.06.018.
[268] Absolute Zero - UK FIRES, (n.d.). https://ukfires.org/absolute-zero/.
[269] J.T. Black, R.A. Kohser, DeGarmo's Materials and Processes in Manufacturing, Wiley, 2020. https://books.google.it/books?id=nh7zDwAAQBAJ.
[270] M. Field, J.F. Kahles, The surface integrity of machined and high strength steels, DMIC Rep (1964) 54–77.